**Lysosomal Calcium Channel TRPML1 in Physiology and Pathology**

by

Lu Yu

A dissertation submitted in partial fulfillment
of the requirements for the degree of
Doctor of Philosophy
(Molecular, Cellular and Developmental Biology)
In the University of Michigan
2019

Doctoral Committee:

Professor Haoxing Xu, Chair
Professor Mohammed Akaaboune
Professor John Y. Kuwada
Professor Daniel Eugene Michele

*The test of a first-rate intelligence is the ability to hold two opposed ideas in mind at the same time and still retain the ability to function.*

*-F. Scott Fitzgerald, 1936.*

Lu Yu

luyu@umich.edu

ORCID iD 0000-0002-6972-6489

## ACKNOWLEDGEMENTS

About six years ago, I started my journey of graduate school. Now I am at the end of the tunnel and looking back, there were lots of people who gave me help and made this work possible. I would like to take this opportunity to extend my gratitude to my advisor, thesis committee members, collaborators, lab members, friends, and family.

First and foremost, I would like to thank my PhD advisor, Prof. Haoxing Xu. There are truly too many things I thank him for. Basically, everything I know about science is learned from Haoxing and the Xu lab. He has always been a responsible advisor, an excellent teacher who impressed me with his passion for doing good science. He is one of the sharpest scientists I have ever seen. There were many times when I presented my data to Haoxing, I was surprised how he would interpret them from a different angle and tell a different story – and his story often made much more sense! I also remember when Haoxing said "Let's get our hands dirty first" – which turned out to be one of the most helpful advices that I always kept in mind. He told me this when I was starting to inject some compounds into mice. These experiments were difficult, since no one had tried to collect *in vivo* data from these compounds before and I needed to figure out everything from scratch. At the beginning I had psychological barrier to try it out but Haoxing convinced me the necessity for doing this experiment and encouraged me to get help from collaborators. Luckily, we did make important findings from these experiments, which you will see in this dissertation. I really appreciate Haoxing for this precious experience, since I learned the courage for trying is important in doing science. Last but not least, I would like to thank him for respecting my thoughts

and opinions and being supportive throughout this process. Overall, it has been a great pleasure and honor for me to work with Haoxing and the rest of Xu lab members.

I would like to extend my gratitude to my thesis committee members for their thought-provoking questions and constructive suggestions. I would like to thank Prof. Mohammed Akaaboune, for his effort to participate in my thesis committee meeting even when he was on sabbatical out of the country. He is a muscle expert and I found his sharp comments on my project very thought-provoking. In addition, I really appreciate his inputs on the manuscript. I would also like to thank Prof. John Kuwada. His knowledge about $Ca^{2+}$ signaling, neuroscience and muscle physiology has provided new angles and insights to my project. The completion of this work would not be possible without the help from Prof. Daniel Michele. As an expert on the muscle field, he was the go-to person whenever I had questions regarding muscle techniques, and he was always responsive to my questions and requests. He also provided insightful comments on the manuscript. Besides, he introduced me to the physiology core in the university, which turned out to be a great help to my thesis work. Overall, I am truly grateful for the guidance and suggestions I have received from my committee members.

I sincerely appreciate all the help from our collaborators. Carol Davis from Prof. Susan Brooks lab helped me perform muscle force measurement. I also received lots of helpful suggestions on data analysis and muscle physiology from Prof. Susan Brooks. I also owe gratitude to Dr. Vincent Mouly from Institut de Myologie in France, who kindly provided us with immortalized patient myoblasts and gave helpful suggestions on the manuscript. Besides, I received guidance and suggestions on drug formulation and dosage from Dr. Jinhui Liao in Prof. Duxin Sun lab. I also learned freezing muscle tissues and cryosectioning from Prof. Renzhi Han, as well as isolation of single muscle fiber from Molly Thorson in Prof. Daniel Michele lab.

I truly enjoyed the time working with all the Xu lab members. In the past six years, I have spent most of my time with them and now they have become not only colleagues, but also close friends to me. I like the atmosphere of the Xu lab where people can be both critical and nice. Among everyone, the person I would like to thank first is Dr. Xiaoli Zhang. Ever since I joined Xu lab, she has been both a good teacher and a loyal friend to me. As a senior postdoc in the lab, I learned a lot from her while working with her, including designing good controls, taking high-quality images, data quantification, etc. Her knowledge on electrophysiology and cell biology often provided me with insightful new ideas when we discussed about science. I also appreciate her a lot for being supportive and encouraging when I encountered difficulties. I would also like to thank Drs. Ping Li and Meiqin Hu. They and I often stayed late in the lab and I thank them for the company. Ping impressed me with his motivation, diligence and persistency, while Meiqin is knowledgeable on electrophysiology, molecular and cell biology assays. I have received lots of helpful comments as well as encouragement from them. I would also like to thank Dr. Wanlu Du, for her helpful suggestions and comments on animal studies. I appreciate help from Mingxue Gu and Ce Wang. Both of them are hard-working PhD students in the lab who are enthusiastic about science. I thank them for their company – I really enjoyed the time we spent together talking about science or life. Interestingly, both of them are good at cooking so I could try lots of good Chinese cuisine made by them. Moreover, I would like to thank several undergraduate students who helped me with experiments, including Yexin (Kathy) Yang, Kaiyuan (Fred) Tang and Zifan Zhao. All of them have shown great enthusiasm about science and been super helpful while working with me. I also appreciate the help from Dr. Dan Li and Wanwan He, who were visiting scholars in the lab and helped me perform experiments. Finally, I would like to thank other lab members including

but not limited to Wei Chen, Spring Gao, Shiyu Xiao, Kathleen Young, Michael Ryan, Sherwin Navaz and Tim Nold for their company and support.

I would also like to extend my gratitude to several previous lab members for their help. Drs. Xiping (Spring) Cheng and Xinran (Roy) Li gave me lots of helpful advices, guidance and encouragement when I was a junior graduate student, especially during my preliminary exam. As the person who initiated the muscle project in the lab, Xiping answered my questions even after she left the lab and I thank her for her patience. I would also like to thank Dr. Nirakar Sahoo, not only because he was knowledgeable about electrophysiology, biochemistry and animal studies, but also due to his happy personality. Furthermore, I would like to thank Dr. Qiong Gao, who was the nicest person I have ever known and was always willing to help people. More importantly, she was the person who brought most joy to the lab. Overall, I truly appreciate all the current and previous lab members, for they have created such a good and friendly environment for learning and doing science. During my stay in the Xu lab, I have always felt joining this lab is the best decision I have made during my PhD.

I would like to thank my friends from Department of MCDB who supported and encouraged me during these years. I thank my roommates and cohorts, Wenjia Wang and Yi Xin, for their friendship and company. I would also like to thank other cohorts, including Jiyuan Yang, Po-Ju Chen, Damian Gatica and Nebibe Mutlu. In the past years we have become friends sharing frustrations and happiness about research and life. I would also like to thank Zhangyuan Yin and Ying Yang, PhD students from MCDB. We became friends when they were doing rotations in Xu lab and I appreciate their company and encouragement during these years.

I owe my deepest gratitude to my family for their unconditional love and support for me. Both of my parents are scientists back in China, which have great influence on me. Besides, they

were all born into families in relatively lower socioeconomic status and strived to achieve their personal goals in life. They have set up best role models for me so I know people should work hard and fight for their goals. Most importantly, both of them have happy personalities which made me a happy and positive person as well. This turned out to be crucial for my completion of PhD, since lots of positive energy is needed to recover from stress and frustrations when doing research.

I realize it is impossible to thank everyone who has contributed, directly or indirectly, to this work, but I would still like to say thanks to all the people who have helped me during this journey. Thank you for what you have done.

## PREFACE

In this dissertation, two individual projects will be presented. The first is about lysosomal TRPML1 (ML1) channels in ROS (reactive oxygen species) sensing and lysosomal adaptation. The project was initiated by Dr. Xiaoli Zhang, a postdoctoral fellow in Xu lab. She is an electrophysiologist who first discovered ML1 channels can be activated by ROS. Then another postdoctoral fellow in the lab, Dr. Xiping Cheng, joined the project to help the cell biology experiments. I was recruited to the project on April 2015, upon Xiping's leaving the lab. I mainly performed cell biology experiments including staining, imaging and quantification. The work was finally published on the journal of *Nature Communications* on 2016, where I was listed as a co-first author. This part of work will be presented in Chapter II. To complete the story, I also included some data generated by Xiaoli and Xiping, which are indicated in the figure legends.

The second project I worked on was about ML1's role in muscle diseases, which will be presented in Chapter III and IV. I started to work on the project from September 2016. At that time, I was also working on several other projects but finally decided to focus on this most promising one from early 2017. At the beginning, I struggled a lot with technical problems on muscle assays. But with the help from the committee members and collaborators, I was able to carry on and finally submitted the manuscript. During this period, I also received lots of help from lab members and collaborators on experiments. Drs. Xiaoli Zhang and Nirakar Sahoo from Xu lab helped me perform electrophysiology and $Ca^{2+}$ imaging, respectively. PhD student Ce Wang helped on Lamp1 surface staining. Several undergraduate students in the lab, Yexin (Kathy) Yang,

Kaiyuan (Fred) Tang and Zifan Zhao, helped with mouse genotyping, tissue sectioning and staining, quantification. Besides, Fred also did Western blot and Zifan helped on qPCR. Our collaborator, Carol Davis from Dr. Susan Brooks lab, helped me perform experiments on muscle force measurements. As I mentioned in the acknowledgement, I am truly grateful for all the lab members and collaborators for their help. Their efforts are also indicated in the figure legends. In Chapter III, effects of ML1 activation on muscular dystrophy will be presented. In Chapter IV, I will present the underlying mechanisms of ML1 in membrane repair and muscular dystrophy.

Last but not least, I would like to thank all the people who are reading my thesis. Doing science is a lonely journey, and knowing someone else may care about your work is always a great comfort. For that, I thank all the readers who have reached this far.

## TABLE OF CONTENTS

## LIST OF FIGURES

### CHAPTER I



### CHAPTER II



### CHAPTER III

**CHAPTER IV**

## LIST OF ABBREVIATIONS

| | |
|---|---|
| 3-MA | 3-methyladenine |
| ACD | autophagic cell death |
| AD | Alzheimer's disease |
| AL | autolysosome |
| ALG | apoptosis-linked gene |
| ALR | autophagic lysosomal reformation |
| AMPK | AMP-activated protein kinase |
| ANOVA | analysis of variance |
| AP | autophagosome |
| aSMase | acid sphingomyelinase |
| ATG | autophagy gene |
| BAPTA | 1,2-bis(o-aminophenoxy)ethane-N,N,N',N'-tetraacetic acid |
| EGTA | ethylene glycol-bis(β-aminoethyl ether)-N,N,N',N'-tetraacetic acid |
| BMD | Becker's muscular dystrophy |
| CaN | calcineurin |
| CCCP | carbonyl cyanide m-chlorophenyl hydrazone |
| ChT | chloramine T |
| CK | creatine kinase |
| ClC | chloride channel |
| CLEAR | coordinated lysosomal enhancement and regulation |
| CMA | chaperone-mediated autophagy |
| CMD | congenital muscular dystrophies |
| CQ | chloroquine |
| CRISPR | clustered regularly interspaced short palindromic repeats |
| CsA | cyclosporin A |
| DAPI | 4',6-diamidino-2-phenylindole |
| DEPTOR | DEP domain-containing mTOR-interacting protein |
| DIA | diaphragm |
| DMD | Duchenne muscular dystrophy |
| DPC | dystrophin protein complex |
| DTNB | 5,5'-dithiobis-(2-nitrobenzoic acid) |
| DTNP | bis(5-nitro-2-pyridyl) disulfide |
| EB | Evans blue |
| EE | early endosome |
| EGFP | enhanced green fluorescent protein |
| ElF2A | eukaryotic translation initiation factor 2α |
| EM | electron microscopy |

| | |
|---|---|
| ER | endoplasmic reticulum |
| ESCRT | endosomal sorting complex required for transport |
| GAA | α-glucosidase |
| GAS | gastrocnemius |
| GBA | β-glucocerebrosidase |
| GPN | gly-phe β-naphthylamide crystalline |
| GSK | glycogen synthase kinase |
| HD | Huntington's disease |
| HE | heamotoxylin and eosin |
| HEK | human embryonic kidney |
| HIF | hypoxia-inducible factor |
| HNE | hydroxynonenal |
| KO | knockout |
| LAMP | lysosome-associated membrane protein |
| LC3 | microtubule-associated protein light chain 3 |
| LCD | lysosomal cell death |
| LE | late endosome |
| LEL | late endosome-lysosome |
| LGMD | limb-girdle muscular dystrophy |
| LSD | lysosomal storage disease |
| LY | lysosome |
| MCK | muscle creatine kinase |
| MD | muscular dystrophy |
| MG53 | mitsigumin-53 |
| MITF | melanocyte inducing transcription factor |
| ML-IV | mucolipidosis type IV |
| ML-SA | mucolipin synthetic agonist |
| ML-SI | mucolipin synthetic inhibitor |
| mLST8 | mammalian lethal with SEC13 protein |
| MPS | mucopolysaccharidosis |
| MSC | mechanosensitive channels |
| MSD | multiple sulfatase deficiency |
| mTORC | mechanistic target of rapamycin complex |
| MVB | multivesicular body |
| NAC | N-acetylcysteine |
| NCL | neuronal ceroid lipofuscinoses |
| NEU1 | neuraminidase |
| NO | nitric oxide |
| NOX | NADPH oxidase |
| NPC | Niemann-Pick disease type C |
| PD | Parkinson's disease |
| PI | propidium iodide |
| $PI(3,5)P_2$ | phosphatidylinositol 3,5-biphosphate |
| $PI(4,5)P_2$ | phosphatidylinositol 4,5-biphosphate |
| PINK1 | PTEN-induced putative kinase protein 1 |

| | |
|---|---|
| PKC | protein kinase C |
| RAPTOR | regulatory-associated protein of mTOR |
| RFP | red fluorescent protein |
| ROS | reactive oxygen species |
| SBMA | spinobulbar muscular dystrophy |
| SERCA | sarcoplasmic reticulum $Ca^{2+}$-ATPase |
| SIM | structured illumination microscopy |
| SLO | streptolysin O |
| SNAP | S-nitroso-N-acetylpenicillamine |
| SNAP23 | synaptosome-associated protein of 23 kDa |
| SNARE | soluble NSF attachment protein receptor |
| SR | sarcoplasmic reticulum |
| Syt7 | synaptotagmin VII |
| TA | tibialis anterior |
| TBHP | tert-butyl hydroperoxide |
| TFEB | transcription factor EB |
| TGN | trans-Golgi network |
| TIRF | total internal reflection fluorescence |
| TPC | two pore channel |
| TRPML/ML | transient receptor potential mucolipin |
| TRPV2 | transient receptor potential vanilloid 2 |
| TV | tubulovesicle |
| VAMP7 | vesicle-associated protein 7 |
| v-ATPase | vacuolar-ATPase |
| WT | wildtype |
| XEMA | X-linked myopathy with excess autophagy |

## ABSTRACT

Not only as the degradation center of the cell, the lysosome has recently been demonstrated to sense and respond to various cellular stresses. Failures of this lysosomal adaptation process to environmental and cellular cues are linked to many diseases. Transient receptor potential mucolipin 1 (TRPML1 or ML1) is the principle $Ca^{2+}$ channel localized to lysosomes. Lysosomal $Ca^{2+}$ release is known to regulate various aspects of lysosomal function, including membrane trafficking, fusion, fission, and lysosomal exocytosis. As an important signal in the cell, lysosomal $Ca^{2+}$ release through ML1 has recently been suggested to act as a trigger for activation of transcription factor (TF)EB. Upon translocating into the nucleus, TFEB upregulates a set of autophagic and lysosomal genes, boosting lysosomal biogenesis and function. Besides, overexpression of TFEB has been shown to activate autophagy and lysosomal exocytosis to promote cellular clearance and ameliorate pathologies in a wide range of disease models. Therefore, ML1, lysosomal $Ca^{2+}$ release, and TFEB together form a pathway to regulate lysosome function under both physiological and pathological conditions. In this dissertation work, I am trying to answer two questions: 1) What is the endogenous cue that activates the ML1-TFEB pathway and its physiological significance (Chapter II); 2) Can activation of ML1 *in vivo*, especially through small molecule agonists, be sufficient to activate TFEB and lysosomal exocytosis, thus ameliorating muscular dystrophy (Chapter III & IV).

Reactive oxygen species (ROS) is an important signal regulating many cellular processes.

We found that ML1 channels can be directly and specifically activated by oxidants and endogenous mitochondria-originated ROS, mediating lysosomal $Ca^{2+}$ release and TFEB nuclear translocation. Our data also showed that ML1 activity is required for ROS-induced autophagosome formation and clearance of damaged mitochondria. Together, our data suggest that the ML1-TFEB mechanism is activated by physiological levels of ROS, initiating autophagy to clean damaged mitochondria and ROS.

Duchenne muscular dystrophy (DMD) is an inherited muscle disease caused by impairment of sarcolemmal repair. Lysosomal exocytosis is an important mechanism that the cell utilizes to repair damaged plasma membrane. ML1 and lysosomal $Ca^{2+}$ release are required for lysosomal exocytosis, and loss of ML1 function causes muscular dystrophy (MD) in both human and mouse. Here, by utilizing genetical and pharmacological tools, we found that activation of ML1 *in vivo* ameliorated all pathological hallmarks of MD mice, including acute necrosis, progressive fibrosis, central-nucleated fibers, reduced muscle force and compromised exercise ability. Sarcolemmal permeability, assayed by serum creatine kinase (CK) release and Evan's blue dye, was also improved upon ML1 activation. Additionally, TFEB was activated by ML1 overexpression and agonists, correcting lysosomal insufficiency seen in MD mice. Finally, we discovered that ML1 agonists activate TFEB and lysosomal biogenesis *in vitro*, preventing human DMD myoblasts from cell death. Taken together, our data demonstrated that ML1 and lysosomal exocytosis can be a potential therapeutic target for treating DMD.

# CHAPTER I

# Introduction

## 1 Overview of the lysosome

### 1.1 Lysosomal physiology

Lysosomes are the primary catabolic organelles in eukaryotic cells. Containing more than 60 different types of hydrolases, lysosomes degrade biomolecules from endocytic and autophagic pathways (Xu and Ren, 2015). Lysosomes also have ~50 membrane proteins including channels, transporters and other regulatory proteins that maintain lysosomal acidification, membrane integrity, ion and nutrient homeostasis, and membrane trafficking (Saftig and Klumperman, 2009). In addition to be an endpoint of cellular degradation pathways, recent studies revealed much more active roles of lysosomes in nutrient sensing, adaptation to multiple cellular cues, plasma membrane repair, cell signaling, membrane trafficking and cell death (Xu and Ren, 2015). Failure of any of these major functions, often caused by mutations in lysosomal proteins, leads to lysosomal storage diseases (LSDs) (Parenti et al., 2015). In this part of introduction, I will discuss about lysosomal contents and function, specifically on autophagy, lysosomal exocytosis, nutrient sensing and lysosomal adaptation.

#### 1.1.1 Lysosomal contents

##### 1.1.1.1 Lysosomal substrate

As the degradation center of the cell, lysosomes receive cargoes from endocytic and autophagic pathways from outside and inside of the cell (Xu and Ren, 2015). Endocytic pathway internalizes fluid, solutes, macromolecules, particles and plasma membrane components via endosomes (Huotari and Helenius, 2011). In specialized cell types, endocytic cargo can also include nutrients, pathogens and cell debris (Huotari and Helenius, 2011). Autophagic cargoes are mainly from the cytosolic components and organelles (Mizushima and Komatsu, 2011), as will be discussed in detail later.

#### 1.1.1.2 Lysosomal enzymes

Lysosomal hydrolases are the major components that degrade substrates. More than 60 different types of hydrolases have been identified in lysosomes including lipase, proteases and glycosidases (Xu and Ren, 2015). Their activity is tightly regulated by lysosomal ion homeostasis and membrane proteins (De Duve, 2005; Saftig and Klumperman, 2009). Catabolites from degradation are then transported out of lysosomes via membrane proteins or membrane trafficking pathways for recycling (Ruivo et al., 2009).

#### 1.1.1.3 Lysosomal membrane proteins

There are ~50 lysosomal membrane proteins identified, with more still being revealed (Lubke et al., 2009; Schroder et al., 2007; Xu and Ren, 2015). These proteins mediate a wide range of function including lysosomal biogenesis, acidification, membrane integrity, transport of ions and catabolites, regulation of fusion and fission events (Schwake et al., 2013). For example, highly glycosylated LAMPs (LAMP1 and LAMP2) are the most abundant membrane proteins in lysosomes (Ruivo et al., 2009). Deficiency of LAMP2 caused vacuolar myopathy in cardiac and skeletal muscles (Danon disease) and the observation was recapitulated in knockout mice (Nishino et al., 2000; Tanaka et al., 2000). Accumulated autophagosomes and cholesterol were seen in mice

lacking LAMP2 or both LAMP1 and LAMP2, likely due to failure of autophagosome-lysosome fusion (Eskelinen et al., 2004; Tanaka et al., 2000).

As another major component of lysosomal membrane proteins, transport proteins are working actively to maintain nutrient and ion homeostasis. These transport proteins consist of transporters that export catabolites from lysosomes and channels/transporters permeable to inorganic ions. Although lysosomes serve as a center for recycling, little do we know about lysosomal catabolites exporters, and most of the known exporters are linked to human diseases (Xu and Ren, 2015). For example, loss of function of cystinosin, a protein that exports cysteine in a $H^+$-dependent way, leads to lysosomal accumulation of cysteine (cystinosis) (Kalatzis et al., 2001). Niemann-Pick disease type C is caused by mutations in NPC1, a cholesterol transporter on lysosomes (Lloyd-Evans et al., 2008). Apparently, more work needs to be done to characterize new lysosomal transporters and their regulatory machineries. Besides, lysosomal catabolites and their exporters play important roles in lysosomal nutrient sensing, as will be discussed later.

Lysosomal ion channels and transporters maintain ion gradient across the membrane and luminal ion homeostasis to regulate activity of hydrolases and exporters, as well as membrane trafficking (Xu and Ren, 2015). Proton pump vacuolar-ATPase (v-ATPase) maintains lysosomes at acidic pH (~4.6) (Ishida et al., 2013; Mindell, 2012). This acidic lumen provides environment for enzymes and catabolites exporters to work properly (Ruivo et al., 2009). It is also required for membrane trafficking processes such as autophagosome-lysosome fusion (Klionsky et al., 2012). Besides, lysosomal $Ca^{2+}$ release triggers various responses such as lysosome and lysosome-related organelle biogenesis, fusion, fission, vesicle transport, lysosomal exocytosis, and plasma membrane repair (Lloyd-Evans et al., 2010). Lysosomal $Ca^{2+}$ gradient (lumen ~0.5 mM versus cytosol ~100 nM) is thought to be maintained by an unidentified $Ca^{2+}/H^+$ exchanger (Yang et al.,

2019). The principle lysosomal $Ca^{2+}$ releasing channel is believed to be transient receptor mucolipin 1 (ML1) (Dong et al., 2008), which will be discussed in section 2.

### 1.1.2 Lysosomal function

#### 1.1.2.1 Lysosomal trafficking

Lysosomes are dynamic organelles that undergo active membrane trafficking processes (Saftig and Klumperman, 2009) (**Fig. 1.1**). Lysosomes receive cargoes from endocytic and autophagic pathways for degradation. Output pathways of lysosomes include exocytosis, reformation and retrograde trafficking back to trans-Golgi network (TGN) (Xu and Ren, 2015). These processes are essential for membrane repair, lysosomal content exocytosis, lysosomal biogenesis, and reuse of lysosomal lipids and proteins (De Duve, 2005). Here, I will mainly discuss about autophagy and lysosomal exocytosis.

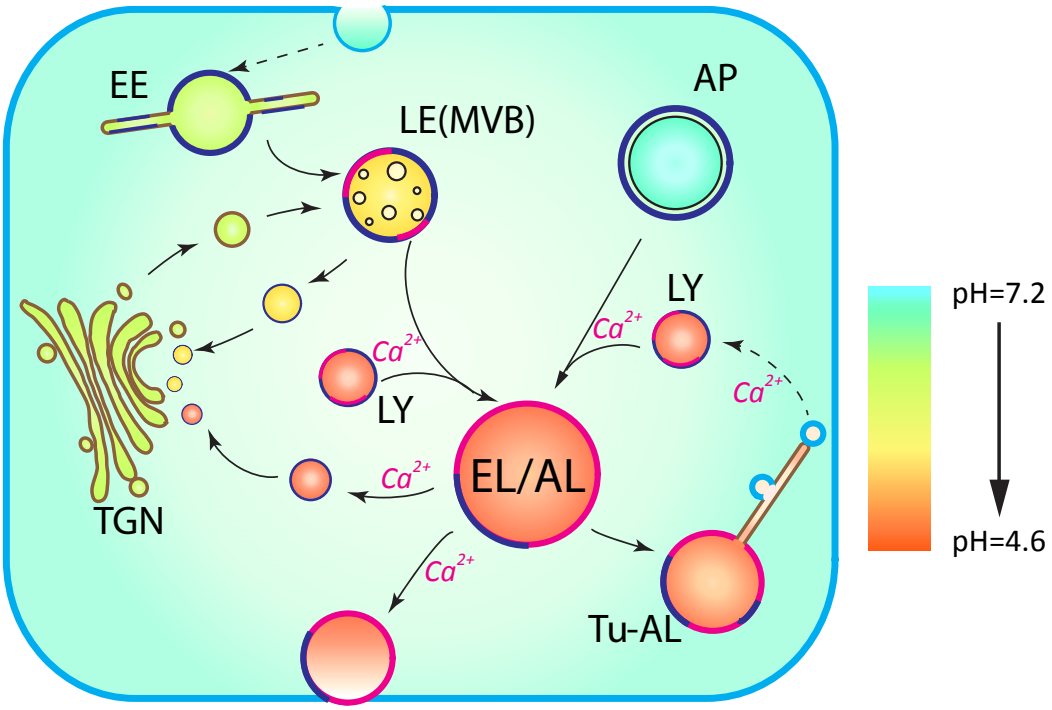


**Figure 1.1 Lysosomal trafficking pathways.** Lysosomes receive inputs from endosomal and autophagic pathways. Output trafficking pathways include lysosomal reformation/fission,

lysosomal exocytosis and retrograde trafficking to trans-Golgi network. Most of these trafficking events require lysosomal $Ca^{2+}$ release. EE, early endosome; LE, late endosome; MVB, multivesicular bodies; AP, autophagosome; LY, lysosome; EL, endolysosome; AL, autolysosome; TGN, trans-Golgi network. Figure is modified from Fig. 1 in ref. (Xu and Ren, 2015), courtesy to Dr. Xinran Li from Xu lab.

#### 1.1.2.1.1 Lysosomal input pathways: endocytosis and autophagy

##### 1.1.2.1.1.1 Endocytosis

During endocytosis, extracellular and plasma membrane components are wrapped by invaginated plasma membrane to form vesicles (Huotari and Helenius, 2011). The endocytic vesicles undergo maturation process to finally become late endosomes (LE) (Huotari and Helenius, 2011). Most of these LEs show multivesicular morphology with intralumenal vesicles, are thus named as multivesicular bodies (MVB) (Huotari and Helenius, 2011). LEs/MVBs then fused with lysosomes to become endolysosomes (EL) (Huotari and Helenius, 2011).

##### 1.1.2.1.1.2 Autophagy

###### 1.1.2.1.1.2.1 Basics of autophagy

Autophagy is an evolutionarily conserved self-eating process (Galluzzi et al., 2014). In general, autophagy is a pro-survival machinery that the cell has adopted in response to environmental cues (Kroemer and Levine, 2008). There are three types of autophagy: macroautophagy, microautophagy and chaperone-mediated autophagy (Galluzzi et al., 2014). Among them, macroautophagy (hereafter referred to as autophagy) is relatively better understood, and it differs from the other two types by the formation of double-membrane autophagosomes. In microautophagy and chaperone-mediated autophagy, cargoes are directly transported into the lysosome lumen for degradation (Galluzzi et al., 2014). In macroautophagy, there are non-selective and selective autophagy (Youle and Narendra, 2011). Non-selective autophagy is often triggered

during nutrient depletion to provide nutrients for cell survival. In contrast, selective autophagy degrades specific types of cargo, usually damaged organelles for quality control purpose (Youle and Narendra, 2011). Examples of selective autophagy include mitophagy (mitochondria), ERphagy (ER), and lysophagy (lysosome). Through genetic screen in yeast, autophagy genes (ATGs) were identified in 1990s, allowing findings of molecular pathways of autophagy initiation (Klionsky et al., 2012; Klionsky et al., 2003).

Initial steps of autophagy include vesicle nucleation and elongation (Hurley and Young, 2017). In yeast, autophagy is initiated from phagophore assembly site (PAS), while in mammals, it is from ER subdomains enriched with PI(3)P (phosphatidylinositol 3-phsophate). Two protein complexes are essential in vesicle nucleation: the ATG1/ULK1 complex and the class III PI3K complex I. Other ATG proteins are then recruited to mediate vesicle elongation. After autophagosomes (AP) are formed, they fuse with lysosomes to become autolysosomes (AL) (**Fig. 1.1)**.

Among all the types of selective autophagy, mitophagy is the best-studied type (Youle and Narendra, 2011). The machinery for autophagosome formation in mitophagy is very similar to those associated with non-selective autophagy mentioned above (Youle and Narendra, 2011). The selectivity of damaged mitochondria is thought to be mediated by PINK1 (PTEN-induced putative kinase protein 1) and E3 ubiquitin ligase Parkin (Youle and Narendra, 2011). When mitochondria are damaged and mitochondrial membrane potential is depolarized, PINK1 quickly accumulates and recruits Parkin to the damaged mitochondria (Youle and Narendra, 2011). Parkin then ubiquitylates mitochondrial proteins and the damaged mitochondria are recognized as cargo for autophagy degradation (Youle and Narendra, 2011).

**1.1.2.1.1.2.2 Monitoring autophagy**

A variety of methods have been developed to monitor autophagy in cultured cells and *in vivo* (Klionsky et al., 2012). ATG8/LC3 is the most commonly used autophagy marker, which is lipidated and recruited to autophagosomes during autophagosome formation and caused a band shift when measuring with western blot. Fluorescence-labeled LC3 can be used for direct imaging of autophagosomes (Mizushima et al., 2004). Furthermore, electron-microscopy is also widely used to monitor double-membrane autophagosomes.

**1.1.2.1.1.2.3 Regulation of autophagy**

As an important stress-response pathway in the cell, the level of autophagy is adjusted according to a variety of stress conditions. Nutrient depletion, energy status, hypoxia and oxidative stress, pathogen invasion, cancer-related genotoxicity can all regulate autophagy (Murrow and Debnath, 2013). At the molecular level, different sensors and respective signaling pathways are involved in autophagy regulation in response to different types of stress. AMPK (AMP activated protein kinase) is an important positive regulator of autophagy (Kim et al., 2011). Being a key energy sensor regulating cell metabolism, AMPK directly phosphorylates ATG1/ULK1 to promote autophagy under glucose starvation (Kim et al., 2011). One of the key negative regulators of autophagy is the mTOR (mechanistic target of rapamycin) kinase, which will be discussed in detail later. Other regulators include ElF2A (eukaryotic translation initiation factor 2α) in ER stress, HIF-1 (hypoxia-inducible factor 1) in hypoxia, and p53 in DNA damage (Galluzzi et al., 2014; Murrow and Debnath, 2013).

**1.1.2.1.1.2.4 Physiological significance of autophagy**

**1.1.2.1.1.2.4.1 Stress response**

Autophagy is an essential pro-survival pathway in response to a wide range of cellular stress (Murrow and Debnath, 2013). During starvation, autophagy is upregulated in almost all

tissues of mice, except brain (Mizushima et al., 2004). Genetic ablation of autophagy essential genes *Atg5* or *Atg7* in mice caused neonatal death, possibly due to nutrient depletion during neonatal stage (Komatsu et al., 2005; Kuma et al., 2004). In the cultured cells, knocking down of Atg7 or treatment with autophagy inhibitor 3-MA resulted in cell death upon growth factor deprivation (Murrow and Debnath, 2013). Hence, multiple pieces of evidence suggest that autophagy is an important mechanism for cellular stress response.

**1.1.2.1.1.2.4.2 Quality control**

Despite its roles in stress-response, basal level of autophagy is required to clean damaged proteins and organelles. Tissue-specific conditional knockout of *Atg5* or *Atg7* in mice showed accumulation of abnormal mitochondria, ER and Golgi in liver, muscles and pancreatic β cells, accompanied with ubiquitin-positive protein aggregation (Ebato et al., 2008; Komatsu et al., 2005; Masiero et al., 2009; Nakai et al., 2007). Collectively, these studies demonstrate that constitutive autophagy is essential for quality control in cells.

**1.1.2.1.1.2.4.3 Cell death**

Intriguingly, autophagy has been linked to cell death pathways by the emergence of the concept, autophagic cell death (ACD) (Kroemer and Levine, 2008). Also known as type II cell death, ACD is described by the ultrastructural criteria that large-scale autophagic vacuolation was found in the cytoplasm (Kroemer and Levine, 2008). Although there were studies accusing autophagy is guilty, at least partially, in killing the cell, more seemed to find it merely an innocent janitor who is helping to clean up the mess and accidentally spotted at the murder scene (Kroemer and Levine, 2008; Levine and Yuan, 2005). Although the roles of autophagy in cell death are still controversial, autophagy seems to be mostly a pro-survival machinery to help the cell recover

when it encounters stress. However, if the stress continues, cellular damage accumulates and the level of autophagy goes too high, cell death pathway may be triggered to minimize the damage.

#### 1.1.2.1.1.2.5 Autophagy defects are linked to pathology

Mutations of multiple genes regulating autophagy are linked to human diseases (Murrow and Debnath, 2013). Mutations of autophagy core component Atg16L1 are linked to Crohn's disease characterized by inflammatory digestive tract, suggesting that autophagy can promote immune response for bacterial clearance (Fritz et al., 2011). Mutations of mitophagy adaptors PINK1 and Parkin are associated with Parkinson's disease (PD), a neurodegenerative disorder (Kitada et al., 1998; Valente et al., 2004). Failure in clearance of damaged mitochondria and accumulation of deletions of mitochondrial DNA during aging are linked to PD (Youle and Narendra, 2011). It is believed that defects of mitochondrial clearance in PINK1- and Parkin-deficient individuals may be a mechanism underlying pathogenesis of the disease (Youle and Narendra, 2011).

### 1.1.2.1.2 Lysosomal output pathways: exocytosis, reformation and retrograde trafficking

#### 1.1.2.1.2.1 Lysosomal exocytosis

##### 1.1.2.1.2.1.1 Basics of lysosomal exocytosis

Lysosomal exocytosis belongs to a "unconventional secretory pathway" describing fusion between autophagosomes, early endosomes, autolysosomes, lysosomes, and MVB, with plasma membrane (Samie and Xu, 2014) (**Fig. 1.1**). In general, the purpose of lysosomal exocytosis is to provide either its membrane or contents (Samie and Xu, 2014). Lysosomal exocytosis was first observed in fibroblasts and epithelial cells by Norma Andrews group, but now we know it is present in all cell types (Rodriguez et al., 1997; Samie and Xu, 2014). As discussed below, machinery regulating lysosome docking, membrane fusion and general pool of lysosomes all play

roles in this process. Lysosomal exocytosis has been linked to a variety of physiological and pathological conditions such as cellular clearance, cell migration, phagocytosis, membrane repair, pathogen defense and neurite growth (Samie and Xu, 2014).

#### 1.1.2.1.2.1.2 Measuring lysosomal exocytosis

Several assays have been developed to measure lysosomal exocytosis *in vitro* (Samie and Xu, 2014). Presence of lysosomal membrane protein such as LAMP1 on plasma membrane has been widely used to measure lysosomal exocytosis (Samie and Xu, 2014). Antibodies against luminal epitopes of LAMP1 are used for staining or flow cytometry to determine LAMP1 proteins on plasma membrane (Andrews, 2017). Upon exocytosis, lysosomal enzymes are secreted into extracellular space. Lysosome-specific enzyme level and activity in culture medium are also used to represent lysosomal exocytosis (Rodriguez et al., 1997). Besides, imaging methods such as TIRF (total internal reflection fluorescent microscopy) detect only sub-plasma membrane biological events. By using fluorescent-labeled lysosomal protein, TIRF has been used to monitor lysosomal exocytosis (Jaiswal et al., 2004).

#### 1.1.2.1.2.1.3 Molecular machineries and regulators of lysosomal exocytosis

##### 1.1.2.1.2.1.3.1 Cytoskeleton and motor proteins

Cytoskeleton and motor proteins are required in lysosomal transport to plasma membrane. While actin filaments mediate short-range of lysosomal trafficking, long-range of movements are more microtubule-based (Luzio et al., 2007b). Manipulation of microtubule-associated motor proteins kinesin and dynein also changes lysosomal mobility and distribution in the cell (Li et al., 2016b; Mrakovic et al., 2012). However, mechanisms regulating lysosomal trafficking to plasma membrane during lysosomal exocytosis, especially under different environmental cues, are largely unknown.

#### 1.1.2.1.2.1.3.2 SNAREs

Docking and fusion between lysosomes and plasma membrane has been found very similar to synaptic vesicle release. SNARE (soluble *N*-ethylmaleimide-sensitive factor-attachment protein receptors) complexes, which initiate exocytosis of synaptic vesicles, dock lysosomes to plasma membrane (Jahn and Scheller, 2006). During exocytosis, VAMP7 (vesicle-associated protein 7), syntaxin-4 and SNAP23 (synaptosome-associated protein of 23 kDa) together form a trans-SNARE complex and pull lysosomes and plasma membrane closer to each other to initiate fusion (Rao et al., 2004).

#### 1.1.2.1.2.1.3.3 $Ca^{2+}$

Fusion between lysosomes and plasma membrane is triggered by a local rise of intracellular $Ca^{2+}$ level (Reddy et al., 2001; Rodriguez et al., 1997) (**Fig. 1.2**). In synaptic vesicle release, a steep $Ca^{2+}$ increase is caused by opening of voltage-gated $Ca^{2+}$ channels at the presynaptic membrane upon membrane potential change (Sudhof, 2013). Increase of intracellular $Ca^{2+}$, caused by $Ca^{2+}$ ionophore or membrane damage, results in increased secretion of lysosomal enzymes and fusion between lysosomes and plasma membrane (Reddy et al., 2001; Rodriguez et al., 1997).

However, the source of $Ca^{2+}$ increase during lysosomal exocytosis is more complicated (Cheng et al., 2015). Upon membrane disruption, influx of $Ca^{2+}$ from extracellular space is believed to be important for triggering lysosomal exocytosis (Reddy et al., 2001). But the role of lysosomal $Ca^{2+}$ store in lysosomal exocytosis remains elusive until recently. Since the predicted local $Ca^{2+}$ concentration for lysosomal exocytosis to happen is 1-5 μM, the ~500 μM lysosomal $Ca^{2+}$ concentration should be enough to provide $Ca^{2+}$ (Martinez et al., 2000). Besides, in a cell-free vesicle assay, $Ca^{2+}$ chelator BAPTA was able to inhibit fusion between late endosomes and lysosomes, while another chelator EGTA cannot. Since BAPTA binds to $Ca^{2+}$ 100 times faster

than EGTA, this study suggests that the $Ca^{2+}$ source is very close to the fusion spot. In other words, lysosomes are most likely providing $Ca^{2+}$ for their own fusion events (Pryor et al., 2000). Together these data suggest the roles of local lysosomal $Ca^{2+}$ source in lysosomal exocytosis may have been underestimated.

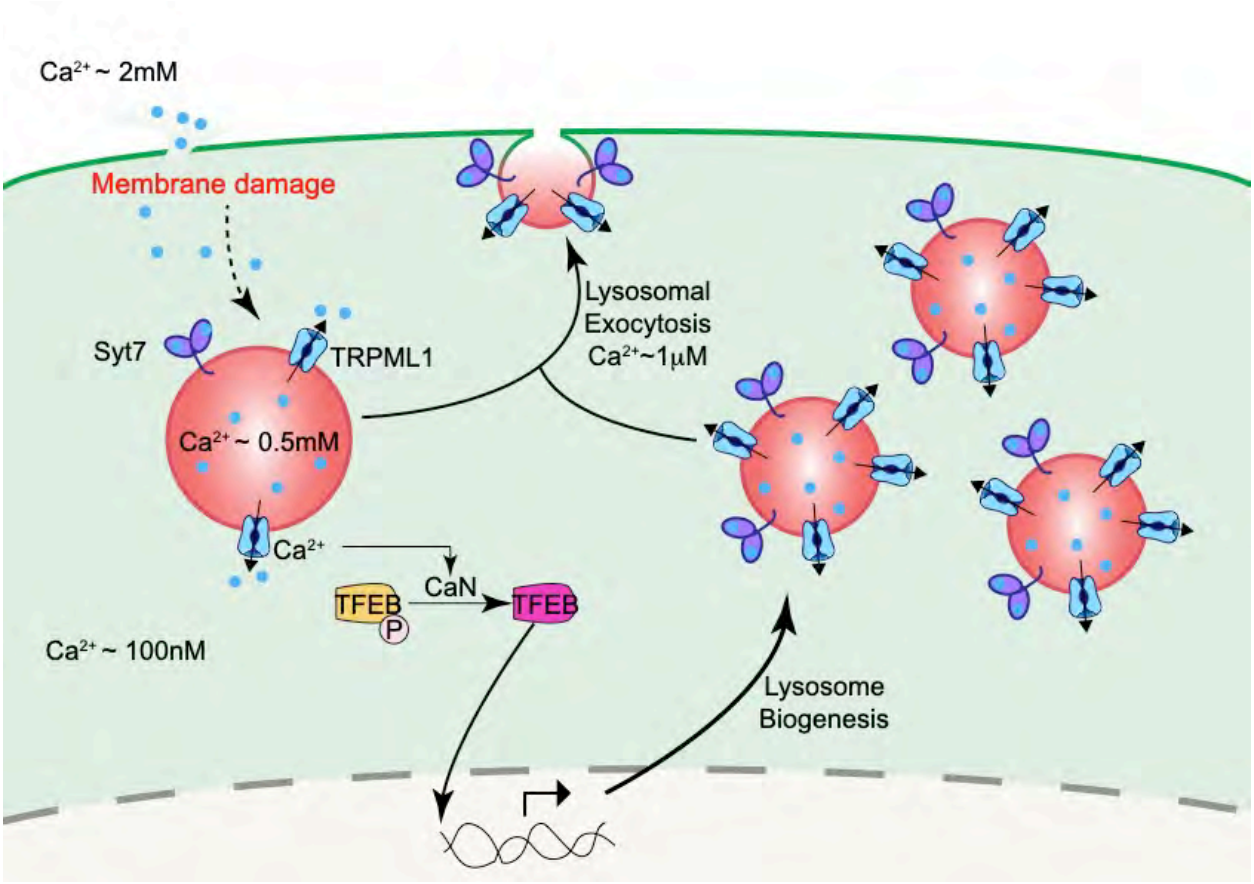


**Figure 1.2 $Ca^{2+}$ in lysosomal exocytosis.** Different $Ca^{2+}$ stores, channels and sensors are involved in multiple steps regulating lysosomal exocytosis. Extracellular $Ca^{2+}$ is required for lysosomal exocytosis. $Ca^{2+}$ release from lysosomal ML1 promotes lysosomal trafficking to plasma membrane, as well as activates TFEB and increases releasable lysosome pool. Lysosomal $Ca^{2+}$ sensor synaptotagmin 7 (syt7) mediates docking of lysosomes to plasma membrane.

### 1.1.2.1.2.1.3.4 Synaptotagmin VII: the $Ca^{2+}$ sensor

Synaptotagmin VII (syt7) has emerged to be the most important $Ca^{2+}$ sensor in lysosomal exocytosis. It belongs to the synaptotagmin family containing two $Ca^{2+}$-binding (C2) domains.

Synaptotagmin I, the most studied family member, is believed as a $Ca^{2+}$ sensor in synaptic vesicle exocytosis. Localized predominantly on lysosomes, syt7 is required for lysosomal exocytosis, since artificially decrease its activity by dominant negative syt7 mutants diminished lysosomal exocytosis (Martinez et al., 2000). Knockout of syt7 in mice macrophages also impaired lysosomal exocytosis (Czibener et al., 2006). However, the depletion of syt7 did not completely abolish lysosomal exocytosis, suggesting presence of other $Ca^{2+}$ sensors during lysosomal exocytosis (Chakrabarti et al., 2003).

**1.1.2.1.2.1.3.5 Releasable lysosome pool**

Releasable lysosome pools also affect lysosomal exocytosis. Interestingly, evidence has suggested that within 2 minutes of $Ca^{2+}$ ionophore stimulus, lysosomes pre-docked to the membrane proximal region readily fuse with plasma membrane, and lysosomal recruitment and docking are not required in this acute lysosomal exocytosis (Jaiswal et al., 2002). In this scenario, membrane proximal, acutely-releasable lysosomal pool seems to vary among cell types. Secretory cells such as macrophages have up to 50% of lysosomal enzymes released within minutes (Samie et al., 2013), while non-secretory cells like fibroblasts only have around 10% (Rodriguez et al., 1997). In LSDs, lysosomes are heavily accumulated in the peri-nuclear region and exocytosis is impaired (Li et al., 2016b; Samie et al., 2013). These lead to outstanding questions in the field that whether there are subpopulations of lysosomes located in different parts of the cell to serve different purposes, and how their dynamics are controlled under pathophysiological conditions.

**1.1.2.1.2.1.3.6 Neuraminidase 1**

Lysosomal enzyme neuraminidase 1 (NEU1) arose to be a negative regulator of lysosomal exocytosis, though with unclear mechanisms. As a lysosomal sialidase, loss-of-function mutations of NEU1 cause sialidosis or mucolipidosis type I, an LSD characterized by accumulation of

carbohydrates in lysosomes. NEU1 deficiency in mice leads to accumulation of over-sialylated LAMP1 proteins and increased lysosomal exocytosis (Yogalingam et al., 2008). Moreover, NEU1-deficient mice showed loss of bone marrow retention and hearing ability, as well as muscle degeneration with significant proliferation of fibroblasts and deposition of collagen (Wu et al., 2010; Yogalingam et al., 2008; Zanoteli et al., 2010). But the links between over-sialylated LAMP1, lysosomal exocytosis and these phenotypes need to be elucidated.

**1.1.2.1.2.1.4 Physiological significance of lysosomal exocytosis**

The biological consequences for lysosomal exocytosis are 1) providing membrane; 2) secreting lysosomal contents to extracellular space (Samie and Xu, 2014). Upon membrane damage, depletion of $Ca^{2+}$ increase or syt7 results in impaired membrane repair (Chakrabarti et al., 2003; Reddy et al., 2001). Besides, lysosomal exocytosis is required in uptake of large particles in macrophages, a process needs large amount of membrane to form pseudopods to wrap the particle (Czibener et al., 2006; Samie et al., 2013). Lysosomal exocytosis has also been proposed to provide membrane for pseudopods during cell migration (Rainero and Norman, 2013).

In specified secretory cells like osteoclasts, astrocytes and immune cells, secretory lysosomes undergo exocytosis to mediate bone reabsorption, ATP release, antigen presentation and pathogen digestion, respectively (Cresswell, 1994; Dou et al., 2012; Mostov and Werb, 1997). Release of lysosomal enzymes by exocytosis can digest extracellular matrix and enable cancer progression. Inhibition of lysosomal exocytosis through interruption of SNARE-associated proteins, synaptotagmin and lysosomal fusion ability has been shown to inhibit cell migration and cancer invasion (Colvin et al., 2010; Dou et al., 2012; Liu et al., 2012; Proux-Gillardeaux et al., 2007). In a recent study, NEU1 insufficiency and increased lysosomal exocytosis were linked to cancer progression, and NEU1 levels and extent of lysosomal exocytosis in human sarcoma cells

determined their invasive potential and responsiveness to chemotherapy (Machado et al., 2015). Overall, lysosomal exocytosis is involved in multiple biological processes and pathologies.

#### 1.1.2.1.2.2 Lysosomal reformation

Lysosomes can be reformed from autolysosome and endolysosome hybrids through membrane fission (Luzio et al., 2007b; Yu et al., 2010) (**Fig. 1.1**). As it will be discussed later, this process is important in lysosomal adaptation.

#### 1.1.2.1.2.3 Lysosomal retrograde trafficking to TGN

Late endosomes and lysosomes also undergo fission to retrogradely transport free lipids to TGN (**Fig. 1.1)**. Moreover, mannose-6-phosphate receptors, which are important for lysosomal enzyme targeting, are retrogradely transported back to TGN for reuse.

### 1.1.2.2 Lysosomes as nutrient sensors

Recent studies have revealed the lysosome as an active player in sensing and regulating cellular nutrient status. Lysosomes serve as a platform to hold molecular machineries for nutrient sensing (Xu and Ren, 2015). The following discussion will be focused on mTORC1, the best studied lysosomal machinery in nutrient sensing.

#### 1.1.2.2.1 mTORC1 as the nutrient sensing node on lysosomes

##### 1.1.2.2.1.1 Basics of mTORC1

Protein complex mTORC1 and its regulatory machineries are the most important nutrient sensors localized on lysosomes. Responding to multiple cellular signals such as growth factors, nutrient and energy status, activation of mTORC1 will ultimately cause increased protein synthesis and cell growth, as well as inhibition of the autophagic-lysosomal pathway (Efeyan et al., 2012; Galluzzi et al., 2014). mTORC1 is composed of the kinase mTOR and regulatory proteins RAPTOR (regulatory-associated protein of mTOR), DEPTOR (DEP domain-containing mTOR-

interacting protein) and mLST8 (mammalian lethal with SEC13 protein) (Efeyan et al., 2012). Subcellular localization of mTORC1 is regulated by nutrient status, as discussed below.

**1.1.2.2.1.2 Regulation machineries of mTORC1 in lysosomal nutrient sensing**

**1.1.2.2.1.2.1 Regulation machineries of mTORC1 in amino acid sensing**

Following its discovery, mTORC1 was found to be suppressed potently by amino acid withdrawal from the culture media (Kroemer et al., 2010). But the link between the kinase mTORC1 and cellular amino acids was missing until regulatory machineries for mTORC1 were revealed by a series of studies. Sancak et al. found that the mTOR kinase is diffused in cytosol upon starvation and addition of amino acids would trigger them go to lysosomes (Sancak et al., 2008). The switch between different subcellular localization is apparently important for mTORC1 function since by fixing mTORC1 either in lysosomes or cytosol (through manipulating its docking machinery), the pathway became dispensable of amino acids levels (Sancak et al., 2010). These findings led to following works identified a lysosomal inside-out amino acid sensing mechanism regulating mTORC1. So far to our knowledge, this mechanism contains 3 parts: 1) Amino acid sensing machinery involves lysosomal arginine transporter SLC38A9 and v-ATPase. SLC38A9 serves as a "sensor" that directly interacts with the catabolites from lysosomes (Rebsamen et al., 2015; Wang et al., 2015a). V-ATPase provides acidic environment enabling amino acid transport across lysosomes, as well as physically interacts with the lysosomal docking machinery of mTORC1 (Zoncu et al., 2011); 2) Lysosomal docking machinery consists of a group of small GTPases, the Rags, and a Rag-binding protein complex Ragulator. The nucleotide loading of Rags can be regulated by amino acids and upon activation Rags bind with mTORC1. The Ragulator complex primarily resides on lysosomes and docks mTORC1 to lysosomes through Rags (Sancak et al., 2010; Sancak et al., 2008); 3) Kinase activation component, specifically another small

GTPase Rheb, localizes to the lysosomes and directly activates the kinase mTOR (Sancak et al., 2010). Taken together, mTORC1 is regulated by cellular amino acid levels via machineries localized on lysosomes.

**1.1.2.2.1.2.2 Regulation machineries of mTORC1 in other nutrient sensing**

Several recent studies have revealed the role of mTORC1 in sensing other types of nutrients. For example, putative lysosomal sugar transporter Spinster is thought to regulate mTOR activity in response to glucose level (Rong et al., 2011). A recent study also found that lysosomal cholesterol activates mTORC1 via putative amino acid transporter SLC38A9 and cholesterol transporter NPC1 (Castellano et al., 2017). These findings revealed the complexity of mTORC1 in nutrient sensing.

**1.1.2.2.1.3 mTORC1 as a key regulator for autophagy initiation and lysosomal adaptation**

mTORC1 is essential for autophagy initiation during starvation. In fed cells, activated mTORC1 directly phosphorylates and inhibits ATG1/ULK1 and its interacting protein ATG13, thus suppresses autophagy (Hosokawa et al., 2009; Kim et al., 2011). mTORC1 also regulates autophagy via interaction with transcription factor EB (TFEB), as discussed later. Upon starvation, mTORC1 is inhibited and autophagy can be initiated (Efeyan et al., 2012). Constitutive active Rags activate mTORC1 independently of amino acid levels (Kim et al., 2008). Mice knocked in with constitutive active Rags have normal development, but fail to survive postnatal day 1 (Efeyan et al., 2013). This neonatal death is similar to what has been seen in mice lacking essential ATG genes (Kuma et al., 2004). Indeed, WT neonates show a drop of plasma amino acid level accompanied with mTOR inhibition, while mice knocked in with constitutive active Rags do not have mTOR inhibition or autophagy initiation (Efeyan et al., 2013). Collectively, these results suggest mTORC1 is important in autophagy initiation.

The mTORC1 regulates lysosomal adaptation through TFEB-dependent transcriptional regulation or lysosomal reformation, as discussed later.

#### 1.1.2.2.2 Other nutrient sensing machineries on lysosomes

Lysosomal ion channels also contribute to nutrient sensing. ATP-sensitive $Na^+$ channels localized on lysosomes were shown to regulate lysosomal membrane potential and physiology in response to cellular ATP levels (Cang et al., 2013).

### 1.1.2.3 Lysosomal adaptation

Number, size, and function of lysosomes are adjusted according to signals from extracellular and intracellular environment (Li et al., 2018). Lysosomal adaptation is important in maintaining cellular homeostasis under stress. Recently, TFEB was discovered as a master regulator for transcriptional regulation of autophagic and lysosomal genes. Here, I will mainly discuss about TFEB in lysosomal adaptation. Besides, lysosomal reformation is a post-translational mechanism for generating more lysosomes using fission-dependent membrane trafficking pathway.

#### 1.1.2.3.1 TFEB is the key regulator for lysosomal adaptation

##### 1.1.2.3.1.1 Basics of TFEB and CLEAR network

Transcription factor EB (TFEB) was re-identified through a series of analysis of lysosomal genes. These analyses led to the finding of the coordinated lysosomal enhancement and regulation (CLEAR) gene network, a set of genes that share a palindromic 10-base site (CLEAR site) in their promoters (Sardiello et al., 2009). A large portion of these genes are related with cellular clearance pathways, particular autophagy and lysosomes (Palmieri et al., 2011). TFEB and other three members from the MiT subfamily, MITF, TFE3 and TFEC, were known to bind to the CLEAR site and trigger target gene transcription (Sardiello et al., 2009). Among all four members, MITF

localizes in specific tissues and cell types such as melanocytes, mast cells and osteoclasts and functions during embryonic stage. TFEB, TFE3 and TFEC are more ubiquitously expressed and there is a redundancy between these family members (Settembre and Ballabio, 2014). As TFEB is the best understood member, the following discussion will mostly focus on it.

By using a combination of genomic approaches, Palmieri et al. identified 471 direct TFEB targets (Palmieri et al., 2011). Among them, 64 targets were involved in the autophagic-lysosomal pathway, including ATGs, lysosomal hydrolases and membrane proteins, and proteins regulating autophagy and lysosomal function (Palmieri et al., 2011). For example, TFEB activation was shown to enhance processing, trafficking, and activity of a destabilized glucocerebrosidase variant and a β-hexosaminidase mutant, two lysosomal enzymes associated with Gaucher disease (GD) and Tay-Sachs disease, respectively (Song et al., 2013). In addition, the ortholog of TFEB in *Drosophila* was reported to regulate components of v-ATPase, mediating lysosomal acidification, biogenesis, and membrane fusion (Bouché et al., 2016; Tognon et al., 2016). Taken together, multiple lines of evidence have suggested that TFEB regulates many aspects of lysosomal function via transcription of lysosomal genes.

Under normal conditions TFEB stays predominantly in the cytoplasm, whereas cellular stress such as starvation and lysosomal dysfunction triggers TFEB go to nucleus, mediating downstream gene transcription (Settembre et al., 2011) (**Fig. 1.3**). Phosphorylation status of TFEB regulates its localization and function: phosphorylated TFEB stays in the cytoplasm and remains inactivated, while dephosphorylated TFEB is active and translocates into the nucleus (Settembre and Ballabio, 2014). Among more than 10 phosphorylation sites have been identified in TFEB protein, serine 142 and 211 are essential in regulating TFEB activity (Settembre and Ballabio, 2014).

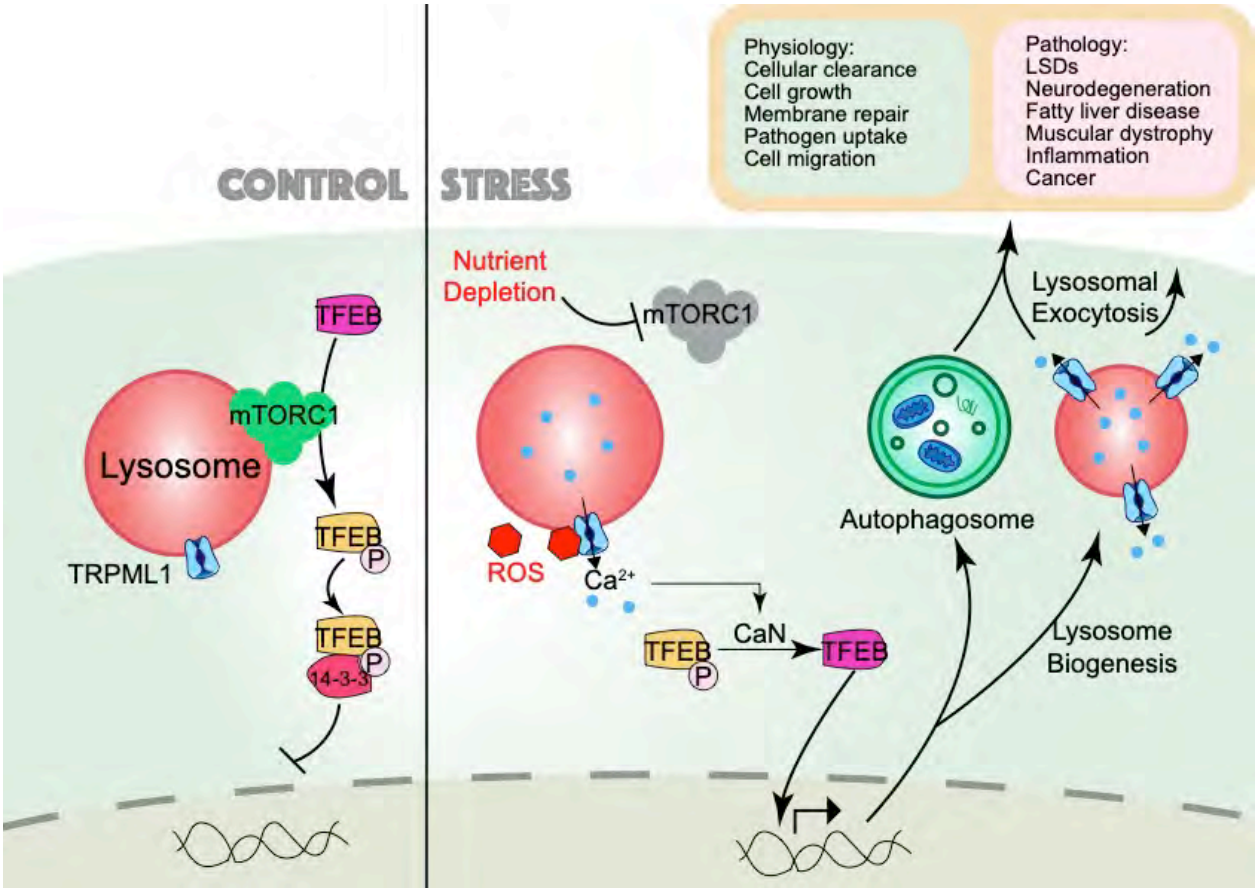


**Figure 1.3 Lysosomal adaptation machineries.** TFEB is regulated by mTOR and ML1 in response to nutrient depletion and ROS, respectively. When TFEB is activated and translocates into nucleus, autophagic and lysosomal genes are upregulated. Manipulation of ML1 and/or TFEB is involved in multiple physiological and pathological conditions. CaN, calcineurin.

#### 1.1.2.3.1.2 Regulation of TFEB

##### 1.1.2.3.1.2.1 TFEB is regulated by mTORC1

In search of TFEB regulators, mTORC1 has emerged as a key negative regulator of TFEB. Under fed condition mTORC1 is active and phosphorylates TFEB at Ser142 and Ser211 (Settembre et al., 2012). Phosphorylation of Ser211 is a recognition site for protein 14-3-3 to retain TFEB in the cytoplasm (Martina et al., 2012; Roczniak-Ferguson et al., 2012) (**Fig. 1.3**).

Interestingly, when staying in the cytoplasm, TFEB has been found both in the cytosol and lysosomes (Martina et al., 2012; Settembre et al., 2011; Settembre et al., 2012). Upon starvation, mTOR is inhibited, releasing the inhibitory effects of TFEB and triggering downstream gene transcription (Martina et al., 2012; Roczniak-Ferguson et al., 2012; Settembre et al., 2012). Working together, these two molecules form a lysosome-to-nucleus pathway to regulate multiple aspects of the lysosome upon intracellular and extracellular stimulus (Settembre and Ballabio, 2014).

**1.1.2.3.1.2.2 TFEB is regulated by lysosomal $Ca^{2+}$ release**

Recent studies found TFEB can be activated by lysosomal $Ca^{2+}$ release via $Ca^{2+}$ channel ML1 (**Fig. 1.3**). This will be discussed in the next section.

**1.1.2.3.1.2.3 Other regulators of TFEB**

TFEB responds to lysosomal stress such as drugs blocking lysosomal acidification, though the underlying molecular mechanism remains to be elucidated (Settembre et al., 2012). Besides, there are other regulators regulating TFEB phosphorylation and activity. For example, extracellular signal-regulated kinase 2 (ERK2) phosphorylates TFEB at Ser142 in response to nutrient status (Settembre et al., 2011). Recently, activation of protein kinase C (PKC) has also been shown to activate TFEB through a GSK3β-dependent signaling pathway (Li et al., 2016c). In this process, mTORC1 is not required and Ser134 and Ser138 are essential (Li et al., 2016c). This work has demonstrated another method to activate TFEB and autophagy.

**1.1.2.3.1.3 Physiological significance of TFEB in lysosomal adaptation**

**1.1.2.3.1.3.1 TFEB coordinates autophagy and lysosomal adaptation in response to nutrient status**

During nutrient depletion, increase of autophagic flux is essential for cell survival (Mizushima and Komatsu, 2011). Previous studies have been focused on the initiation step of autophagy in response to stress (Murrow and Debnath, 2013). Yet, completion of autophagy requires lysosomal function. Regulatory machineries for lysosomal adaptation during nutrient depletion remained unclear until the recent discoveries of TFEB. As the master regulator for autophagic and lysosomal genes, TFEB is activated during nutrient depletion and triggers autophagosome and lysosome biogenesis (Palmieri et al., 2011; Settembre et al., 2011). Liver specific knockout of TFEB resulted in accumulation of lipids droplets in liver when given high-fat diet, possibly due to failure of autophagy induction (Settembre et al., 2013a). Overexpression of TFEB induces autophagy both *in vitro* and *in vivo* and promote cellular clearance (Settembre et al., 2013a; Settembre et al., 2011). Other than nutrient status, TFEB also incorporates inputs from other cellular stress conditions, connecting the autophagic-lysosomal pathway to cellular adaptation to a wide range of environmental cues (Settembre and Ballabio, 2014).

**1.1.2.3.1.3.2 TFEB in lysosomal exocytosis**

Lysosomal exocytosis is another important aspect of lysosomal adaptation in response to stress like plasma membrane damage (Samie and Xu, 2014). Since acutely-releasable lysosomal pool may not always meet cellular needs, long-term regulatory machinery is necessary for cellular adaptation (Samie and Xu, 2014). TFEB, as the master regulator of lysosomal genes, triggers lysosomal biogenesis and increases total lysosomal pool in the cell (Sardiello et al., 2009). Overexpression of TFEB increases the pool of lysosomes close to the proximity of plasma membrane and induces lysosomal exocytosis (Medina et al., 2011). In Pompe disease, an LSD characterized by accumulation of enlarged autophagosomes and autolysosomes, activation of

TFEB was found to trigger docking of autolysosomes to plasma membrane (Spampanato et al., 2013). These data suggest that TFEB is critical in lysosomal exocytosis.

#### 1.1.2.3.2 Other mechanisms of lysosomal adaptation

Membrane fission-dependent lysosomal reformation is another mechanism for lysosomal adaptation (**Fig. 1.1**). After prolonged starvation, Yu et al. found that lysosome number and size recovered, accompanied by tubular structure extending from autolysosomes. These tubular structures are considered to serve as platforms for lysosomal fission events and this process is named as autophagic lysosomal reformation (ALR). In this process, mTOR is reactivated, and suppression of mTOR prevents ALR. Moreover, cathepsin inhibitors seem to abolish both mTOR reactivation and ALR, suggesting that catabolic signals from lysosomal lumen may be important for this process (Yu et al., 2010). These data demonstrated another mechanism for lysosomal biogenesis and adaptation.

## 1.2 Lysosomal pathology

Lysosomes are active players in regulating cellular clearance and adapting to environmental cues. Lysosomal dysfunction leads to pathologies (Xu and Ren, 2015). Here, I will be discussing about two types of diseases: 1) diseases directly caused by mutations of lysosomal proteins or proteins regulating lysosomal function (LSDs); 2) common diseases implicated with lysosomal dysfunction in pathogenesis. Finally, I will discuss about studies targeting TFEB to treat these diseases.

### 1.2.1 Lysosomal storage diseases (LSDs)

#### 1.2.1.1 LSDs: symptoms and causes

Lysosomal storage diseases describe a group of inherited rare diseases characterized by accumulation of lysosomal materials (Neufeld, 1991). LSDs are caused by mutations affecting

lysosomal enzymes, membrane proteins and regulators for lysosomal function (Parkinson-Lawrence et al., 2010). More than 50 lysosomal storage diseases have been identified so far (Parenti et al., 2015). Even though each individual disease is very rare, together the prevalence add up to around 1 in 8000 live births (Meikle et al., 1999). The clinical manifestations of LSDs usually involve multiple systems and organs, suggesting the fundamental roles of lysosomes in physiology. Neurological, skeletomuscular, and visceral (hepatosplenomegaly) abnormities are typical in LSDs, possibly because these organs are either susceptible to lysosomal storage or metabolically active (Parenti et al., 2015). Other organs, including kidney, blood system, heart, respiratory tracts and lungs, skin, stomach and intestines, can all be affected in LSDs (Parenti et al., 2015).

Most LSDs are caused by mutations in lysosomal enzymes, but the primary storage of undegraded cargoes often leads to secondary defects in membrane trafficking (Futerman and Van Meer, 2004). For example, the autophagic-lysosomal pathway is interrupted in many LSDs (Parenti et al., 2015). In Pompe disease, a myopathy caused by mutations in acid α-glucosidase (GAA) and glycogen storage, enlarged autophagosomes and autolysosomes are accumulated in muscles, possibly due to defects in fusion and fission (Shea and Raben, 2009). Some LSDs are also linked to lysosomal transmembrane proteins or non-lysosomal proteins regulate lysosome function. Mutations in cholesterol exporter NPC1 leads to NPC disease characterized by accumulation of lipid in lysosomes (Vanier, 2010). Mucolipidosis type II is caused by deficiency of Golgi phosphotransferase (Tiede et al., 2005). Loss-of-function of this enzyme results in mis-localization of lysosomal enzymes and lysosomal storage phenotype (Tiede et al., 2005). Taken together, lysosomal function is fine-tuned by different molecules and biological events, and defects in any step can lead to pathology.

#### 1.2.1.2 Treatment of LSDs

##### 1.2.1.2.1 Enzyme replacement therapy

Ever since the causes of LSDs were discovered, enzyme replacement therapy has been proposed and tested in many different LSDs (Parenti et al., 2015). The logic of injecting a working, recombinant protein to replace the malfunctional one is straightforward, and studies in Gaucher's disease have been encouraging (Brady, 2006). However, certain technical barriers still exist, including the ability of these big molecules to pass blood brain barrier and patients' immune responses to recombinant proteins (Parenti et al., 2015).

##### 1.2.1.2.2 Gene therapy

Gene therapy by transducing the non-mutated gene using virus seems to be most promising, especially with CRISPR Cas9 technology. In fact, clinical trials for gene therapy in a wide range of LSDs are already in progress (Parenti et al., 2015). The main caveats of gene therapy in LSDs are the transduction efficiency and gene expression level in different tissues (Parenti et al., 2015).

##### 1.2.1.2.3 Substrate reduction therapy

Substrate reduction therapy is another strategy to ameliorate the storage. For example, cyclodextrin has been found to reduce cholesterol accumulation in NPC animal models and patients through unclear mechanisms (Matsuo et al., 2013; Ward et al., 2010). However, the limitation of this strategy is certain drugs need to be found to decrease the substrate via interruption of biosynthesis or other mechanisms (Parenti et al., 2015).

### 1.2.2 Lysosome-associated diseases

Recently, it was brought to our attention that some diseases not considered to be classic LSD also showed similar storage phenotype or were implicated with lysosomal dysfunction in pathogenesis. Here, I will discuss about roles of lysosomes in these lysosome-associated diseases.

#### 1.2.2.1 Common neurodegenerative diseases

Recent studies have revealed unexpected connections between LSDs and common neurodegenerative diseases (Deng et al., 2015; Schweitzer et al., 2009). Neurodegenerative diseases are characterized by abnormal aggregation of proteins inside and outside of cells, leading to progressive neuronal death (Nixon, 2013). Interestingly, accumulation of unwanted substrate is also a hallmark for LSDs, and about two-thirds of LSD patients show neurological impairment, particular childhood neurodegeneration (Parenti et al., 2015). Several lysosomal genes have been found as risk factors for Parkinson's disease (PD) including β-glucocerebrosidase (GBA), mutations of which cause Gaucher disease (GD). Consistently, GD patients have ~20 folds higher possibility to develop PD (Deng et al., 2015; Mc Donald and Krainc, 2017). Amyloid peptides, the pathological hallmark in Alzheimer's disease (AD), are also found accumulated intracellularly in NPC cells (Nixon, 2004). Besides, impaired autophagic-lysosomal pathway has also been demonstrated in multiple neurodegenerative diseases (Nixon, 2013). Taken together, these studies suggest that lysosomes are involved in pathogenesis of common neurodegenerative diseases.

#### 1.2.2.2 Liver diseases

As the major cellular degradation pathway, autophagy has been implicated in liver physiology and diseases (Rautou et al., 2010). Autophagy is important in lipid metabolism and quality control in liver cells (Komatsu et al., 2005; Murrow and Debnath, 2013). Dysregulation of autophagy has been seen in hepatitis, fatty liver diseases and hepatocellular carcinoma (Rautou et al., 2010). Autophagy has been proposed as a potential therapeutic target for treating liver diseases (Rautou et al., 2010).

#### 1.2.2.3 Muscle diseases

Autophagy and lysosomal exocytosis are essential in regulating muscle physiology and pathology. This will be discussed in section 3.

#### 1.2.2.4 Cancer

According to our current knowledge, lysosomes have several different roles in cancer (Kirkegaard and Jäättelä, 2009). First, release of lysosomal hydrolases to extracellular space through exocytosis helps cancer cell migration (Kirkegaard and Jäättelä, 2009). Second, increased lysosomal membrane permeability and release of hydrolases to intracellular space triggers programmed cell death pathways in cancer cells, a process termed as lysosomal cell death (LCD) (Kirkegaard and Jäättelä, 2009). Third, as a major input for lysosomes, autophagy has been suggested to have controversial roles in cancer progression (Kirkegaard and Jäättelä, 2009). The roles of lysosomes in cell proliferation and migration during cancer progression still remain to be elucidated.

### 1.2.3 Targeting TFEB to treat diseases

#### 1.2.3.1 Targeting TFEB to treat LSDs

Compared with enzyme replacement or gene therapy for individual LSD, targeting TFEB is becoming increasingly attractive recently since it seems to be the one key to solve multiple diseases. By using cell lines derived from patients and murine models, TFEB overexpression has been shown to help lysosomal exocytosis and cellular clearance in multiple sulfatase deficiency (MSD), mucopolysaccharidosis type IIIA (MPS-IIIA), Batten disease, and neuronal ceroid lipofuscinoses (NCL) (Medina et al., 2011). In Pompe disease, TFEB overexpression promotes docking of accumulated enlarged autolysosomes to plasma membrane, ameliorating glycogen storage in muscles (Spampanato et al., 2013). In cystinotic kidney cells derived from patients, TFEB overexpression is able to decrease substrate storage and lysosomal number and size (Rega

et al., 2016). TFEB activation in Gaucher disease and Tay-Sachs disease also boosted lysosomal proteolysis (Song et al., 2013). Putting together, as the master regulator of lysosomal function, TFEB is a potential therapeutic target for treating LSDs.

#### 1.2.3.2 Targeting TFEB to treat common neurodegenerative diseases

Since abnormal protein storage is found in many common neurodegenerative disorders, the lysosome has long been proposed as a potential target for treatment (Lie and Nixon, 2019). Indeed, genetic and pharmacological activation of TFEB decreased aggregated α-synuclein in PD cell and mouse models through the autophagic-lysosomal pathway (Decressac et al., 2013; Kilpatrick et al., 2015). Similarly, studies in AD and Huntington's disease (HD) have also revealed that TFEB activation helps clearance of protein aggregation and improves neurological function (Polito et al., 2014; Sardiello et al., 2009; Tsunemi et al., 2012; Xiao et al., 2014). These studies have demonstrated that TFEB can be a potential therapeutic target for neurodegeneration.

#### 1.2.3.3 Targeting TFEB to treat liver diseases

As a metabolically active organ, liver requires autophagy and TFEB activity in response to stress (Komatsu et al., 2005; Settembre et al., 2013a). More importantly, liver-specific overexpression of TFEB decreased lipid accumulation in mice fed with high-fat diet (Settembre et al., 2013a). TFEB overexpression has also been shown effective in triggering autophagy and helping cellular clearance in mouse models of α1-antitrypsin deficiency, the most common genetic cause of liver disease (Pastore et al., 2013a; Pastore et al., 2013b). Overall, TFEB overexpression seems to have therapeutic effects on liver diseases caused by different triggers.

#### 1.2.3.4 Targeting TFEB to treat muscle diseases

TFEB was reported to regulate energy and glucose homeostasis in muscles during exercise (Mansueto et al., 2017). TFEB activation in spinobulbar muscular atrophy (SBMA), a

neuromuscular disorder caused by mutations in androgen receptor gene, enhanced autophagy and ameliorated aggregation of mutated proteins (Chua et al., 2013). More evidences are needed to further demonstrate TFEB's role in regulating muscle pathophysiology.

## 2 ML1 as the principle lysosomal $Ca^{2+}$ channel

Transient receptor potential mucolipin 1 (TRPML1 or ML1) is the primary $Ca^{2+}$ channel localized to lysosomes (Cheng et al., 2010). Encoded by MCOLN1 gene in human, loss-of-function of ML1 leads to mucolipidosis type IV (ML-IV) (Bach et al., 2010). Here, I will be discussing about the channel structure, properties, function, as well as its involvement in diseases.

### 2.1 TRPML family and channel structure

TRPML subfamily belongs to the TRP channel family and has 3 members, TRPML1-3 (Cheng et al., 2010). In mammals, ML1 is ubiquitously expressed, whereas expression of ML2 and ML3 are more restricted to tissues like thymus, kidney and spleen (Cheng et al., 2010). Primarily localized on endosomes and lysosomes, TRPMLs are cation channels regulating lysosomal functions (Cheng et al., 2010). Loss-of-function mutations in human ML1 lead to ML-IV, an LSD characterized by childhood neurodegeneration, muscular dystrophy, iron deficiency anemia and abnormal stomach acid secretion (Boudewyn and Walkley, 2018; Cheng et al., 2014; Dong et al., 2008; Sahoo et al., 2017). Gain-of-function mutations of mouse ML3 cause the varitint-waddler (Va) phenotype that is characterized by deafness, circling behavior and pigmentation defects (Di Palma et al., 2002).

Several recent studies have revealed high-resolution crystal and electron microscopy (EM) structures of ML1 and ML3 (Chen et al., 2017; Hirschi et al., 2017; Li et al., 2017; Schmiege et al., 2017). TRPMLs are tetrameric channels containing six transmembrane segments S1-S6

(Cheng et al., 2010) (**Fig. 1.4**). TRPML family proteins share about 75% amino acid sequence similarity, with the highest similarity being in the pore region (more than 90% sequence similarity) (Puertollano and Kiselyov, 2009). Similar to other TRP channels, ML1 S5 and S6 form the pore region (Chen et al., 2017). A large luminal linker loop between S1 and S2, which accounts for about one-third of total length, was considered to form tetramer and regulate ML1 assembly (Li et al., 2017). Several single-amino acid mutations in this region are related with ML-IV and mis-localization of the channel (Li et al., 2017). Besides, channel structures allowed deeper understanding of permeation and gating properties of ML1, as discussed below.

**2.2 Subcellular localization of ML1**

Due to the limitations of currently available ML1 antibodies, subcellular localization of ML1 was studied by overexpression of ML1 with fluorescent tags (Cheng et al., 2010). These studies have revealed ML1 to be primarily localized to LAMP1- and Rab7-positive late endosomes and lysosomes (Dong et al., 2008; Kiselyov et al., 2005). Two di-leucine motifs are considered important for ML1's lysosomal localization (Vergarajauregui and Puertollano, 2006b). One is at N-terminal and interacts with clathrin adaptors AP1/AP3 to mediate trafficking of the protein from trans-Golgi network (TGN), while the other one at C-terminus binds with AP2 and enables internalization of the channel from plasma membrane (Vergarajauregui and Puertollano, 2006a).

Our lab recently found ML1 is expressed in gastric tubulovesicles (TVs) and regulates gastric acid secretion, demonstrating ML1's role in lysosome-related organelles in specialized cell types (Sahoo et al., 2017).

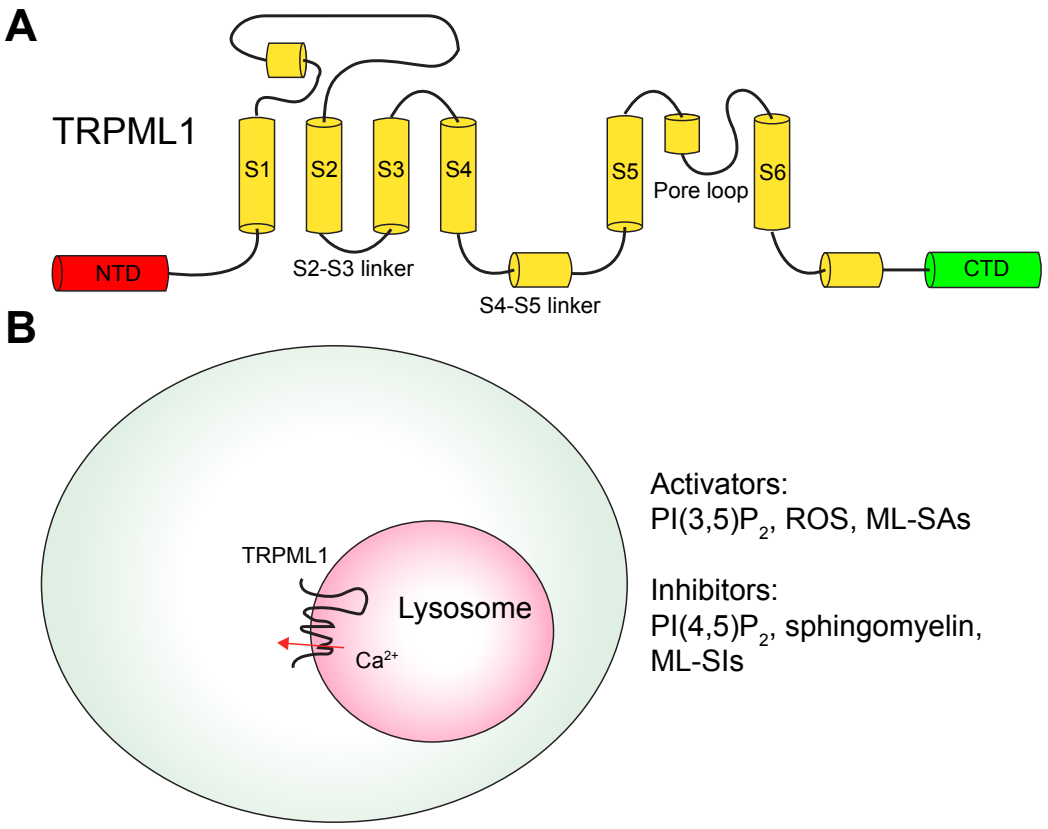


**Figure 1.4 ML1 structure diagram and topology.** (**A**) ML1 contains 6 transmembrane domains, with the channel pore located at S5 and S5. (**B**) ML1 is located primarily on lysosomal membrane, with both N and C terminus in cytoplasm. The channel is modulated by endogenous and synthetic agonists and antagonists. Upon activation, ML1 releases $Ca^{2+}$ from lysosomal lumen to cytosol.

### 2.3 Permeation properties of ML1

Using drugs to artificially induce homotypic fusion of late endosomes and lysosomes, electrophysiologists were able to isolate enlarged lysosomes from cells and study lysosomal channels in their native environment (Dong et al., 2008). According to whole-endolysosomal patch clamp, ML1 conducts $Ca^{2+}$, $Fe^{2+}$, $Zn^{2+}$, $Na^{+}$ and $K^{+}$, but not proton (Dong et al., 2008). Under physiological conditions, ML1 mainly releases $Ca^{2+}$, $Fe^{2+}$ and $Zn^{2+}$ from lysosomal lumen to cytosol (Xu and Ren, 2015). EM structure revealed selectivity filter of ML1 is localized in the

channel pore loop and composed of conserved, negatively charged amino acid residues (Chen et al., 2017). Surprisingly, the large luminal loop between S1 and S2 also forms a luminal pore atop the channel pore (refer to side view of the channel) (Chen et al., 2017). With high electronegative charge, this pore forms a trap for cations, especially divalent cations, at luminal side of the channel pore (Chen et al., 2017; Li et al., 2017). Thus, the selectivity of ML1 may come from both luminal pore and selectivity filter in the channel pore.

### 2.4 Gating properties of ML1

#### 2.4.1 Endogenous agonists: $PI(3,5)P_2$

Phosphatidylinositol 3,5-bisphosphate [$PI(3,5)P_2$] is a phosphoinositide primarily localized in late endosomes and lysosomes that regulates lysosomal membrane trafficking (McCartney et al., 2014). Like $PI(4,5)P_2$, the phosphoinositide localized on plasma membrane and regulates transporters and channels there, $PI(3,5)P_2$ has been found to activate lysosomal ML1 and two pore channel (TPC) in physiological nanomolar range (Dong et al., 2010b; Falkenburger et al., 2010; McCartney et al., 2014; Wang et al., 2012a). As modeled in EM structure of ML1, $PI(3,5)P_2$ binds to positively charged amino acids close to the N-terminus in S1, causing conformational change in S2 and S3 which leads to channel opening (Chen et al., 2017). Based on N-terminal segment of ML1, a genetically encoded $PI(3,5)P_2$ probe was generated and observed transient increase of $PI(3,5)P_2$ level prior to fusion between two LAMP1-positive vesicles, suggesting $PI(3,5)P_2$'s role in lysosomal membrane trafficking (Li et al., 2013). Consistently, inhibition of $PI(3,5)P_2$ synthesis by interrupting its synthetic enzyme complex leads to failure of lysosomal exocytosis and reformation (McCartney et al., 2014). Indeed, $PI(3,5)P_2$-deficent cells developed lysosomal storage phenotype resembles ML-IV which can be ameliorated by overexpression of ML1, suggesting ML1 may be its major downstream molecule in regulating lysosomal functions (Dong

et al., 2010b). However, how $PI(3,5)P_2$ synthesis and turnover respond to environmental cues and regulate the channel function still remains unclear.

We recently found ROS also activate lysosomal ML1 channel directly and increase autophagic flux. This part will be presented in Chapter II.

### 2.4.2 Endogenous inhibitors: $PI(4,5)P_2$ and sphingomyelin

$PI(4,5)P_2$ and sphingomyelin, two lipids primarily localized to plasma membrane, are shown to inhibit lysosomal ML1 (Shen et al., 2012; Zhang et al., 2012). The physiological significance of these machineries is to guarantee that lysosomal channels are only functional in the right place. Under pathological conditions, levels of these lipids in lysosomes can be increased and contributes to pathology through ML1. For example, in NPC cells, sphingomyelin is accumulated in lysosomal lumen and inhibit ML1 channel activity and $Ca^{2+}$ release, leading to impaired membrane trafficking (Shen et al., 2012).

### 2.4.3 Synthetic small molecule agonists and antagonists of ML1

Small molecule agonists and antagonists have been screened to manipulate ML1 channel and lysosomal $Ca^{2+}$ release (Shen et al., 2012). The first generation of mucolipin synthetic agonist ML-SA1 has recently been shown to bind with a hydrophobic pocket in the S5-S6 pore segments according to the EM structure (Schmiege et al., 2017). Notably, the ML-SA1 binding site is different from $PI(3,5)P_2$ binding site, and mutations interrupting ML-SA1 binding do not affect $PI(3,5)P_2$ binding (Schmiege et al., 2017). Recently, we have also developed more potent small molecule ML1 agonists and antagonists which can be useful tools in studying ML1- and lysosomal $Ca^{2+}$-related physiology and pathology.

## 2.5 ML1 in physiology

### 2.5.1 Metal export: $Fe^{2+}$ and $Zn^{2+}$

As a cation channel, ML1 exports $Fe^{2+}$ and $Zn^{2+}$ from lysosomal lumen to cytosol (Dong et al., 2008; Eichelsdoerfer et al., 2010). Consistently, ML1 KO cells have overloaded lysosomal $Fe^{2+}$ and $Zn^{2+}$ and iron deficiency in cytosol, which is related with anemia seen in ML-IV patients (Dong et al., 2008).

### 2.5.2 Lysosomal $Ca^{2+}$ release via ML1 mediates membrane trafficking and transport

As the primary lysosomal $Ca^{2+}$ channel, loss of function of ML1 leads to defects in membrane trafficking including lysosomal fusion, fission, exocytosis, and transport, suggesting that ML1 and lysosomal $Ca^{2+}$ release regulate these processes (Cheng et al., 2010).

#### 2.5.2.1 $Ca^{2+}$-dependent membrane fusion

ML1-deficienct cells exhibit defects in membrane fusion (Cheng et al., 2010; Xu and Ren, 2015). Delayed delivery of plasma membrane growth factor receptors to lysosomes suggests defective endosome-lysosome fusion and lysosomal maturation (Thompson et al., 2007). Fusion between autophagosomes and lysosomes is also impaired by ML1 knockout, causing autophagosome accumulation (Curcio-Morelli et al., 2010; Vergarajauregui et al., 2008; Wong et al., 2012). Together, these data suggest that ML1 activity is required in lysosomal membrane fusion.

#### 2.5.2.2 $Ca^{2+}$-dependent membrane fission

Accumulation of enlarged late endosomes and lysosomes (LEL) is considered as a hallmark of ML1-deficient cells from human, mouse, *C. elegans* and *Drosophila* (Dong et al., 2008; Treusch et al., 2004; Venkatachalam et al., 2008; Venugopal et al., 2007). Since membrane fission is a $Ca^{2+}$-dependent process, this naturally led to the assumption that ML1 plays a role in lysosomal fission and reformation (Luzio et al., 2007a; Luzio et al., 2007b). Indeed, retrograde trafficking of lipid from LEL to TGN is defective in ML-IV cells, and acute knockdown of ML1

also confirmed that (Chen et al., 1998; Pryor et al., 2006; Thompson et al., 2007). Indeed, additional attention needs to be paid when analyzing ML1's role in membrane trafficking events using ML1 KO cells, since any observed defects can be just secondary effects of lysosomal storage. For instance, defects in autophagosome-lysosome fusion were also seen in other LSDs (Parenti et al., 2015). Besides, membrane fusion and fission may dynamically regulate each other (Xu and Ren, 2015). Thus, acute manipulation of ML1 and methods directly detecting fusion and fission events need to be utilized in answering these questions.

#### 2.5.2.3 ML1 in lysosomal exocytosis

As discussed in the last section, local $Ca^{2+}$ store may play a role in regulating lysosomal exocytosis. The source of $Ca^{2+}$ release during lysosomal exocytosis remained unclear until recent findings suggested ML1's role in regulating this process. ML1 is a downstream gene of TFEB and lysosomal exocytosis induced by TFEB overexpression is abolished in ML1-deficient cells (Medina et al., 2011). Defects of lysosomal exocytosis and following pathogenesis were observed in different tissue of ML1 KO mice. In muscle tissues where lysosomal exocytosis is believed to repair disrupted membrane, progressive muscle degeneration was observed in ML1 KO mice (Cheng et al., 2014). ML1 KO macrophages also showed impaired lysosomal exocytosis and particle uptake (Samie et al., 2013). In gastric parietal cells, knockout of ML1 channels leads to failure of TV exocytosis and acid secretion, which is consistent with what has been seen in ML-IV patients (Bargal et al., 2000; Sahoo et al., 2017). These data suggest that the ML1 activity is required for lysosomal exocytosis. Moreover, overexpression of a gain-of-function mutation of ML1 boosted lysosomal exocytosis in HEK293T cells (Dong et al., 2009). Consistently, ML1 agonist ML-SA1 triggered lysosomal exocytosis in mouse macrophages, which can be blocked by

$Ca^{2+}$ chelator BAPTA-AM (Samie et al., 2013). Together, these data suggest ML1 is both necessary and sufficient for lysosomal exocytosis.

#### 2.5.2.4 ML1 in lysosomal transport

A recent study revealed the role of ML1 in regulating lysosomal transport and positioning (Li et al., 2016b). ML1 directly interacts with ALG-2 (apoptosis-linked gene 2), a cytosolic protein with five EF-hand motifs, in a $Ca^{2+}$-dependent manner (Li et al., 2016b; Vergarajauregui et al., 2009). More importantly, ALG-2 also physically associates with motor protein dynein and is required in ML1 activation-induced lysosome retrograde transport towards peri-nucleus region (Li et al., 2016b). Under starvation, lysosomes undergo retrograde transport to fuse with autophagosomes (Korolchuk et al., 2011). ML1 or ALG-2 depletion blocked this transport, leaving accumulated autophagosomes in the peri-nucleus region (Li et al., 2016b). This study uncovered a novel role of ML1 in regulating lysosomal positioning.

### 2.5.3 Lysosomal $Ca^{2+}$ release via ML1 activates TFEB

As one of the most important messengers in the cell, $Ca^{2+}$ transduces signals from different sources by interacting with a variety of its sensors and downstream signaling pathways. Similarly, lysosomal $Ca^{2+}$ release through ML1 triggers downstream signaling pathways to regulate lysosomal function. Upon ML1 activation and lysosomal $Ca^{2+}$ release, calcineurin is activated (Medina et al., 2015). The phosphatase then dephosphorylates TFEB at Ser142 and Ser211 and promotes its downstream autophagic and lysosomal gene transcription (Medina et al., 2015) (**Fig. 1.3**). Since lysosomal channel activity is modulated by a diverse of lysosomal and cellular stress, this observation has linked TFEB to these stress conditions in health and disease. A good example will be presented in Chapter II, where ROS trigger activation of TFEB and autophagy via gating ML1 channels. Besides, ML1 channels are easily manipulated by small molecule compounds as

suggested in many of our previous works (Shen et al., 2012), allowing TFEB to be a therapeutic target for a variety of diseases involving autophagy and lysosomal function. Relevant data will be shown in Chapter III and IV.

**2.6 ML1 in pathology**

ML1 is encoded by MCOLN1 gene, and mutations in MCOLN1 cause rare disease ML-IV in human (Bach et al., 2010). ML-IV patients manifest psychomotor retardation, corneal opacity, retinal degeneration and constitutive achlorhydria (Slaugenhaupt, 2002). ML1 KO mice reproduced most of the symptoms, including early-onset neurodegeneration, muscular dystrophy, iron deficiency anemia, hyposecretion of gastric acid, and ophthalmological abnormalities (Venugopal et al., 2007). This mouse model has helped us to gain profound understanding of ML1's and lysosome's role in physiology and pathology (Cheng et al., 2014; Dong et al., 2008; Sahoo et al., 2017).

ML1 has been proposed as a therapeutic target for other LSDs. In NPC cells, overexpression of ML1 and ML-SA1 ameliorate cholesterol storage, suggesting ML1 activation may facilitate lysosomal function (Shen et al., 2012). Indeed, since ML1 regulates many aspects of lysosomal function, manipulating channel activity might be a potential therapeutic strategy for LSDs and lysosome-associated diseases. More importantly, as it will be presented in Chapter II, ML1 activation via ML-SAs robustly and potently triggers TFEB nuclear translocation and downstream gene transcription. Since activation of TFEB has been suggested to have therapeutic effects in many diseases, as discussed earlier, small molecule agonists of ML1 can potentially be used to treat these diseases. And activation of TFEB by small molecule compounds will be much easier to achieve than overexpression *in vivo.* In general, with the potent small molecule agonists

and antagonists, ML1 can be a potential therapeutic target for treating LSDs and lysosome-associated diseases.

## 3 Lysosomes in muscle physiology and pathology

Being both metabolically and mechanically active, it is essential for the terminally-differentiated muscle tissues to be adaptive to a wide range of environmental and cellular cues (Allen et al., 2016; Sandri, 2010). Lysosomes regulate both aspects via autophagy and lysosomal exocytosis. Autophagy is required for muscle renovation and mass maintenance, while lysosomal exocytosis facilitates sarcolemmal repair (Allen et al., 2016; Sandri, 2010). Consistently, genetic mutations impairing autophagy and lysosomal exocytosis lead to myopathies (Cheng et al., 2014; Malicdan and Nishino, 2012; Sandri, 2010). More importantly, autophagic and lysosomal defects have been reported in muscle diseases such as muscular dystrophy (De Palma et al., 2014; Pal et al., 2014). Thus, lysosomes can be potential therapeutic targets for treating muscle pathologies.

### 3.1 Lysosomes in muscle physiology

#### 3.1.1 Autophagic-lysosomal pathway is required for maintenance of muscle mass and function

For terminally-differentiated organs like muscles, autophagy is essential for renovation of cellular contents (Mizushima and Komatsu, 2011). Basal and stress-induced autophagy have been shown important in muscle mass and function maintenance under physiological and pathological conditions (Sandri, 2010). In an early study comparing gene expression pattern in different models of muscle atrophy, characterized by muscle wasting and mass loss, a small subset of genes was found upregulated and named as atrophy-related genes (Bodine et al., 2001). Interestingly, many of these genes are involved in ubiquitin-proteasome system and autophagic-lysosomal pathway

including LC3, a protein now commonly used as an autophagosome marker (Bodine et al., 2001; Klionsky et al., 2012). Later, by utilizing transgenic mouse line expressing GFP-labeled LC3, Mizushima et al. found autophagy was significantly induced in skeletal muscles under starvation (Mizushima et al., 2004). Notably, basal autophagosomes were inconspicuous in muscles and even fasted muscle fibers showed smallest autophagosomes compared with liver, pancreas and heart, possibly due to specified cytoskeleton and sarcoplasmic reticulum (SR) structure in these cells (Mizushima et al., 2004).

To build more direct connections between autophagy and muscle pathology, several *Atg* genes were deleted specifically in skeletal and cardiac muscles in mouse models (**Table 1.1**). As a key protein involved in autophagosome formation, ATG5 deficiency in cardiac muscles showed normal heart function under basal level (Nakai et al., 2007). However, under pressure overload challenge, ATG5-deficient hearts developed left ventricle dilatation and heart failure (Nakai et al., 2007). Consistently, acute induction of cardiac ATG5 deficiency by tamoxifen also triggered disorganized sarcomeres, aggregated mitochondria and ventricular dilatation (Nakai et al., 2007). Similarly, muscle-specific depletion of ATG7, another key protein in autophagy initiation, caused profound muscle atrophy in mice (Masiero et al., 2009). Progressive loss of muscle mass and force was observed in these mice, accompanied with upregulated atrophy-related genes, aggregated autophagy substrates, enlarged vacuoles, abnormal mitochondria and SR, and disorganized sarcomeres (Masiero et al., 2009). More importantly, denervation and fasting exacerbated all these symptoms (Masiero et al., 2009). However, although degeneration occurs, muscle membrane permeability seems not severely affected, evidenced by normal creatine kinase (CK) level and mildly-increased immunoglobulin-positive fibers (Masiero et al., 2009). These data suggest that autophagy is essential for basal as well as adaptive muscle function.

**Table 1.1 Muscle phenotypes of autophagic-lysosomal gene deficiency**

| Genotype (species) | Phenotype | Reference |
|---|---|---|
| *Atg4C* KO (mouse) | Diaphragm-specific autophagy defects under starvation | (Mariño et al., 2007) |
| *Atg5* cardiomyocyte KO (mouse) | Pressure overload-induced ventricle dilatation and heart failure; accumulated damaged cellular organelles | (Nakai et al., 2007) |
| *Atg6/beclin 1* heterozygous (mouse) | Decreased pressure overload-induced heart failure; decreased heart damage upon ischemia/reperfusion | (Matsui et al., 2007) |
| *Atg7* muscle KO (mouse) | Muscle atrophy and accumulated damaged cellular contents; phenotypes are exacerbated by starvation and denervation | (Masiero et al., 2009) |
| LAMP2 deficiency (human and mouse) | Danon disease; skeletal and cardiac myopathy; accumulation of enlarged autophagosomes | (Tanaka et al., 2000) |
| GAA deficiency (human and mouse) | Pompe disease; vacuolar skeletal and cardiac myopathy; accumulation of glycogen | (Hers, 1963) |
| VMA21 deficiency (human) | X-linked myopathy with excess autophagy | (Ramachandran et al., 2013) |

Except for proteins involved in early autophagy initiation step, several lysosomal proteins have been linked to human myopathies with aberrant autophagy (**Table 1.1**). As mentioned previously, mutations in lysosomal membrane protein LAMP2 and glucosidase GAA lead to Danon and Pompe disease, respectively. Both diseases are characterized by hypertrophic cardiomyopathy, muscle weakness, and accumulation of enlarged autophagosomes (Malicdan and Nishino, 2012). Notably, patients of Danon and Pompe disease showed different degree of serum CK increase, suggesting muscle membrane leakage (Chien et al., 2011; Malicdan and Nishino, 2012). Recently, X-linked myopathy with excess autophagy (XMEA) was identified to be caused by mutations in VMA21, a gene encoding a protein involved in v-ATPase assembly (Ramachandran et al., 2013). Pathology of XMEA patients exhibits similar phenotypes as what have been seen in Danon disease (Sugie et al., 2005). Except genetic ablation, pharmacological inhibition of lysosomal acidification using chloroquine (CQ) also leads to skeletal and cardiac

myopathy, characterized by increased autophagosomes in muscle fibers (Suzuki et al., 2002). Together these data demonstrated that the autophagic-lysosomal pathway is required in muscle physiology.

### 3.1.2 Lysosomal exocytosis facilitates membrane repair in muscles

#### 3.1.2.1 Cellular membrane repair mechanisms

Intact plasma membrane is essential for cell survival. Muscles undergo constant mechanical stretch and are therefore susceptible to plasma membrane/sarcolemmal damage (Cooper and McNeil, 2015). Upon damage, cells immediately trigger multiple repair machineries depending on the size of injury (Cooper and McNeil, 2015; McNeil and Kirchhausen, 2005). For tiny injuries less than a nanometer, membrane lipids diffuse and spontaneously reseal the membrane (Cooper and McNeil, 2015; McNeil and Kirchhausen, 2005). In liposomes and red blood cells which lack organelles, damaged membrane is efficiently resealed even at very low concentration of extracellular $Ca^{2+}$ (Hoffman, 1992). But in mechanically active cells like skeletal and cardiac muscle cells, damage is often more severe and facilitated resealing machineries are required (Cooper and McNeil, 2015). Although the mechanisms of this active resealing are not fully understood, it is universally agreed that $Ca^{2+}$ influx upon damage is essential in membrane repair (Cooper and McNeil, 2015). In the early study using sea urchin egg, cells can repeatedly repair sequential wounds more than 1,000 square microns in a few seconds but cannot survive a single insult in the absence of extracellular $Ca^{2+}$ (McNeil and Kirchhausen, 2005; Terasaki et al., 1997). Significant increase of $Ca^{2+}$ at the injury site has been detected, and chelating this increase prevents membrane repair (Cai et al., 2009a; Chakrabarti et al., 2003). However, caution should be taken when analyzing these results since removing extracellular $Ca^{2+}$ often eliminates intracellular $Ca^{2+}$ stores at the same time (Cheng et al., 2015).

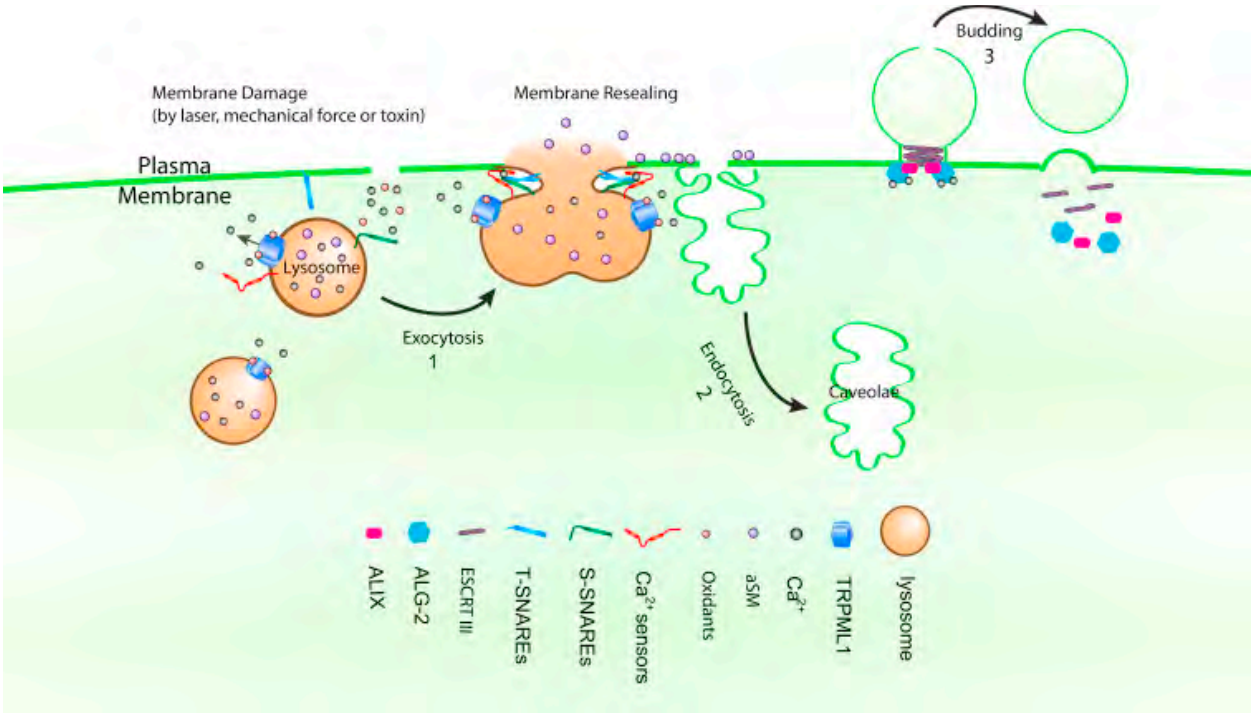


**Figure 1.5 Membrane repair mechanisms.** Three models for membrane repair: 1) Lysosomal exocytosis; 2) Secretion of aSMase through lysosomal exocytosis triggers endocytosis of membrane lesion; 3) Budding of damaged membrane. All of these processes are $Ca^{2+}$-dependent. Figure is modified from Fig. 1 in ref. (Cheng et al., 2015), courtesy to Dr. Xiping Cheng from Xu lab.

Several models have been proposed for facilitated resealing (Cheng et al., 2015) (**Fig. 1.5**). First, in the "lipid patch" model, intracellular vesicles dock to plasma membrane and fuse to patch the damaged site. Lysosomes, endosomes and specified organelles in special cell types have been suggested to repair the damaged membrane (McNeil and Kirchhausen, 2005). Among these, the evidence about lysosomal exocytosis may be stronger than others, especially after identification of lysosome-localized $Ca^{2+}$ sensor synaptotagmin VII (Martinez et al., 2000; Reddy et al., 2001). The second mechanism is the "endocytic removal" model, which proposes membrane lesions are removed by endocytosis. Interestingly, this model also relies on lysosomal exocytosis. Secretion of lysosomal aSMase (acid sphingomyelinase) mediates hydrolysis of sphingomyelins, triggering

ceramide-driven membrane invagination and lesion removal (Idone et al., 2008; Tam et al., 2010). The third one is called "macro-vesicle shedding", in which damaged membrane undergoes budding towards extracellular direction to remove the injury. This model involves ESCRT (endosomal sorting complex required for transport), a protein complex mediates membrane budding and fission events (Jimenez et al., 2014). It has been shown that injury-induced $Ca^{2+}$ increase triggers ESCRT assembly via $Ca^{2+}$-binding ALG-2 (Scheffer et al., 2014). Thus, all of these proposed resealing mechanisms are $Ca^{2+}$-dependent.

#### 3.1.2.2 Lysosomal exocytosis is required for membrane repair in muscles

The lysosome is a candidate vesicle for membrane repair. We and colleagues have found that activation of lysosomal $Ca^{2+}$ channel ML1 through genetic upregulation and channel agonists promotes lysosomal exocytosis (Medina et al., 2011; Samie et al., 2013). Interestingly, ML-IV patients and ML1 KO mice showed early-onset, progressive muscular dystrophy and defected sarcolemmal repair (Bach et al., 2010; Cheng et al., 2014). Sarcolemmal permeability, assayed by EB-positive fibers and serum CK levels, are significantly increased in ML1 KO mice, and worsened by exercise (Cheng et al., 2014). Membrane repair in fibers from ML1 KO mice after laser and mechanical damage is also dramatically impaired compared with WT (Cheng et al., 2014). Upon bacterial streptolysin O (SLO) toxin treatment which digs pores on plasma membrane, ML1 KO fibroblasts showed less lysosomal enzyme release than WT, and pharmacological inhibition of ML1 channel also caused more cell death measured by propidium iodide (PI) dye (Cheng et al., 2014). Based on these results, we demonstrated that ML1 is required for lysosomal exocytosis, sarcolemmal repair and cell survival during injury. It is likely that lysosomal $Ca^{2+}$ store and channels serve as sources to provide $Ca^{2+}$ release for their own exocytosis.

Apart from ML1, other players regulating lysosomal exocytosis have been found important in membrane repair in muscles. For example, mice lacking syt7 showed extensive inflammation, fibrosis and collagen deposition in skeletal muscles (Chakrabarti et al., 2003). Moreover, serum CK level is significantly elevated, suggesting increased membrane permeability in syt7 KO mice (Chakrabarti et al., 2003). Notably, as previously discussed, patients with Pompe/Danon/XEMA all show serum CK increase, suggesting membrane integrity may also be compromised, possibly due to defects in lysosomal function (Malicdan and Nishino, 2012; Malicdan et al., 2008). Putting together, these results demonstrate lysosomal exocytosis is required in maintenance of sarcolemma integrity.

### 3.2 Lysosomes in muscle pathology

Autophagy and lysosomal exocytosis have been implicated in muscle pathologies (De Palma et al., 2014). In MD, compromised sarcolemma repair is considered to be a crucial step in pathogenesis (Allen et al., 2016). Since lysosomes are important in membrane repair, they have become potential therapeutic targets for treating MD (Reddy et al., 2001). In this part, I will discuss about the role of lysosomes in myopathies, with a focus on the best-known MD, Duchenne muscular dystrophy (DMD).

#### 3.2.1 Lysosomes in muscular dystrophy

##### 3.2.1.1 Basics of MD

###### 3.2.1.1.1 Clinical manifestations and molecular basis

Muscular dystrophy (MD) is more than 30 inherited diseases characterized by progressive muscle weakness and degeneration. Described by Duchenne in 1868, DMD is an X-linked, rare disease with the prevalence of 1 in 3000 boys (Allen et al., 2016; Van Deutekom and Van Ommen, 2003). Duchenne's report included 13 cases with progressive muscle weakness initially affecting

lower limbs and the early hypertrophy followed by atrophy (Allen et al., 2016). He also tracked the patients and obtained samples for muscle biopsy during their lives, thus established the characteristic histology (Allen et al., 2016). Other clinical features include mental retardation, curvature of the spine, cardiac dysfunction, and respiratory failure caused by weakness of thoracic muscles and diaphragm (Bushby et al., 2010). The latter is considered to be the reason resulting in premature death around mid 20s in DMD patients (Bushby et al., 2010). The X-linked trend was noticed later and dystrophin gene was finally cloned in 1980s (Gowers, 1879; Kunkel et al., 1985).

With 2.5 megabases, dystrophin turned out to be the largest known gene in human genome (Kunkel, 1986; Prior and Bridgeman, 2005). Different mutations in dystrophin lead to DMD or Becker muscular dystrophy (BMD), the milder form of MD, depending on whether the protein function is completely or partially lost (Kunkel, 1986; Prior and Bridgeman, 2005). Since loss-of-function of dystrophin mainly affects muscles, it was first believed that dystrophin and its associated protein complex were exclusively expressed in striated and smooth muscles (Haenggi and Fritschy, 2006). However, recent studies have found dystrophin protein products in a variety of cell types, including in the brain (Haenggi and Fritschy, 2006). Development of dystrophin antibody helped determination of its subcellular localization (Hoffman et al., 1987; Watkins et al., 1988). Dystrophin protein is located in the intracellular side of the plasma membrane, where it forms a large protein complex to connect muscle fibers to their extracellular matrix, as well as to transduce signals across the plasma membrane (Allen et al., 2016; Hoffman et al., 1987; Watkins et al., 1988) (**Fig. 1.6**).

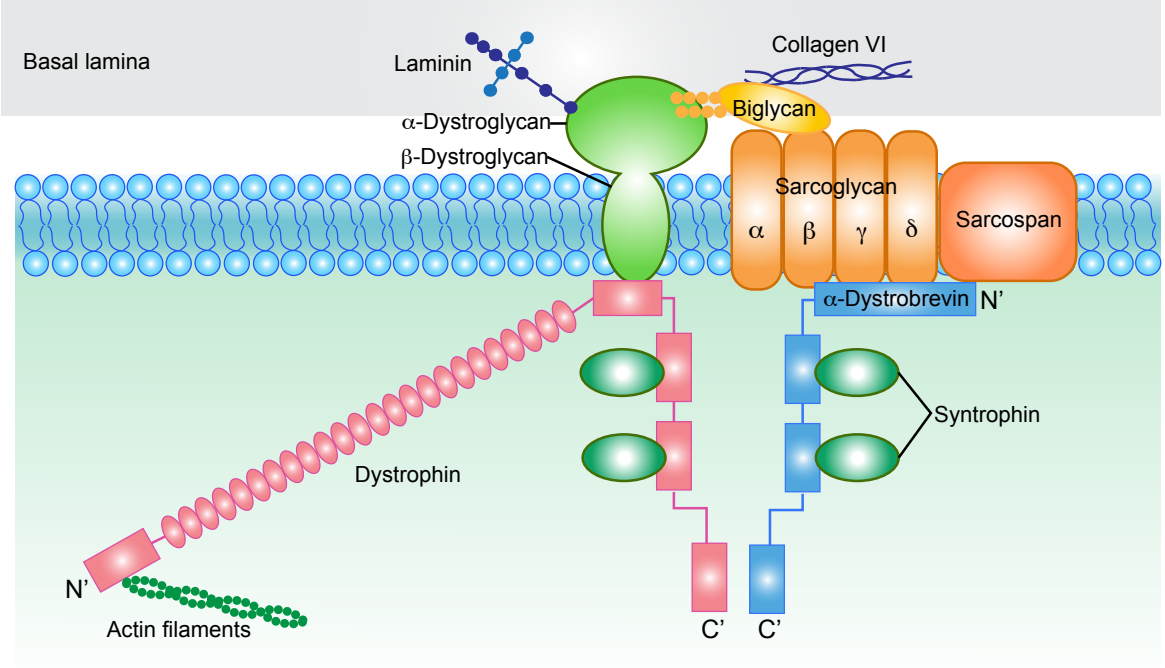


**Figure 1.6 The dystrophin protein complex (DPC).** DPC connects the extracellular matrix to cytoskeleton proteins. Shown is the interaction between core components of the DPC, including dystrophin, α-dystrobrevin, syntrophin, sarcoglycans, sarcospan, α- and β-dystroglycan, and biglycan.

Through binding with cytoskeleton γ-actin and membrane proteins, dystrophin forms dystrophin protein complex (DPC) (Allen et al., 2016) (**Fig. 1.6**). Upon its discovery, it was believed that DPC physically maintains sarcolemma integrity as well as attachment of muscle fibers to their extracellular matrix (Durbeej and Campbell, 2002). However, recent evidence also suggests that several DPC members play active roles in signal transduction through direct and indirect interaction with cellular messengers such as $Ca^{2+}$ and ROS (Allen et al., 2016). Except dystrophin, mutations or knockout of other DPC members have been reported to cause different degree of MD in human and mouse models (Grady et al., 1999; Mathews and Moore, 2003; Mercuri and Muntoni, 2012). For example, congenital muscular dystrophies (CMD) is a group of genetic disorders characterized by mental retardation, ocular defects, and skeletal muscle

pathology (Straub and Campbell, 1997). Genetic characterization of CMD patients has revealed that mutations in Laminin-2, collagen type VI, and abnormal glycosylation of a-dystroglycan underline these diseases (Schessl et al.). Similarly, limb-girdle muscular dystrophies (LGMD), which have lots of overlap of symptomatology with BMD patients, are linked to sarcoglycans (Guglieri et al., 2008). Deficiency of α-dystrobrevin in mice also resulted in skeletal muscular dystrophy and cardiomyopathy (Grady et al., 1999). More importantly, overexpression of several DPC members has been reported to ameliorate MD in dystrophin-deficient animal models (Peter et al., 2008; Young and Fallon, 2012).

The role of dystrophin in maintaining sarcolemma integrity is evidenced by increased membrane permeability in DMD and BMD patients (Allen et al., 2016). In fact, leakage of muscle-specific enzymes into serum such as CK has become a pathological hallmark and diagnostic characteristic of DMD (Allen et al., 2016). Other diagnostic standards include clinical manifestations, histology and immunostaining results for dystrophin (Bushby et al., 2010). Identification of the genetic mutation can also help treatment and prognosis (Bushby et al., 2010). So far, no treatment is available to all types of mutations of DMD (Bushby et al., 2010). Steroids have been used to delay disease development and prolong survival (Allen et al., 2016; Bushby et al., 2010). Recently, growing evidence suggests that gene therapy to induce expression of a partial or fully functional dystrophin or its homolog protein is beneficial for DMD patients (McGreevy et al., 2015; Van Deutekom and Van Ommen, 2003). These efforts finally made the FDA-approved drug Eteplirsen, a morpholino antisense oligomer triggers skipping of exon 51 and yields a partial functional dystrophin protein product (Aartsma-Rus and Krieg, 2017; Mendell et al., 2013). Recently, progress of CRISPR-Cas9 in mammalian gene editing has made gene therapy even more attractive for treating DMD (Amoasii et al., 2017; Nelson et al., 2016). However, certain caveats

do exist. For example, most available gene therapy only targets some types of mutations - Eteplirsen is estimated to be effective on mutations making up 13% of DMD patients, not to mention patients who cannot afford its high cost (Aartsma-Rus and Krieg, 2017). Since a variety of mutations in the large dystrophin gene can cause DMD, the use of this exon-skipping strategy may be limited. In addition, transduction of a reduced dystrophin gene (e.g. mini- or micro-dystrophin) via AAV has been shown effective in DMD mouse models, but transduction and expression efficiency, as well as the immune response have been major drawbacks (Van Deutekom and Van Ommen, 2003). Thus, it is necessary to develop easily-achieved therapeutic strategies to target on more general mechanisms in the pathogenesis of DMD.

**3.2.1.1.2 Animal models to study MD**

Various mouse and canine models have been generated for DMD (McGreevy et al., 2015). The most widely used is the *mdx* mice, found in 1984 due to elevated serum CK level and muscle damage and regeneration (Bulfield et al., 1984). Later characterization located the spontaneous, nonsense point mutation in dystrophin gene that aborted full-length protein expression in *mdx* mice (Sicinski et al., 1989). Despite the identical genotype as human patients, the phenotype of *mdx* mice is much milder. In the first 2 weeks, *mdx* mice are indistinguishable from their wildtype peers (McGreevy et al., 2015). From 3 to 6 weeks, they developed massive necrosis, which is more acute and severe than necrosis seen in human patients (McGreevy et al., 2015). Later on, the majority of muscles in *mdx* mice undergoes robust regeneration, characterized by central-nucleated muscle fibers (McGreevy et al., 2015). This regeneration phenotype is absent in patients either (McGreevy et al., 2015). Instead, muscle histology from patients suggests extensive and progressive muscle fibrosis at later stage of the disease (McGreevy et al., 2015). The only skeletal muscle shows similar fibrotic phenotype in *mdx* mice is the diaphragm, though the mechanism is still largely

unknown (Stedman et al., 1991). Besides, cardiac muscle is not affected in the *mdx* mice until very late stages and their lifespan is almost normal (Allen et al., 2016; McGreevy et al., 2015). Although disadvantages exist, due to its identical genotype, muscle weakness phenotype and easy availability, *mdx* strain is still the most commonly used animal model for studying DMD. In 1989, four chemical variant (cv) *mdx* lines were generated by mutagen (Chapman et al., 1989). Named as $mdx^{2cv}$, $mdx^{3cv}$, $mdx^{4cv}$ and $mdx^{5cv}$, each of them carries a different point mutation in dystrophin that leads to deficiency of full-length protein and shorter forms in other tissues like brain (Chapman et al., 1989). Generally speaking, the phenotypes of these mice are very similar to *mdx* mice, though the $mdx^{5cv}$ was reported to have more severe skeletal muscle phenotype (Beastrom et al., 2011).

The phenomenon that *mdx* mice have much milder phenotypes than DMD has raised an interesting question in the field. So far, the best explanation is the existence of utrophin proteins compensating for dystrophin loss in mice (Allen et al., 2016). Utrophin is structurally similar as dystrophin but its expression is more restricted to the neuromuscular junction in adults (Blake et al., 2002). It was shown that sarcolemmal utrophin level was increased in *mdx* mice, and overexpression of utrophin protein in *mdx* mice ameliorated the symptoms (Matsumura et al., 1992; Tinsley et al., 1998). Additionally, knockout of utrophin in *mdx* mice yields very severe phenotype considered to better mimic DMD (Deconinck et al., 1997; Grady et al., 1997). These mice showed weight loss, curved spine, progressive muscle degeneration and regeneration, cardiac dysfunction, and their lifespan is around 3 months (Deconinck et al., 1997; Grady et al., 1997). However, these mice are difficult to breed and care for, which have limited their use. Other DPC members, as well as proteins play roles in pathogenesis of DMD, have been knocked out in *mdx* mice to “humanize” the model (McGreevy et al., 2015). Yet, these mouse models all carry

mutations in genes other than dystrophin, which may affect the interpretation of data collected from them.

So far, the dystrophin-null golden retriever dystrophy model is considered the best to mimic DMD, for identical genotype and phenotype (McGreevy et al., 2015). Due to similar immune responses as human, the canine models are especially helpful in analyzing gene therapy (Amoasii et al., 2018; McGreevy et al., 2015). But apparently, these animals are much more costly and hard to maintain, setting limitations to their use.

#### 3.2.1.1.3 Membrane damage and repair in MD

Defects in sarcolemmal repair is an important step in early pathogenesis of MD (Allen et al., 2016). However, it is necessary to point out that various molecules, cellular organelles, and muscle physiology aspects all play roles in these devastating diseases (Allen et al., 2016). Here, I will be focused on membrane damage and repair in MD pathogenesis, since it is most relevant to lysosomal function.

##### 3.2.1.1.3.1 Increased membrane permeability in MD: biomarkers

Increased membrane permeability is thought to be one of the major early pathological changes in MD (Allen et al., 2016). Two types of biomarkers are used to measure membrane permeability *in vivo*. First, upon damage, muscle-specific enzymes such as CK is leaked into blood stream and its activity can be detected in serum (Allen et al., 2016). In normal people, physical activity, especially eccentric exercise like resistance training, can cause CK level to increase mildly (Brancaccio et al., 2007). However, in many types of MD, as well as animal models such as *mdx*, serum CK activity is dramatically increased by more than 100-fold after exercise (Zatz et al., 1991). The other type of biomarkers commonly used is influx of proteins or membrane-impermeable dyes such as albumin, procion orange and Evan's blue (EB) dye (Allen et al., 2016).

Stimulated by eccentric contraction, the magnitude of EB increase in *mdx* mice is much greater than WT (Hamer et al., 2002).

Although commonly used, some cautions need to be taken when interpreting these assays. For example, CK is reported to be modified by ROS and oxidation, which results in reduction of its activity (Nuss et al., 2009). Therefore, it may be necessary to look at the protein level as well when studying ROS-related muscle biology. Besides, EB dye is found to preferentially stain some types of muscle fibers *in vivo,* such as the branched ones (Head, 2010). More importantly, neither CK activity nor EB dye increase is correlated with muscle force loss (Allen et al., 2016). In *mdx* mice, EB dye positive fibers constitute ~ 20% of total after exercise, while muscle force undergoes a drop around 70% (Moens et al., 1993; Whitehead et al., 2006). This inconsistency may be explained by some fibers are more susceptible to EB staining. But it is more likely that increased membrane permeability is just one piece of the whole picture. In MD, mutations of muscle proteins may cause pathological changes in many aspects of the muscle, including sarcolemma, $Ca^{2+}$ store, vesicle trafficking, SR and contraction machinery, NO (nitric oxide), ROS, and these all contribute to muscle degeneration and dysfunction (Allen et al., 2016). In the following discussion, I will present the connections between some of these players, from a membrane damage-repair angle.

**3.2.1.1.3.2 Exacerbated membrane damage in MD: a story of $Ca^{2+}$ and ROS**

In both healthy individuals and MD patients, membrane damage constantly occurs in muscle tissues during contraction (Allen et al., 2016). Ever since the discovery of dystrophin/DPC, it is believed that dystrophin physically supports the sarcolemma, thus the loss of it would lead to more damage in DMD patients during contraction (Petrof et al., 1993). To demonstrate this point, Whitehead et al. designed a study to test procion orange dye entry into *mdx* muscles at early time course after eccentric contraction (Whitehead et al., 2006). Surprisingly, they found muscles

collected immediately after exercise have only a few percent more positive fibers than resting controls, yet the number rise up to 15% in muscles collected 60 minutes after exercise (Whitehead et al., 2006). This finding suggests that the majority of membrane damage happens after the physical disruption. It is likely that muscle contraction mainly serves as a primary trigger to downstream damage signaling cascades, and the latter can be regulated by dystrophin.

$Ca^{2+}$ turned out to be a major damage signal regulated by dystrophin (Allen et al., 2016). Elevated intracellular $Ca^{2+}$ was found in *mdx* mice and is considered to cause protein degradation and eventually cell death through proteases like calpains (Franco Jr and Lansman, 1990; Spencer et al., 1995; Turner et al., 1988). In fact, by blocking $Ca^{2+}$-permeable mechanosensitive channels (MSCs), dye uptake in *mdx* mice after exercise was significantly reduced (Whitehead et al., 2006). Consistently, although the genetic identity is still under debate, studies have shown MSCs are more active in *mdx* and DMD myotubes (Franco Jr and Lansman, 1990; Franco-Obregón and Lansman, 2002; Vandebrouck et al., 2001). In addition, overexpression of SR $Ca^{2+}$ pump (SERCA), which pumps $Ca^{2+}$ from myoplasm back to SR, yields robust improvement of sarcolemma permeability as well as muscle performance in *mdx* mice (Goonasekera et al., 2011). Together, multiple pieces of evidence suggest that intracellular $Ca^{2+}$ increase mediates the membrane permeabilization and is regulated by dystrophin.

ROS are another important player. ROS are oxygen-containing molecules that can directly interact with macromolecules to modify their structure and function (Barbieri and Sestili, 2012). In MD patients and animal models, ROS levels are elevated under resting and stimulation (Kim et al., 2013; Rando, 2002). This elevation is considered to be crucial for sarcolemma permeabilization, since antioxidant treatments such as NAC (N-acetylcysteine), vitamin E and green tea extract have all been reported to ameliorate sarcolemmal leak and dystrophy (Call et al.,

2008; Gamstorp et al., 1986; Howard et al., 2011; Whitehead et al., 2008). In skeletal muscles undergoing contractions, ROS are predominantly generated by NADPH oxidase (NOX), but not mitochondria (Michaelson et al., 2010). And blocking NOX prevented most of the ROS production (Shkryl et al., 2009). NOX is a multiprotein enzyme complex producing superoxide and $H_2O_2$ (Mofarrahi et al., 2008). Having several isoforms of catalytic subunits, NOX2 and NOX4 are found in muscles (Mofarrahi et al., 2008). Interestingly, NOX2 level is also raised in dystrophic muscles and it can be activated by stretch, possibly through a microtubule-dependent mechanism (Khairallah et al., 2012; Whitehead et al., 2010). It has been demonstrated that in MD, increased NOX2 leads to more ROS production upon stretch, resulting in cell damage (Allen et al., 2016).

The search for downstream molecules for ROS in muscles revealed an unexpected link between ROS and $Ca^{2+}$. A MSC candidate has been found activated by ROS to trigger $Ca^{2+}$ release, and NOX inhibitors prevented $Ca^{2+}$ influx (Gervásio et al., 2008; Khairallah et al., 2012; Shkryl et al., 2009; Whitehead et al., 2010). Thus, the NOX-ROS-MSC-$Ca^{2+}$ axis has been proposed and is still one of the most popular explanations for damage in dystrophic muscles (Allen et al., 2016). Besides, ROS can regulate other aspects in MD pathogenesis. Recently, increased NOX2 and ROS in *mdx* mice have been indicated to impair autophagy and lysosomes, contributing to pathogenesis (Pal et al., 2014). ROS are also reported to oxidize membrane lipids, changing membrane property and permeability in DMD (Dudley et al., 2006).

Notably, although ROS and $Ca^{2+}$ have deleterious roles in muscle damage, both of them are active signals in the cell and regulate a variety of biological events. Under physiological conditions, ROS operate important functions in skeletal muscles such as regeneration, metabolism and mitochondria function, and $Ca^{2+}$ is essential in muscle contraction and physiology (Barbieri and Sestili, 2012; Cheng et al., 2015; Ebashi and Endo, 1968). Paradoxically, they also play roles

in membrane repair (Cai et al., 2009a; Cheng et al., 2015). Indeed, for active messengers like $Ca^{2+}$ and ROS, cells have adopted machineries to make sure they only function locally. Take $Ca^{2+}$ as an example, diffusion and cellular buffering for $Ca^{2+}$ can produce 100 nM to 10 μM $Ca^{2+}$ concentration drops in a distance of 30 nm surrounding the releasing $Ca^{2+}$ channel within a few milliseconds (Cheng et al., 2015; Clapham, 2007). This guaranteed $Ca^{2+}$ signaling to be accurately controlled responding to precise cellular needs. It is likely that upon sarcolemmal damage, $Ca^{2+}$ from varied sources are involved in different biological processes by triggering diverse downstream signaling pathways through different local sensors, and possibly at different time. Therefore, concentration, source and sensor should all be carefully examined when discussing about the physiological and pathological roles of $Ca^{2+}$ and ROS.

**3.2.1.1.3.3 Impaired membrane repair in MD**

**3.2.1.1.3.3.1 Impaired exocytosis and membrane repair in MD**

**3.2.1.1.3.3.1.1 Dysferlin acts as the $Ca^{2+}$ sensor and is required in membrane repair**

Some genes underlying MD have been found directly involved in membrane repair. Loss of dysferlin results in limb girdle muscular dystrophy type 2B (LGMD2B) and Miyoshi myopathy (Cooper and McNeil, 2015). Patients of these diseases often show normal physical ability during childhood but developed MD as a teenager or adult after an injury that is difficult to recover from (Cooper and McNeil, 2015). Dysferlin-deficient mice showed similar late-onset MD, and closer look into their muscles have uncovered impaired membrane repair (Bansal et al., 2003). Bansal et al. developed a membrane damage-repair assay using FM1-43 dye, a water-soluble dye that cannot cross membranes (Bansal et al., 2003). Upon laser irritation, the FM dye accumulates at the damage site rapidly, but plateaued within 30s in WT fibers, suggesting effective membrane resealing (Bansal et al., 2003). In contrast, dysferlin-null fibers presented prolonged dye entry until

up to 2 minutes, and the kinetics are similar to WT fibers damaged in the absence of $Ca^{2+}$ (Bansal et al., 2003). Indeed, dysferlin is a $Ca^{2+}$-binding protein with C2 domains similar as synaptotagmins (Anderson et al., 1999; Evesson et al., 2010). It is ubiquitously expressed but have highest expression levels in skeletal and cardiac muscles (Anderson et al., 1999; Evesson et al., 2010). In the cellular level, it predominantly locates on sarcolemma, but recent findings have suggested that it shuttles between sarcolemma and endolysosomal vesicles (Anderson et al., 1999; Evesson et al., 2010). The mechanisms for dysferlin to repair damaged membrane is not fully understood, but it is believed that dysferlin is recruited to the injured site within 10 seconds after damage, and it can be cleaved by calpain (activated by local $Ca^{2+}$ influx) to yield a synaptotagmin-like module with two C2 domains (Cooper and McNeil, 2015; Han and Campbell, 2007). This cleaved fragment may mediate vesicle fusions in a manner similar as synaptotagmins (Cooper and McNeil, 2015; Han and Campbell, 2007). Consistently, accumulation of vesicles close to sarcolemma was observed in dysferlin-null muscles (Bansal et al., 2003). Interestingly, deficiency of syt7 in mice also results in myopathy characterized by increased CK level and massive fibrosis (Chakrabarti et al., 2003). Putting together, these data suggest that dysferlin plays a role in membrane repair, though the mechanisms still remain to be elucidated.

**3.2.1.1.3.3.1.2 MG53 acts as a potential ROS sensor and is required in membrane repair**

Mitsigumin-53 (MG53) is a ROS sensor candidate belonging to the E3 ubiquitin ligase TRIM family (Waddell et al., 2011; Weisleder et al., 2008). It is highly expressed in skeletal and cardiac muscles, and subcellularly localized to both sarcolemma and cytosol (Waddell et al., 2011; Weisleder et al., 2008). Although not implicated in human disease, MG53-deficient mice showed progressive myopathy and impaired membrane repair (Cai et al., 2009a). MG53 is associated with intracellular vesicles via phosphatidylserine (Cai et al., 2009a). When membrane damage occurs,

released ROS cause MG53 oligomerization, leading to recruitment of MG53-positive vesicles to injury site (Cai et al., 2009a). Absence of $Ca^{2+}$ partially blocked recruitment process, suggesting both $Ca^{2+}$-dependent and -independent pathways underlying it (Cai et al., 2009a). Interestingly, the same study also showed 0 $Ca^{2+}$ solution could significantly increase FM dye uptake upon injury in WT fibers, and this is exacerbated when treating the WT fibers with antioxidant in 0 $Ca^{2+}$ solution (Cai et al., 2009a). These findings have not only identified the importance of MG53 in sarcolemmal resealing, but also revealed complicated roles of ROS in membrane damage-repair. Three-dimensional structured illumination microscopy (3D-SIM) also showed rapid recruitment of MG53 to injury site within 2 s, followed by dysferlin which is recruited in 10 s (Lek et al., 2013). The two proteins are largely colocalized with each other at the injury site, and co-immunoprecipitaion suggests they have interactions in MD (Cai et al., 2009b; Lek et al., 2013; Waddell et al., 2011). However, how they coordinate in membrane repair is still unknown. Besides, the nature of vesicles in these studies is not well characterized.

**3.2.1.1.3.3.1.3 Membrane repair in DMD**

Whether membrane repair efficiency or machineries are impaired dystrophin-deficient human or mice, however, is still under debate (Allen et al., 2016). This is partially due to technical difficulties, since assays currently available cannot differentiate membrane damage and repair. According to previous discussions, damage signaling still continues and causes more damage to the membrane after the initial irritation. Besides, mutations of muscle proteins often result in more fragile muscles (Allen et al., 2016). In the laser irradiation assay, for instance, increased FM dye in MD fibers may due to either exacerbated, continuing damage or impaired membrane repair, especially given that membrane repair is triggered immediately after damage (Allen et al., 2016).

This problem may be resolved when more knowledge is gained about the underlying mechanisms of membrane damage and repair.

Although direct evidence is still lacking, studies have shown MG53 was upregulated in MD patients (Waddell et al., 2011). Besides, the family member of dysferlin, myoferlin, is upregulated in dystrophin-null mice (Davis et al., 2000). However, the double knockout mice of dysferlin and dystrophin showed more severe phenotype than single knockout of any of them, implying the two proteins may regulate muscle function via different pathways (Han et al., 2011). In summary, it is still unclear whether the membrane repair pathway is affected in dystrophin-deficient mice. However, multiple pieces of evidence have suggested boosting membrane repair pathway in MD animal models ameliorates muscle phenotypes, as discussed below.

**3.2.1.1.3.3.2 Triggering membrane repair to treat MD**

Since membrane damage is an important step in the pathogenesis of MD, triggering membrane repair has been proposed as a strategy for therapeutics. Membrane sealant poloxamer 188 has been shown to improve cardiac failure in *mdx* mice (Yasuda et al., 2005). Myocytes isolated from *mdx* mice were susceptible to stretch-induced $Ca^{2+}$ overload, resulting in cell death (Yasuda et al., 2005). Poloxamer 188 corrected these changes *in vitro*, and injection of this drug into *mdx* mice also ameliorated dobutamine-induced heart failure (Yasuda et al., 2005). In another study, recombinant human MG53 (rhMG53) protein was able to promote plasma membrane repair in both muscle and non-muscle cells *in vitro* (Weisleder et al., 2012). Injection of the recombinant protein through different routes into *mdx* mice also showed improvement of muscle pathology (Weisleder et al., 2012). Together, these data suggest that membrane repair can be a potential target for MD therapy. Since ML1 activation has been shown to trigger lysosomal exocytosis, it is possible that activation of ML1 may also induce sarcolemmal repair in MD.

#### 3.2.1.2 Autophagic-lysosomal defects in MD

Impairment of autophagy has been reported in DMD (De Palma et al., 2014). Defects of autophagy were observed in *mdx* mice, due to abnormal activation of Akt and mTOR (De Palma et al., 2012; Pal et al., 2014). Additionally, NOX2 was also upregulated in *mdx* mice, leading to increased oxidative stress and impaired autophagosome formation (Pal et al., 2014). Furthermore, inhibition of the Akt-mTOR pathway and NOX2, as well as activation of autophagy through low protein diet or AMPK were shown to ameliorate dystrophic phenotypes in *mdx* mice (Bibee et al., 2014; De Palma et al., 2012; Pal et al., 2014; Pauly et al., 2012).

The defects of lysosomes in DMD is less clear. Increased NOX2 and oxidative stress in *mdx* mice were shown to impair lysosome formation, resulting in decreased LAMP1 level, whereas inhibition of NOX2 enhanced LAMP1 protein and ameliorated MD (Pal et al., 2014). However, in an earlier study, LAMP1-positive vesicles were found accumulated in *mdx* myofibers, consistent with immunohistochemistry of LAMP1 staining in *mdx* muscle sections (Duguez et al., 2013). Analysis of secretome profile of these fibers also revealed enrichment of LAMP1 protein, suggesting LAMP1-positive vesicles were undergoing active exocytosis (Duguez et al., 2013). These findings have demonstrated controversial roles of lysosomes in DMD which need to be resolved by further studies.

Defects in autophagic-lysosomal pathway have also been reported in other MDs. In a MD mouse model deficient of extracellular matrix protein collagen-6, autophagy is impaired via activation of Akt and mTOR, resulting in accumulation of abnormal mitochondria and SR and cell death (Grumati et al., 2010). More importantly, activation of autophagy in this disease model has been found beneficial and helps cellular clearance (Grumati et al., 2010). Overall, these studies

suggest that autophagy and lysosomes are impaired in MD, and boosting their function may be a potential treatment.

### 3.2.2 Lysosomes in other myopathies

Autophagic and lysosomal defects have been found in other myopathies. In muscle atrophy, the autophagic-lysosomal pathway is overactivated to remove proteins and organelles, contributing to the muscle loss (Bonaldo and Sandri, 2013). In patients of ischemia or with pressure overload, accumulation of autophagosomes was found in the hearts, which can be reproduced in animal or cell culture models (Terman and Brunk, 2005). Interestingly, drugs exacerbating ischemia such as β-adrenergic receptor agonist reduced autophagy, while drugs ameliorating heart failure like β-adrenergic receptor antagonist increased autophagy (Bahro and Pfeifer, 1987). Together, these data suggest that the autophagic-lysosomal system may contribute to the pathogenesis of myopathies.

## 4. Central goal of this study

Lysosomes are essential in cellular adaptation to stress. Through releasing $Ca^{2+}$ from lysosomal lumen, ML1 regulates multiple aspects of lysosomal function in health and disease. It was reported that by artificially activating ML1, TFEB translocates into nucleus, triggering downstream autophagic and lysosomal gene transcription. However, the endogenous cue for ML1 and TFEB activation under physiological conditions remains unknown. In Chapter II, I will try to answer this question and provide physiological significance for ML1 in regulation of TFEB and lysosomal adaptation.

Lysosomal $Ca^{2+}$ release via ML1 also triggers lysosomal exocytosis. Moreover, TFEB activation by ML1 leads to lysosomal biogenesis, meaning bigger pool for lysosomal exocytosis.

Thus, ML1 activation boosts lysosomal exocytosis via both short-term and long-term mechanisms. Lysosomal exocytosis has been shown important in membrane repair, and impaired membrane repair is linked to MD. Consistently, ML1-deficient human and mice exhibit compromised sarcolemmal integrity, as well as progressive MD. Therefore, ML1 activity is required for lysosomal exocytosis and sarcolemmal repair. Since ML1 activation upregulates lysosomal exocytosis, I hypothesize that activation of ML1 *in vivo* may help sarcolemmal repair and ameliorate MD. This is especially of clinical interest due to the availability of small molecule agonists of ML1, for these compounds can activate lysosomal exocytosis, as well as TFEB robustly and potently *in vitro.* By using genetic and pharmacological tools to upregulate ML1 in MD mouse models, I will investigate the effects of ML1 activation in MD (Chapter III & IV).

# CHAPTER II

## ML1 Is a ROS Sensor in Lysosomes That Regulates Autophagy


### Abstract

Cellular stresses, such as nutrient deprivation and oxidative bursts, trigger autophagy to remove damaged macromolecules and organelles. Lysosomes, the primary digestive force in the cell, "host" multiple stress-sensing mechanisms that trigger the coordinated biogenesis of autophagosomes and lysosomes. For example, TFEB, which regulates autophagy and lysosome biogenesis, is activated following the inhibition of mTOR. Here, we show that ROS activate TFEB via a mechanism that is dependent on lysosomal $Ca^{2+}$ but not mTOR. Exogenous application of oxidants or pharmacologically-increasing mitochondrial ROS levels results in direct, specific, and sustained activation of lysosomal ML1 channels, inducing $Ca^{2+}$ release from the lysosomal lumen. This activation triggers calcineurin-dependent TFEB nuclear translocation, autophagy induction, and lysosome biogenesis. When ML1 was genetically inactivated or pharmacologically inhibited, clearance of damaged mitochondria was blocked. Hence, ML1 is a ROS sensor localized on the lysosomal membrane that orchestrates an autophagy-dependent negative-feedback program to mitigate oxidative stress in the cell.

## Introduction

ROS are generated mainly as byproducts of mitochondrial respiration, and their cytosolic levels are tightly controlled by multiple anti-oxidant mechanisms (Scherz-Shouval and Elazar, 2011). A regulatory imbalance can result in elevated ROS levels and oxidative stress, which are believed to underlie a variety of metabolic and neurodegenerative diseases, as well as aging (Barnham et al., 2004; Scherz-Shouval and Elazar, 2011). Although high levels of ROS may additionally cause severe oxidative damage of proteins and lipids, a moderate ROS increase may serve as a sufficient "signal" to trigger autophagy and other cell-survival mechanisms (Barnham et al., 2004; Scherz-Shouval and Elazar, 2011). Autophagy can target oxidized and damaged biomaterials selectively for lysosomal degradation (Murrow and Debnath, 2013). Because unhealthy mitochondria may further augment ROS production, ROS-induced mitophagy is required for effective removal of excess ROS (Narendra et al., 2008; Scherz-Shouval and Elazar, 2011; Wang et al., 2012b). Hence, ROS and autophagy may constitute a negative feedback mechanism that mitigates oxidative stress and promotes cell survival.

Autophagy is a multi-step catabolic process that involves initiation (i.e., phagophore formation), autophagosome biogenesis, lysosome biogenesis, autophagosome-lysosome fusion, and lysosomal degradation (Murrow and Debnath, 2013; Shen and Mizushima, 2014). ROS are known to induce autophagy, but the mechanisms underlying this induction are poorly understood (Li et al., 2015; Scherz-Shouval and Elazar, 2011). ATG4, a cysteine protease and component of the cellular autophagy machinery, was recently identified as a direct target of ROS (Scherz-Shouval et al., 2007). Oxidized ATG4 promotes lipidation of LC3, a process that is essential for autophagy initiation (Scherz-Shouval et al., 2007). Because coping with prolonged oxidative stress may require sustained autophagy and sufficient lysosome supplies to achieve efficient

autophagosome-lysosome fusion in an ongoing manner, it is hypothesized that the lysosome-participating steps of autophagy need to be upregulated in a coordinated fashion by ROS signaling (Li et al., 2015; Medina et al., 2015; Scherz-Shouval and Elazar, 2011; Shen and Mizushima, 2014; Wang et al., 2015b). Indeed, given the essential role of lysosomes in autophagic clearance (Shen and Mizushima, 2014), inadequate lysosomal function inevitably leads to metabolic and neurodegenerative diseases, even though autophagy induction is often elevated under these pathological conditions (Murrow and Debnath, 2013; Shen and Mizushima, 2014).

Lysosomes are organelles that "host" important nutrient-sensitive molecules (Settembre et al., 2013b). Under starvation conditions, inhibition of mTOR results in a decrease in the phosphorylation of TFEB, a master transcriptional regulator of both autophagy and lysosomal biogenesis (Martina et al., 2012; Roczniak-Ferguson et al., 2012; Sardiello et al., 2009; Settembre et al., 2012). Dephosphorylated TFEB proteins translocate rapidly to the nucleus from the cytosol and lysosomes, inducing or increasing the expression of a unique set of genes that are related specifically to autophagosome and lysosome biogenesis (Roczniak-Ferguson et al., 2012; Settembre et al., 2012). It is not yet known whether the mTOR-TFEB pathway regulates lysosome function in response to other cellular stresses. Very recently, it was reported that TFEB nuclear translocation can also be stimulated by lysosomal $Ca^{2+}$ release through ML1 and the $Ca^{2+}$-dependent phosphatase calcineurin (Medina et al., 2015). However, it is unclear whether and how ML1 is activated by specific autophagy-inducing conditions, e.g., oxidative stress and nutrient starvation.

Lysosomes are required for quality-control regulation of mitochondria, and oxidative stress is a common feature of LSDs (Xu and Ren, 2015). Recent studies suggest that mitochondria, the major source of endogenous ROS, are localized in close physical proximity to lysosomes (Elbaz-

Alon et al., 2014; Li et al., 2015). Hence the lysosomal membrane is potentially an accessible and direct target of ROS signaling. Given that ROS reportedly regulate ion channels (Bogeski and Niemeyer, 2014), we *hypothesize* that lysosomal conductances, particularly through lysosomal $Ca^{2+}$ channels such as ML1, may mediate ROS-regulation of lysosomal function.

## Methods

**Molecular biology.** ML1 mutants were constructed with a site-directed mutagenesis kit (Qiagen) using mouse ML1 as the template. GCaMP7-ML1 was generated using a similar approach that was described previously for GCaMP3-ML1 (Shen et al., 2012). The mCherry-PARKIN construct was provided by Dr. Richard Youle through Addgene (Narendra et al., 2008). All constructs were confirmed by DNA sequencing.

**Mammalian cell culture.** COS-1 and HEK-293T were cultured in a 1:1 mixture of DMEM and Ham's F12 (DF12) media with 10% fetal bovine serum (FBS). HeLa and HAP1 cells were maintained in DMEM and IMDM, respectively, both with 10% FBS. Lipofectamine 2000 (Invitrogen) was used for the transfection of above cells. Human skin fibroblast cells from a mucolipidosis IV (ML1 KO) patient (clone GM02048) and a healthy control (clone GM05659) were obtained from the Coriell Institute for Medical Research (NJ, USA). Fibroblasts were transfected with a Neon electroporation kit (Invitrogen). Culture media were refreshed 18–24 h post-transfection, and cells were imaged 48 h post-transfection to allow sufficient recovery time following transfection.

**Stable cell lines.** The mCherry-PARKIN stable cell line was generated in HeLa cells under the selection of 500 mg/L Geneticin (G418, Invitrogen). The mCherry-TFEB stable cell line was generated using the Flip-In T-Rex 293 cell line (Invitrogen) under blasticidin selection. GFP–mRFP–LC3 and GFP-TFEB stable cell lines were kindly provided by Drs. David Rubinsztein

(Vicinanza et al., 2015) and Shawn M. Ferguson (Roczniak-Ferguson et al., 2012), respectively. Unless otherwise indicated, all cell lines were maintained in DMEM medium supplemented with 10% Tet-free FBS at 37 °C in a humidified 5% $CO_2$ incubator.

**Confocal imaging.** For TFEB and TFE3 immunofluorescence detection, cells were grown on glass coverslips and then fixed with 4% paraformaldehyde and permeabilized with 0.3% Triton X-100 after treatments. The cells were then blocked with 1% bovine serum albumin in phosphate buffered saline (PBS). Endogenous TFEB and TFE3 were recognized by incubating cells with anti-TFEB (1:200; Cell Signaling Technology) or anti-TFE3 antibody (1:1,000 Sigma) at 4 °C overnight. Cells were then washed 4–5 times with PBS and incubated with anti-rabbit secondary antibodies conjugated to Alexa Fluor 568 or 488 (Invitrogen) for 1 h. After three washes with PBS, coverslips were mounted on the slides with Fluoromount-G (Southern Biotech). Images were acquired with an Olympus Spinning-Disk Confocal microscope.

**Western blotting.** Cells were lysed with ice-cold RIPA buffer (Boston BioProducts) in the presence of 1× protease inhibitor cocktail (Sigma), 1 mM NaF, and 1 mM $Na_3VO_4$. Total cell lysates were mixed with 2× SDS loading buffer and were boiled at 95 °C for 10 min. Protein samples (10–100 μg) were then loaded and separated on 4–12% gradient SDS-PAGE gels (Invitrogen) and transferred to polyvinylidene difluoride membranes. The membranes were blocked for 1 h with 1% bovine serum albumin in PBS supplemented with 0.1% Tween20 and were incubated with antibodies against GFP (1:10,000; Covance), LC3 (1:2,000; Sigma), Lamp1 (1:1,000; Developmental Studies Hybridoma Bank), γ-tubulin (1:4,000; Sigma), TFEB (1:1,000; Cell Signaling Technology), TFE3 (1:4,000; Sigma). Bound antibodies were detected using horseradish peroxidase-conjugated anti-rabbit or anti-mouse secondary antibodies (1:5000) and

enhanced chemiluminescence reagent (Amersham Pharmacia Biotech). Band intensities were quantified in Image J software.

**$Ca^{2+}$ imaging.** Fura-2 $Ca^{2+}$ imaging was carried out in cells loaded with 5 μM Fura-2 AM (Invitrogen) at 37 °C for 1 h, as described previously (Shen et al., 2012). Fluorescence, at two excitation wavelengths, $F_{340}$ and $F_{380,}$ was recorded with an EasyRatioPro system (PTI). Fura-2 ratios ($F_{340}/F_{380}$) were used to monitor changes in intracellular [$Ca^{2+}$]. Lysosomal $Ca^{2+}$ release was measured under a zero-$Ca^{2+}$ external solution, which contained 145 mM NaCl, 5 mM KCl, 3 mM $MgCl_2$, 10 mM glucose, 1 mM EGTA, and 20 mM HEPES (pH 7.4); free $[Ca^{2+}]_o$ < 10 nM (estimated with Maxchelator software http://maxchelator.stanford.edu/).

GCaMP imaging was performed in HeLa cells transfected with GCaMP7-ML1, a lysosome-targeted genetically-encoded $Ca^{2+}$ sensor (Shen et al., 2012). The fluorescence intensity at 488 nm (F488) was recorded at 37 ºC with the spinning disk confocal live-imaging system, which included an Olympus IX81 inverted microscope, a 60X or 100X objective (Olympus), a CSU-X1 scanner (Yokogawa), an iXon EM-CCD camera (Andor), and MetaMorph Advanced Imaging acquisition software v.7.7.8.0 (Molecular Devices).

**ROS imaging.** ROS levels were detected with a CM-H2DCFDA dye assay (Invitrogen). Briefly, cells were incubated with 2.5–5 μM CM-H2DCFDA in the culture media without FBS at 37 °C for 30 min, and then recovered in the complete media for 10 min before imaging. The fluorescence was visualized with a DP71 camera (Olympus) mounted on an Olympus IX-71 inverted microscope. Images were captured at 20× magnification with DPController software. The fluorescence intensity was quantified with the ImageJ software (NIH).

**Mitochondrial membrane potential measurement.** Human fibroblasts were incubated with 1 μM JC-1 (Invitrogen) in complete culture medium at 37 °C for 30 min before imaging. The fluorescence was detected at 520 nm for J-monomer and 600 nm for J-aggregates (excitation wavelength= 488 nm), respectively, by a Leica confocal microscope.

**Whole-endolysosome electrophysiology.** Isolated endolysosomes were subjected to whole-endolysosomal electrophysiology by a modified patch-clamp method (Dong et al., 2010b; Wang et al., 2012b). Briefly, cells were treated with 1 μM vacuolin-1 overnight to selectively increase the size of late endosomes and lysosomes (Cerny et al., 2004). Enlarged vacuoles were released into the dish by mechanical disruption of the cell membrane with a fine-tip glass electrode. Unless otherwise indicated, vacuoles were bathed continuously in an internal (cytoplasmic) solution containing 140 mM $K^+$-Gluconate, 4 mM NaCl, 1 mM EGTA, 2 mM $Na_2$-ATP, 2 mM $MgCl_2$, 0.39 mM $CaCl_2$, 0.1 mM GTP, and 10 mM HEPES (pH adjusted with KOH to 7.2; free $[Ca^{2+}]_i \approx$ 100 nM). The pipette (luminal) solution contained 145 mM NaCl, 5 mM KCl, 2 mM $CaCl_2$, 1 mM $MgCl_2$, 10 mM HEPES, 10 mM MES and 10 mM glucose (pH adjusted to 4.6 with NaOH). The whole-endolysosome configuration was achieved as described previously (Wang et al., 2012a). After formation of a gigaseal between the patch pipette and an enlarged endolysosome, voltage steps of several hundred millivolts with a millisecond duration were applied to break into the vacuolar membrane (Wang et al., 2012a). All bath solutions were applied via a fast perfusion system that produced a complete solution exchange within a few seconds. Data were collected via an Axopatch 2A patch clamp amplifier, Digidata 1440, and processed with pClamp 10.0 software (Axon Instruments). Whole-endolysosome currents were digitized at 10 kHz and filtered at 2 kHz. All experiments were conducted at room temperature (21–23 °C) and all recordings were analyzed in pCLAMP10 (Axon Instruments) and Origin 8.0 (OriginLab).

**Whole-cell and inside-out patch-clamp electrophysiology.** Whole-cell recordings were performed with pipette electrodes (resistance 3–5 MΩ) filled with (in mM): 1) 133 Cs methanesulfonate, 4 NaCl, 10 EGTA, 2 $Na_2$-ATP, 2 $MgCl_2$, and 20 HEPES (pH 7.2, adjusted with CsOH; free $[Ca^{2+}]_i$ < 10 nM), or 2) 140 K-gluconate, 4 NaCl, 1 EGTA, 2 $MgCl_2$, 0.39 $CaCl_2$ , and 20 HEPES (pH 7.2; free $[Ca^{2+}]_i$ ~ 100 nM). The standard extracellular bath solution (Tyrode's solution) contained (in mM): 153 NaCl, 5 KCl, 2 $CaCl_2$, 1 $MgCl_2$, 20 HEPES, and 10 glucose (pH 7.4). For excised inside-out patch recordings, pipette electrodes with 1–2 MΩ resistance were used. The bath solution and pipette solution were the same as those used for whole-endolysosome recordings.

**Reagents.** The following reagents were purchased: ML-SA1 (Princeton BioMolecular Research Inc), ML-SI3 (AKOS), Torin 1 (Tocris), NAC (Sigma), CCCP (Sigma), $H_2O_2$ (Sigma), ChT (Sigma), NSC (Sigma), DTNP (Sigma), 4-HNE (Caymen), Ionomycin (Sigma), BAPTA-AM (Invitrogen), and vacuolin-1 (Calbiochem).

**Data analysis.** Data are presented as mean ± standard errors of the mean (SEM). Statistical comparisons of confocal images were performed with analyses of variance (ANOVA). Protein expression levels were compared using paired *t*-test. A *P* value < 0.05 was considered statistically significant.

## Results

### Oxidants and endogenous ROS activate lysosomal ML1 channels directly and specifically.

We investigated the effects of oxidants on whole-endolysosome conductances in vacuolin-1-enlarged endolysosomes (Dong et al., 2010b; Wang et al., 2012b) under a variety of experimental conditions in various cell types. In cells overexpressing enhanced green fluorescent

protein (EGFP)-tagged ML1 (**Fig. 2.1A**), whole-endolysosome ML1-mediated currents ($I_{TRPML1}$) were activated strongly by bath application of chloramine T (ChT), a non-selective strong oxidant. ChT-activated $I_{TRPML1}$ was inhibited by the mucolipin-specific synthetic inhibitors [ML-SIs], but at concentrations higher than that are typically used to block ML1 (Wang et al., 2015b). Several other commonly-used oxidants, including NaOCl, N-chlorosuccinimide, thimerosal, $H_2O_2$, and tert-butyl hydroperoxide (TBHP) also readily, albeit less potently, activated $I_{TRPML1}$ (**Fig. 2.1B**). On the other hand, cysteine-modifying oxidants that are known to modulate several TRP channels, such as DTNP and DTNB (Chuang and Lin, 2009), failed to activate $I_{TRPML1}$ (**Fig. 2.1B**). Likewise, the NO donor SNAP and the reactive lipid peroxidation intermediate 4-HNE (Kozai et al., 2014) did not affect $I_{TRPML1}$ (**Fig. 2.1B**). Unlike mouse and human ML1, oxidants failed to activate several other closely-related lysosome-localized channels, which include mouse TRPML2, mouse TRPML3, mouse TPC2 (**Fig. 2.1D**), and a zebrafish homolog of mammalian ML1 (zTRPML1.1; **Fig. 2.1C, D**). Taken together, these results suggest that oxidants activate lysosomal ML1 channels specifically via a distinct and novel mechanism.

Because mitochondria are the primary source of endogenous ROS (Narendra et al., 2008; Scherz-Shouval and Elazar, 2011; Wang et al., 2012b), to evaluate the effect of endogenous ROS on ML1, we exposed cells to mitochondrial respiration inhibitor carbonyl cyanide m-chlorophenylhydrazone (CCCP), which is commonly used to induce ROS production, mitochondrial damage, and subsequent mitophagy (Benard et al., 2007; Nishikawa et al., 2000). Following 1 hour exposure to CCCP (5–10 μM), intracellular ROS levels increased significantly (**Fig. 2.1E**), as reflected by visualization of CM-H2DCFDA, a ROS-sensitive fluorescent dye (Nishikawa et al., 2000). N-acetyl-cysteine (NAC), a commonly used membrane-permeable antioxidant (Underwood et al., 2010), abolished CCCP-induced increases in ROS levels (**Fig.**

**2.1E**). Because drugs like CCCP might produce ROS-independent effects due to mitochondrial depolarization/damage in addition to ROS production (Benard et al., 2007; Nishikawa et al., 2000), NAC sensitivity test was routinely performed in various cellular assays in the current study.

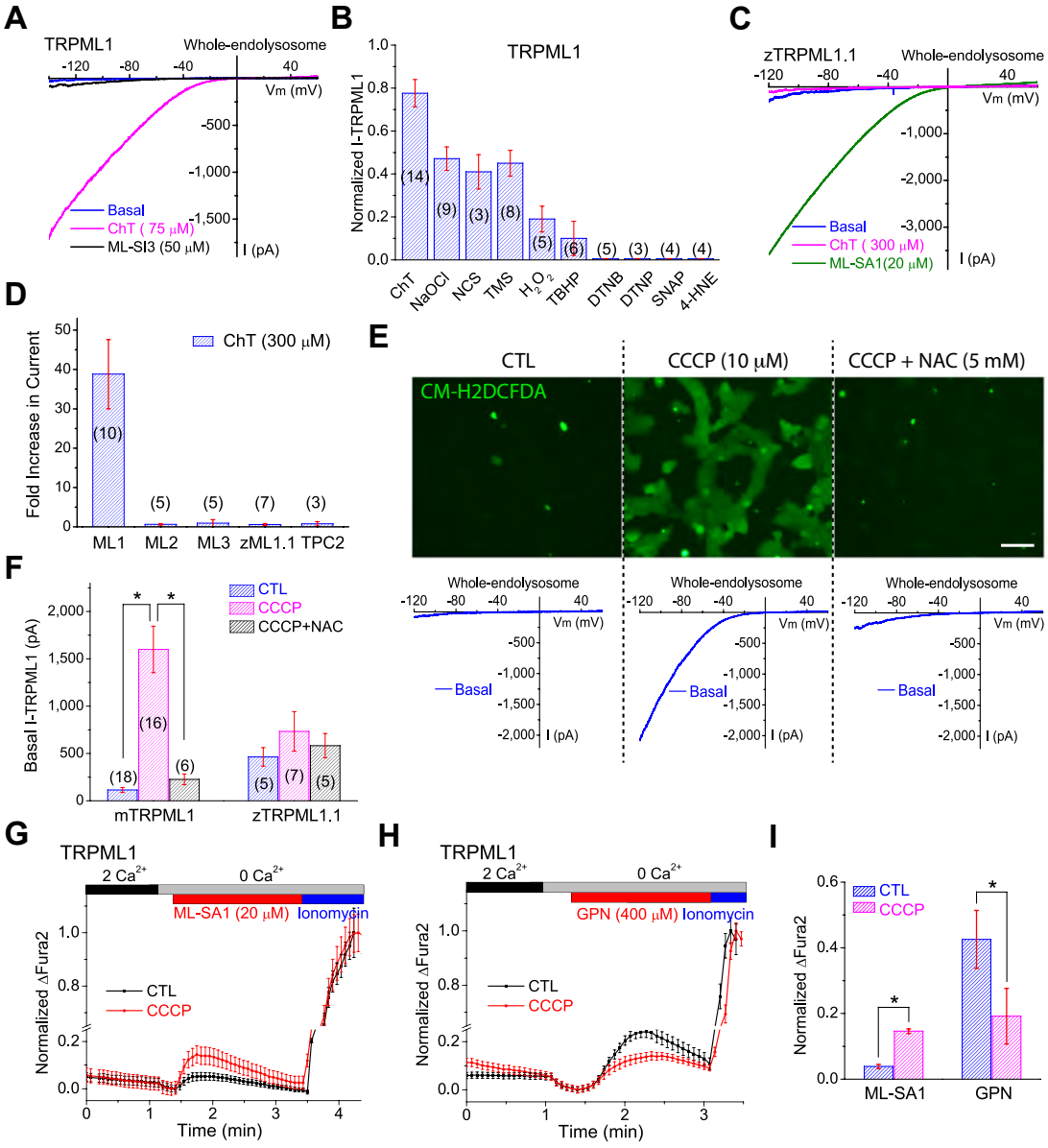


**Figure 2.1 Direct and specific activation of lysosomal ML1 channels by oxidants and endogenous ROS.** (**A**) Representative traces of basal (blue), ChT-activated (magenta), and ML-SI3-inhibited (black) $I_{TRPML1}$ from whole-endolysosomal patch clamp of EGFP-ML1-

overexpressing COS1 cells. (**B**) Oxidant-specific activation of $I_{TRPML1}$. Active oxidants included ChT (150 μM), NaOCl (3 mM), N-chlorosuccinimide (NCS, 500 μM), thimerosal (TMS, 50 μM), $H_2O_2$ (10 mM), and tert-butyl hydroperoxide (TBHP, 1 mM). Other tested oxidants included cysteine-specific oxidants (DTNB and DTNP, both at 100 μM), an NO-donor (SNAP, 100 μM), and a reactive lipid (4-HNE, 300 μM). The effects of oxidants were normalized to that of ML-SA1 (20 μM). (**C**) Insensitivity of zTRPML1.1 to ChT. (**D**) ChT activated mTRPML1 specifically, but not mTRPML2, mTRPML3, zTRPML1.1, or mTPC2. (**E**) Upper panels: application of CCCP increased the fluorescence intensity of CM-H2DCFDA (green) *vs*. the DMSO-treated control (CTL) group. The increase was inhibited by co-application of NAC (5 mM). Lower panels: representative traces of basal whole-endolysosomal currents under each condition (CTL, CCCP, CCCP+NAC) in ML1-expressing COS1 cells. Scale bar = 50 μm. (**F**) Summary of CCCP pretreatment effects in basal $I_{TRPML1}$ and $I_{zTRPML1.1}$. *$P < 0.05$, ANOVA. (**G**) Pretreatment of CCCP (10 μM) for 1 h increased ML-SA1-induced $Ca^{2+}$ release measured by Fura-2 imaging in ML1-expressing HEK293 cells. (**H**) CCCP pretreatment reduced GPN-induced lysosomal $Ca^{2+}$ release, which is presumed to reflect the lysosomal $Ca^{2+}$ store. Mean values (± SEM) are shown for more than 30 cells per coverslip. (**I**) Quantification of results shown in **G** and **H** from at least three independent experiments (mean ± SEM). *$P < 0.05$, paired *t*-tests. Data are presented as mean ± SEM. Figure generated by Drs. Xiaoli Zhang and Xiping Cheng from Xu lab.

Remarkably, after CCCP pretreatment in ML1-expressing COS-1 cells, basal whole-endolysosome $I_{TRPML1}$ was increased significantly (**Fig. 2.1E, F**). The CCCP-induced increase in basal $I_{TRPML1}$, however, was largely abolished by NAC (**Fig. 2.1E, F**). Next, we investigated the effect of CCCP-generated mitochondrial ROS on lysosomal $Ca^{2+}$ release. In COS-1 cells transfected with EGFP-ML1, ML-SA1-evoked lysosomal $Ca^{2+}$ release (Wang et al., 2015b) was increased upon CCCP (10 μM) pretreatment for 1 hour (**Fig. 2.1G**). The constant $Ca^{2+}$ release in CCCP-treated cells, presumably mediated by constitutive activity of ML1, is expected to continuously decrease $Ca^{2+}$ stores in lysosomes. To test this possibility, GPN, a lysosome-specific substrate that causes channel-independent "leakage" of $Ca^{2+}$, was employed to probe lysosome $Ca^{2+}$ stores (Morgan et al., 2015). In contrast to ML-SA1-induced release, GPN-induced $Ca^{2+}$ release was reduced in CCCP-treated cells (**Fig 2.1G-I**). Taken together, these results suggest that

lysosomal ML1 is activated or sensitized by mitochondria-generated ROS, mediating more $Ca^{2+}$ release from lysosomes.

**ML1 is specifically required for ROS-induced autophagy induction.**

CCCP-induced mitochondrial depolarization and/or ROS production is known to induce general autophagy, and mitophagy if there is extensive mitochondrial damage (Wang et al., 2012b). To investigate the role of ML1 in this process, we measured autophagic induction in HeLa cells stably expressing mRFP-GFP-LC3 (Vicinanza et al., 2015). Because LC3-II is recruited specifically to phagophores and autophagosomes, and because of the pH sensitivity of the GFP signal, $mRFP^+$ $GFP^+$ and $mRFP^+$ $GFP^-$ puncta indicate non-acidified autophagosomes and acidified autolysosomes, respectively (Murrow and Debnath, 2013). Three-hour exposure to CCCP (5 μM) led to a dramatic increase in autophagosomes, and this increase could be prevented by 3-methyladenine (3-MA), an inhibitor of autophagy induction (Murrow and Debnath, 2013) (**Fig. 2.2A-D** ). All these effects of CCCP were abolished by NAC (**Fig. 2.2A, B**), suggesting that CCCP-induced autophagy is mediated exclusively by ROS. Consistent with the hypothesis that ROS mediated the CCCP effect, $H_2O_2$ (100 μM, 3 h) treatment was sufficient to enhance autophagosome formation (**Fig. 2.2E, F**). Remarkably, CCCP- and $H_2O_2$- induced autophagosome formation was blocked by BAPTA-AM (membrane-permeable $Ca^{2+}$ chelator (Morgan et al., 2015)) or ML-SI3 (**Fig. 2.2A, B, E, F**), suggesting that ROS induce autophagy via a $Ca^{2+}$- or ML1-dependent mechanism. On the other hand, artificial activation of ML1 by the synthetic agonist ML-SA1, or the more potent agonists ML-SA3 and ML-SA5 (Wang et al., 2015b), was sufficient to induce $mRFP^+$ $GFP^+$ LC3 puncta formation, but these effects were insensitive to NAC treatment (**Fig. 2.3**). Taken together, these results suggest that CCCP treatment may increase mitochondrial ROS, thereby activating ML1 to induce autophagy.

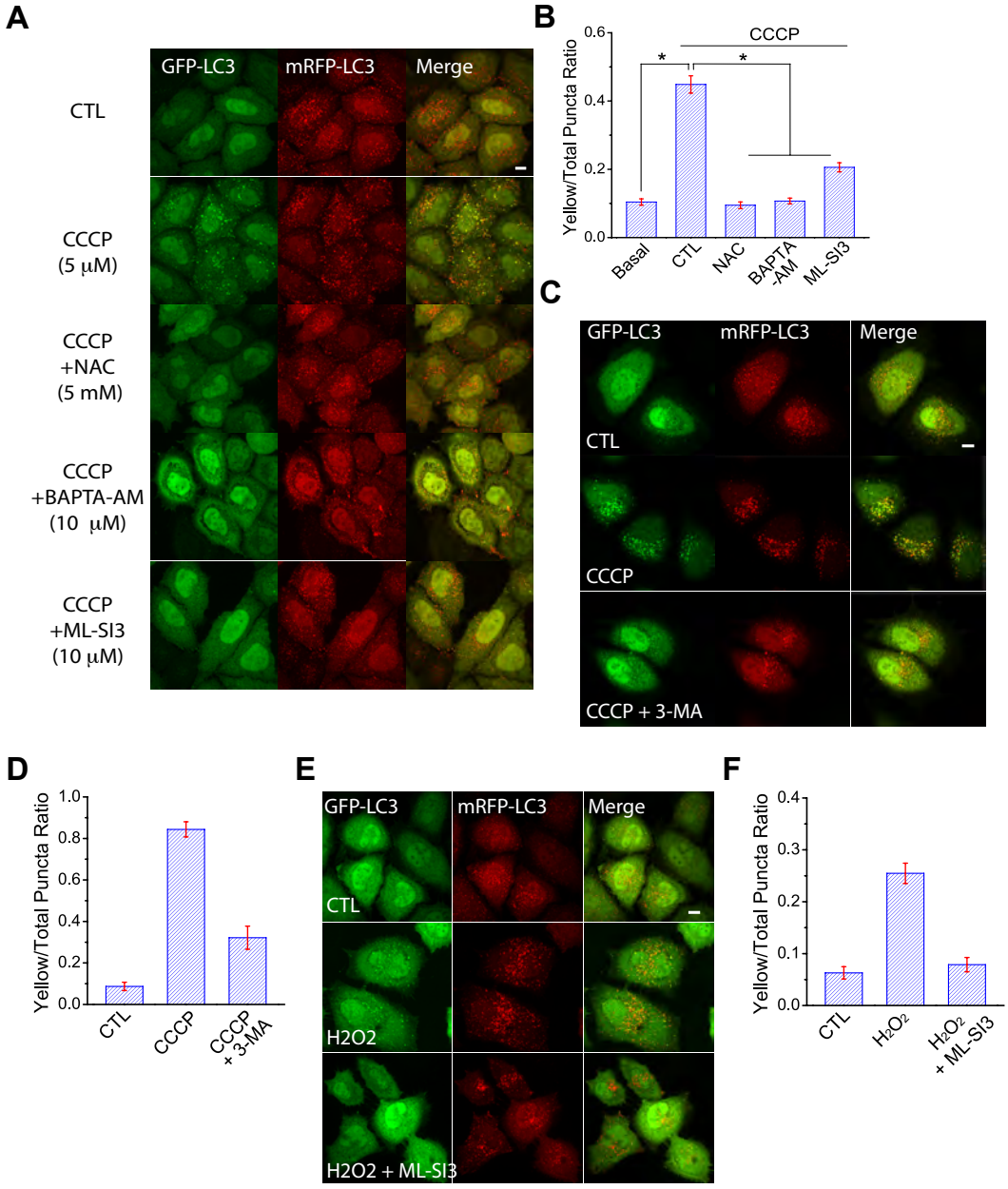


**Figure 2.2 ROS-dependent autophagy induction requires $Ca^{2+}$ and ML1.** (**A**) In HeLa cells stably expressing mRFP-GFP-LC3, CCCP treatment (5 μM for 3 h) increased the formation of autophagosomes, "visualized" as $mRFP^+$ $GFP^+$ puncta. Co-treatment with NAC, BAPTA-AM, or ML-SI3 abolished the increases. Scale bar = 10 μm. (**B**) Quantification of various treatment conditions on CCCP-induced autophagosome formation. $*P < 0.05$, ANOVA. (**C, D**) CCCP pretreatment (5 μM) for 3 h increased the number of $GFP^+mRFP^+$ LC3 puncta in GFP-mRFP-LC3 stable cells, and the increase was blocked by co-application of 3-MA (5 mM), a drug inhibiting autophagosome formation. **(E, F)** $H_2O_2$ treatment (100 μM for 3 h) increased the number of $GFP^+mRFP^+$ LC3 puncta in HeLa cells, and the increase was inhibited by co-application of ML-

SI3. Data are presented as mean ± SEM; *$P < 0.05$, paired *t*-tests. Images in panel A was taken by Dr. Xiping Cheng from Xu lab.

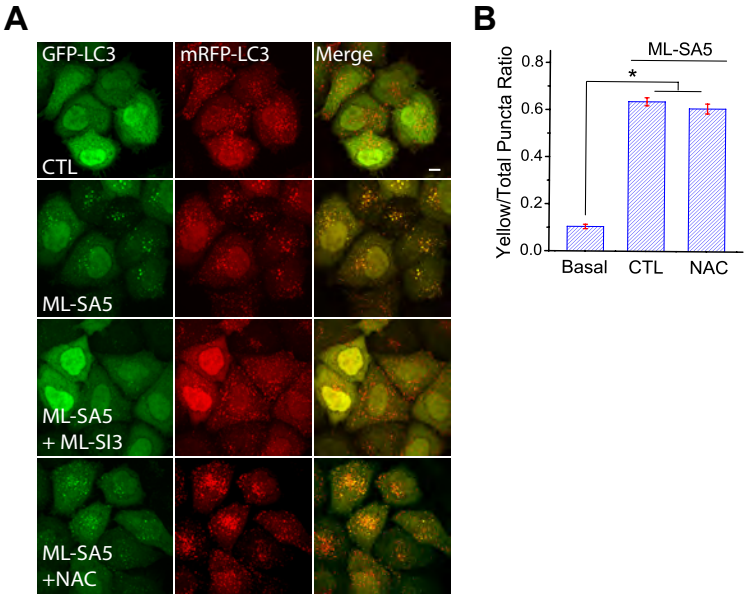


**Figure 2.3 ML1 activation is sufficient to promote autophagosome formation**. (**A**) Effects of ML-SA5 on $GFP^+$ LC3 puncta formation in the presence and absence of ML-SI3 or NAC. Scale bar = 10 μm. (**B**) NAC did not affect ML-SA5-induced autophagosome formation. Data are presented as mean ± SEM. *$P < 0.05$, paired *t*-test.

### ML1 is required for the clearance of damaged mitochondria

Sustained elevation of ROS levels can cause severe oxidative damage to mitochondria, triggering mitophagy (Scherz-Shouval and Elazar, 2011). ROS-induced mitophagy may facilitate the removal of damaged mitochondria and excess ROS products in the cell (Scherz-Shouval and Elazar, 2011). To investigate the role of ML1 in ROS-induced autophagic clearance of damaged mitochondria, we induced severe mitochondrial damage and fragmentation by exposing cells to high concentrations of CCCP for extended periods of time (e.g., 10–20 μM for 3 h). Using JC-1 fluorescence dye (Smiley et al., 1991) to monitor mitochondrial membrane potential, we found that such CCCP treatment resulted in rapid depolarization of mitochondria (data not shown).

PARKIN proteins are known to be recruited specifically to the damaged mitochondria, which are then autophagocytosed and delivered to lysosomes for degradation (Narendra et al., 2008). In HeLa cells stably expressing mCherry-Parkin (PARKIN stable cells), PARKIN-positive puncta were increased significantly following CCCP treatment (**Fig. 2.4A, B**). After CCCP washout, the majority of the PARKIN-positive puncta disappeared, and most mitochondria returned to the repolarized state (**Fig. 2.4A-D**). In contrast, acute inhibition of ML1 with ML-SI3 or ML-SI4 during the CCCP treatment phase was sufficient to block the disappearance of PARKIN, even though ML-SI3 or ML-SI4 alone did not induce the prolonged accumulation of PARKIN (**Fig. 2.4A, B**). Furthermore, JC-1 recovery was also blocked in ML-IV fibroblasts, compared with WT fibroblasts (**Fig. 2.4C, D**). Taken together, these results suggest that ML1 is required for ROS- and mitophagy-dependent clearance of damaged mitochondria.

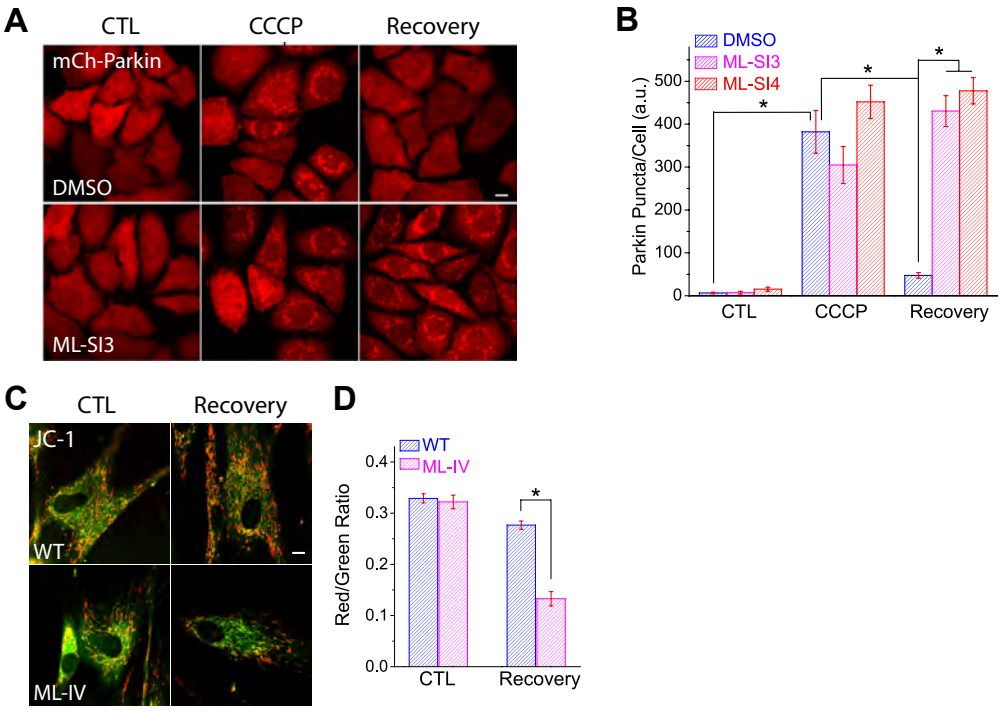


**Figure 2.4 ML1 is required for autophagic clearance of damaged mitochondria.** (**A**) Effects

of ML-SI3 (10 μM) co-administration on the accumulation of PARKIN-positive puncta (red) induced by CCCP treatment (10 μM for 3 h) followed by 1 h recovery (without CCCP) in PARKIN stable cells. Scale bar = 10 μm. (**B**) Quantitative analysis of ML-SI3 and ML-SI4 effects on the clearance of PARKIN puncta. (**C**) Effects of CCCP treatment on mitochondrial membrane potential monitored by JC-1 fluorescent dyes in WT and ML-IV fibroblasts. After CCCP (10 μM for 3 h) treatment, removal of CCCP for 1 h led to repolarization (re-energization) of mitochondrial membrane potential (green: J monomer, de-energized; red: J aggregates, energized) in WT but not ML-IV cells. Scale bar = 10 μm. (**D**) The ratio of red to green fluorescence of JC-1 was quantified for more than 30 randomly selected cells. Means are shown with SEM; **P* < 0.05, ANOVA.

**ML1 mediates ROS-, but not starvation-induced TFEB activation**

We next investigated the mechanisms by which ML1 activation leads to enhanced autophagy induction and mitophagic clearance. TFEB regulates biogenesis of both autophagosomes and lysosomes (Settembre et al., 2011). Recent evidence suggests that ML1 and TFEB may form a positive-feedback loop in regulating autophagy (Medina et al., 2015; Wang et al., 2015b). In HEK293 cells stably expressing mCherry-TFEB (TFEB stable cells), we found that a mild increase in ROS levels due to CCCP treatment (5 μM for 1 h) was sufficient to induce TFEB nuclear translocation (nuclear to cytosol ratio increased from 0.54 ± 0.02 to 2.67 ± 0.14; see **Fig. 2.5A, B**). Likewise, endogenous TFEB in human fibroblasts was also activated (i.e., underwent nuclear translocation) in response to CCCP administration (**Fig. 2.5C, D**). Likewise, rotenone (10 μM for 2 h), another drug interrupting mitochondrial respiratory chain (**Fig. 2.6B, C**), or $H_2O_2$ treatment (50 μM for 1 h) was also sufficient to induce TFEB translocation in WT HeLa cells (**Fig. 2.6A, D**). Remarkably, in all cases, TFEB-nuclear translocation, induced by CCCP, rotenone, or $H_2O_2$, was largely blocked by NAC, BAPTA-AM, ML-SI3, or ML1 KO (**Fig. 2.5A-D** and **Fig. 2.6A, D**).

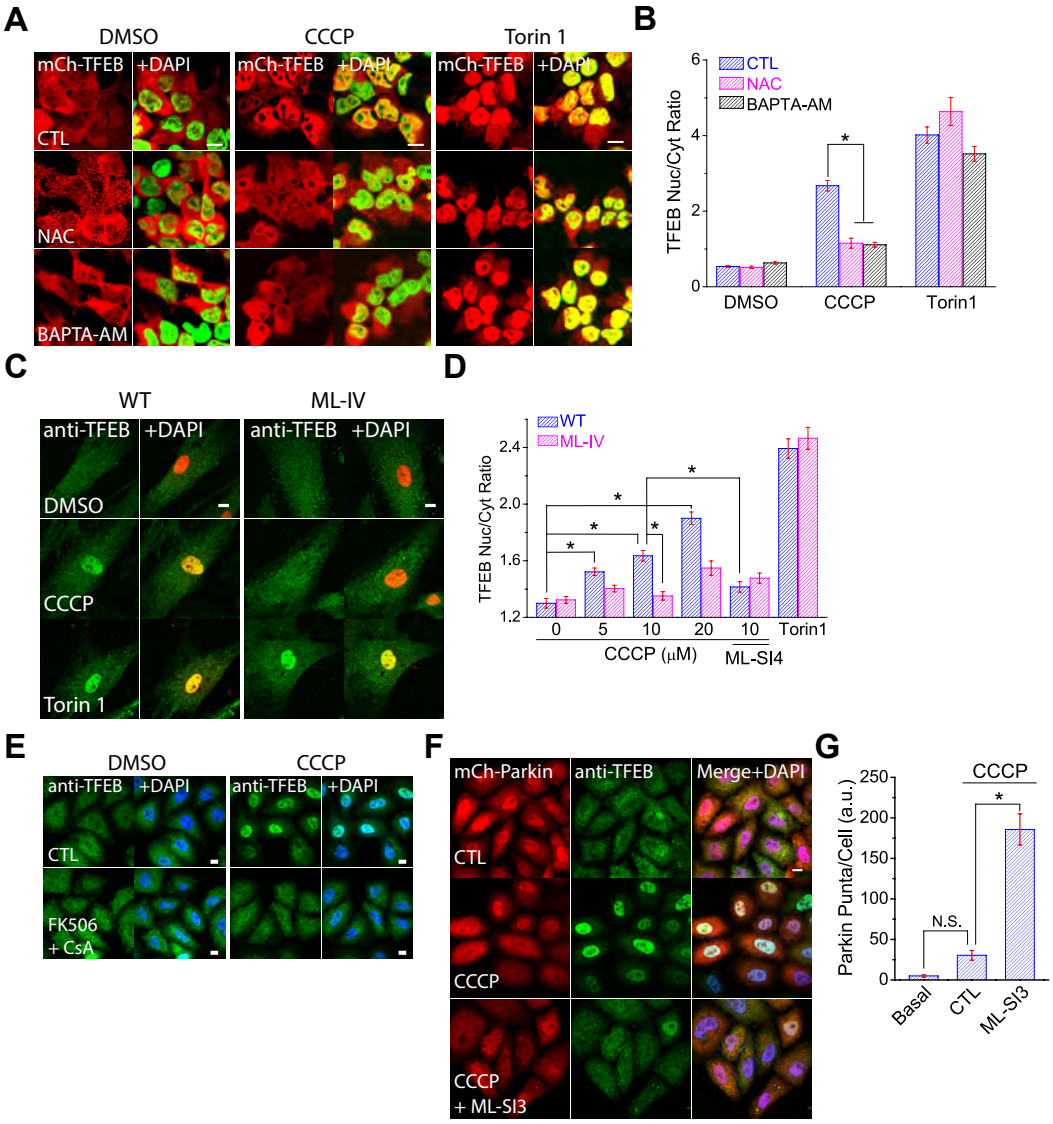


**Figure 2.5 ML1 channel activity is required for ROS-induced TFEB nuclear translocation.** (**A**) Differential effects of BAPTA-AM and NAC on CCCP- and Torin-1-induced TFEB nuclear translocation in HEK293 cells stably expressing mCherry-TFEB. Cells were treated with CCCP (5 μM) and Torin 1 (1 μM) for 1 h to induce TFEB nuclear translocation. Nuclei were counterstained with DAPI (pseudo-colored in green). Scale bar = 10 μm. (**B**) Ratio of nuclear *vs.* cytosolic TFEB (>100 cells per experimental condition). (**C**) CCCP (10 μM for 1 h) induced accumulation of TFEB, detected by anti-human TFEB antibody, in the nuclei of WT, but not ML-IV cells. In contrast, Torin-1 induced TFEB nuclear translocation in both WT and ML-IV cells. Nuclei were labeled with DAPI (pseudo-colored in red). Scale bar = 10 μm. (**D**) Average ratios of nuclear *vs.* cytosolic TFEB immuoreactivity (>100 randomly-selected cells per experiment). ML-SI4 (10 μM) inhibited TFEB nuclear translocation induced by CCCP (10 μM) treatment for 1 h. **(E)** CCCP (5 μM for 1 h)-induced TFEB nuclear translocation was blocked by co-application of FK506 (5 μM) and CsA (10 μM) in HeLa cells. Nuclei were counterstained with DAPI. Scale bar = 10 μm. (**F**) Inhibition of ML1 blocks TFEB nuclear translocation and promotes CCCP-induced

mitochondrial damage. In PARKIN stable cells, CCCP treatment (5 μM for 3 h) led to minimal PARKIN aggregation, but strong TFEB nuclear translocation. Co-application of ML-SI3 enhanced PARKIN accumulation but inhibited TFEB activation. Scale bar = 10 μm. (**G**) Quantification of PARKIN puncta shown in **F** (>50 cells per experimental condition; mean ± SEM). **P* < 0.05, ANOVA. Images from panels A&C were taken by Dr. Xiping Cheng from Xu lab.

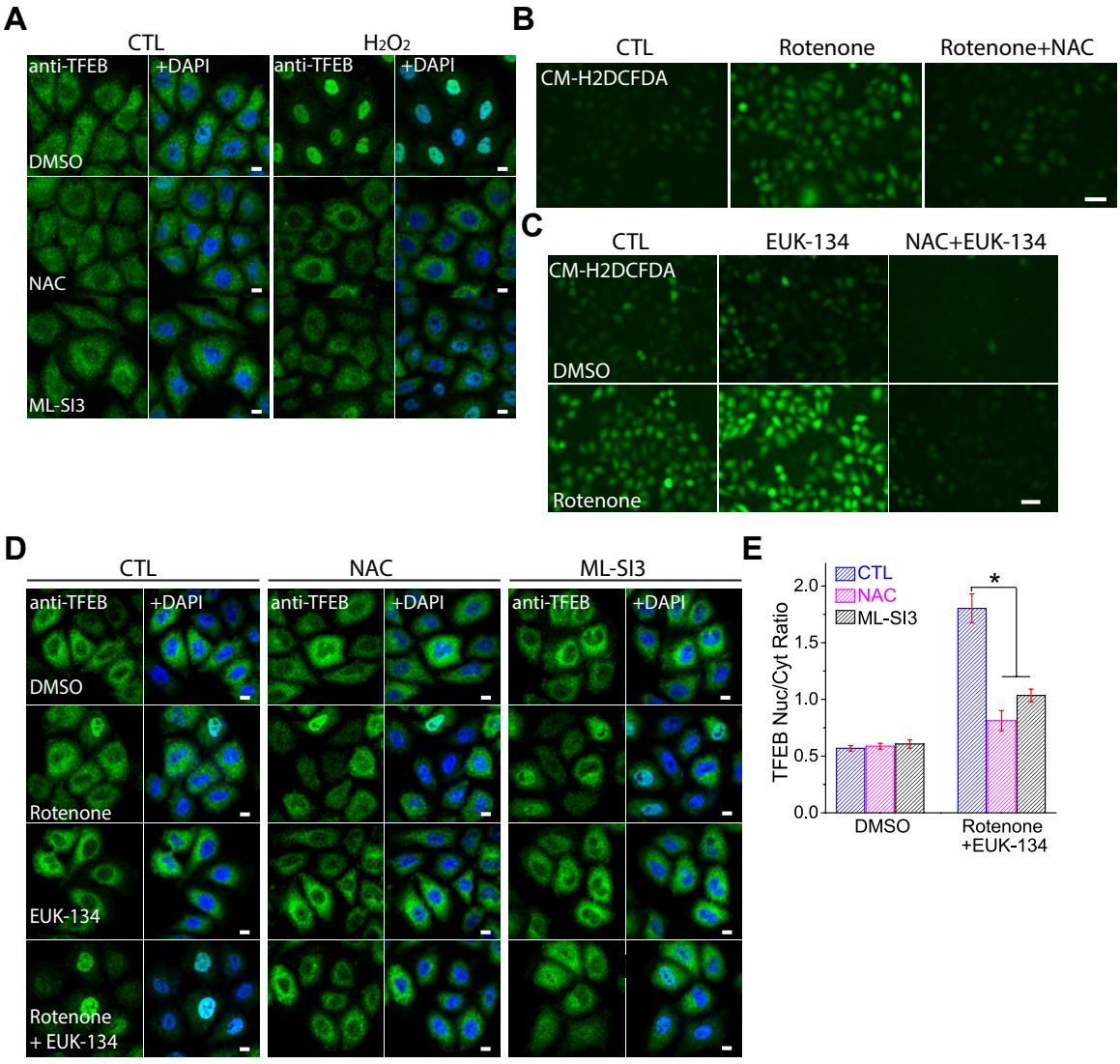


**Figure 2.6 Different oxidants induce TFEB nuclear translocation. (A)** TFEB nuclear translocation induced by $H_2O_2$ (50 μM) was effectively blocked by NAC or ML-SI3. Nuclei were counterstained with DAPI. Scale bar = 10 μm. **(B)** Rotenone (10 μM) treatment for 1 h increased the fluorescence intensity of CM-H2DCFDA compared with the DMSO-treated control group (CTL). The increase was inhibited by co-application of NAC. Scale bar = 50 μm. **(C)** ROS levels (detected with CM-H2DCFDA) were augmented by rotenone (10 μM, 2h), which was further increased by co-application of EUK-134. NAC abolished CM-H2DCFDA fluorescence in cells

treated with rotenone alone, or together with EUK-134. Scale bar = 50 μm. **(D)** Although rotenone alone only induced mild TFEB nuclear translocation, co-application of EUK-134 (a synthetic dismutase/catalase mimetic) markedly enhanced TFEB activation. Both NAC and ML-SI3 blocked rotenone-induced TFEB activation. Nuclei were counterstained with DAPI. Scale bar = 10 μm. **(E)** Quantification of **D** from at least 50 cells for each experimental condition. Images from panels B&C were taken by Dr. Xiaoli Zhang from Xu lab.

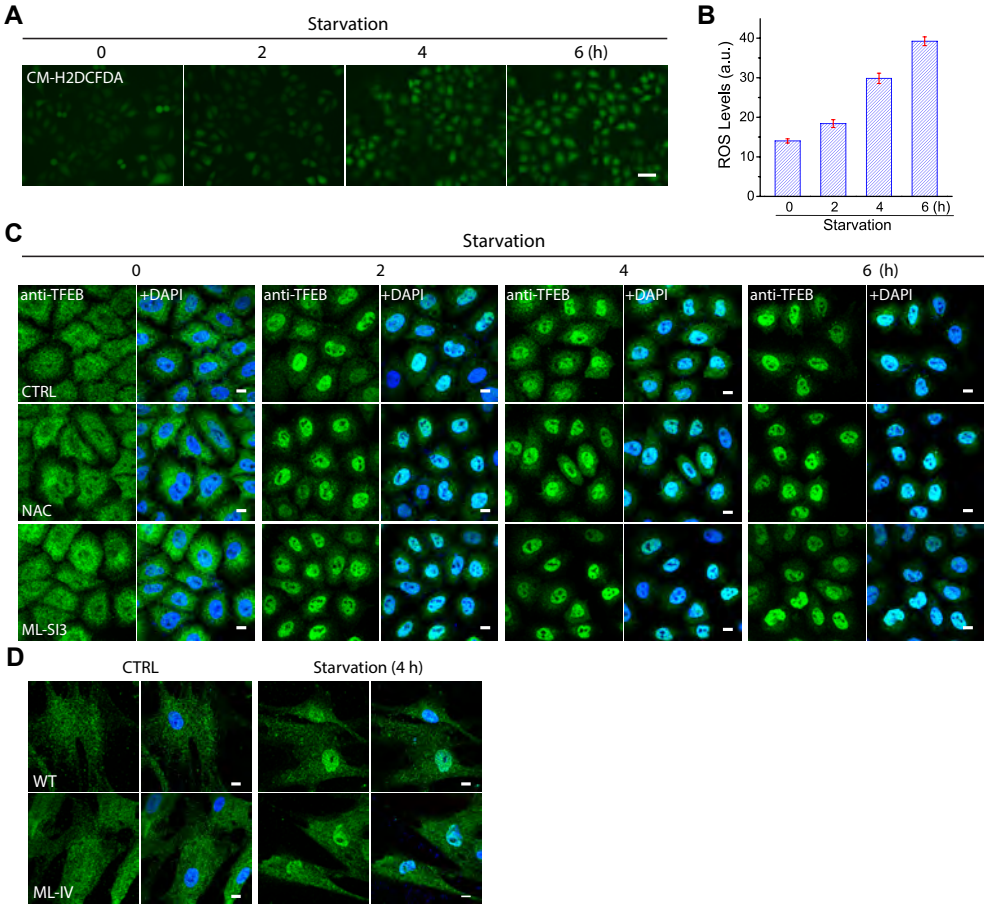


**Figure 2.7 Starvation-induced TFEB nuclear translocation does not require ROS or ML1.** **(A, B)** Starvation-induced time-dependent increment in ROS levels as quantified in **B**. Starvation is induced by deprivation of both FBS and amino acids in the culture media. Scale bar = 50 μm. **(C)** Neither NAC not ML-SI3 diminished TFEB activation induced by short term (2, 4, 6 h) starvation. Nuclei were counterstained with DAPI. Scale bar = 10 μm. **(D)** Starvation (4h) activated TFEB in both WT and ML-IV human fibroblasts. Nuclei were counterstained with DAPI. Scale bar = 10 μm. Images from panel A were taken by Dr. Xiaoli Zhang.

ROS levels are reportedly elevated during starvation (Scherz-Shouval et al., 2007), a condition that activates TFEB and promotes autophagy (Medina et al., 2015). Indeed, short-term

(4-6 hrs) starvation increased ROS levels and caused TFEB nuclear translocation (**Fig. 2.7**). However, starvation-induced TFEB activation was not blocked by NAC, nor by ML-SI3 (**Fig. 2.7C**). These results suggest that starvation may induce TFEB-activation via mechanisms that do not require ML1. Consistently, 4h-starvation induced TFEB nuclear translocation in both WT and ML-IV human fibroblasts (**Fig. 2.7D**). Collectively, these results suggest that whereas ROS activation of ML1 is sufficient to activate TFEB, additional ML1-independent mechanisms may be responsible for starvation-induced TFEB activation.

CCCP-mediated TFEB translocation was largely abolished in ML-IV fibroblasts, as well as cells treated with ML-SI3 (**Fig. 2.5C, D**). Furthermore, ML-SA5 alone was sufficient to cause TFEB nuclear translocation in WT cells (**Fig. 2.8**). This ML-SA5-induced TFEB translocation was sensitive to BAPTA-AM, but not NAC (**Fig. 2.8C-E**). Neither CCCP nor ML-SA5 affected the activity of mTOR, as reflected by levels of phosphorylated S6K, a primary mTOR substrate (Settembre et al., 2013b) (**Fig. 2.8F**). On the other hand, Torin-1–induced TFEB nuclear translocation, observed in both WT and ML-IV cells (**Fig. 2.5C**), was not sensitive to BAPTA-AM (**Fig. 2.5A**). Hence, ML1 and lysosomal $Ca^{2+}$ appear to play a specific role in ROS-induced, but not the general mTOR-inhibition-mediated, autophagy. More strikingly, in PARKIN stable cells, when TFEB translocation was blocked by ML-SI3, obvious aggregation of PARKIN-positive puncta was observed even with a low-dose CCCP treatment (**Fig. 2.5F, G**). Consistent with the reported role of calcineurin in TFEB activation, we found that TFEB translocation induced by CCCP was also largely blocked by calcineurin inhibitors, FK506 and Cyclosporin A (CsA) (**Fig. 2.5E**). Taken together, these results suggest that ML1-dependent activation of TFEB plays a crucial role in ROS-induced autophagy and mitophagy.

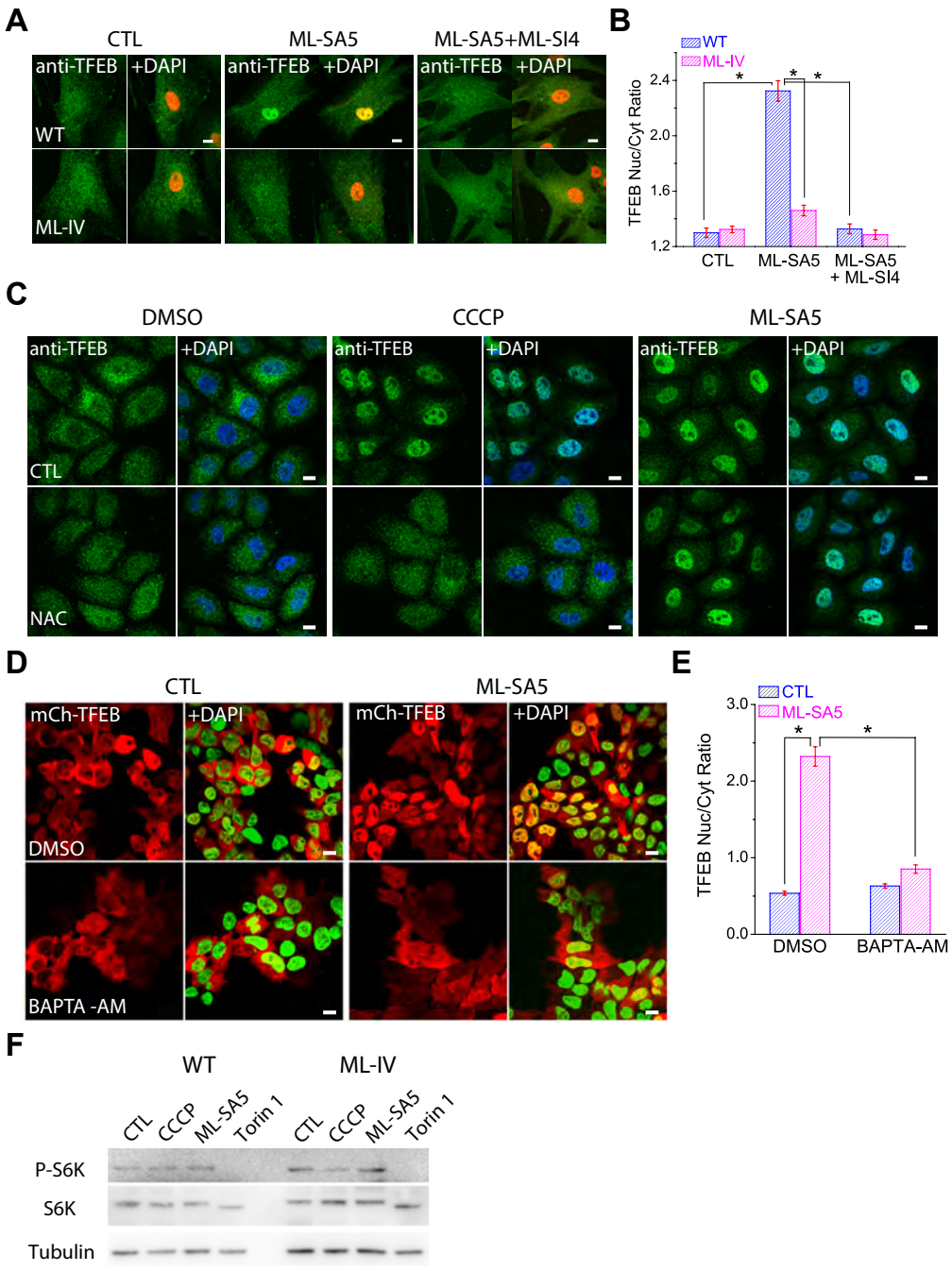


**Fig. 2.8 ML1 agonists induce TFEB nuclear translocation. (A)** The effects of ML-SA5 (1 μM for 1 h) on TFEB nuclear translocation in the presence and absence of ML-SI4 (10 μM) in WT and ML-IV cells. Scale bar = 10 μm. **(B)** Average ratios of nuclear *vs.* cytosolic TFEB immuoreactivity (>50 randomly-selected cells per experiment). (**C**) CCCP-induced, but not ML-SA5–induced, TFEB nuclear translocation was blocked by NAC in HeLa cells. (**D**) ML-SA5 (1 μM for 1 h)-induced TFEB nuclear translocation was blocked by BAPTA-AM in TFEB stable cells. Nuclei were counterstained with DAPI. Scale bar = 10 μm. (**E**) Quantification of TFEB

activation by ML-SA5 (>100 randomly-selected cells per experimental condition). (**F**) The activity of mTOR was assessed by phosphorylated S6K level assays in WT and ML-IV fibroblasts. Torin1 was used as a positive control. All quantification data are presented as mean ± SEM; **P* < 0.05, paired *t*-test for western blots and ANOVA for all other comparisons. Images from panels D&F were taken by Dr. Xiping Cheng from Xu lab.

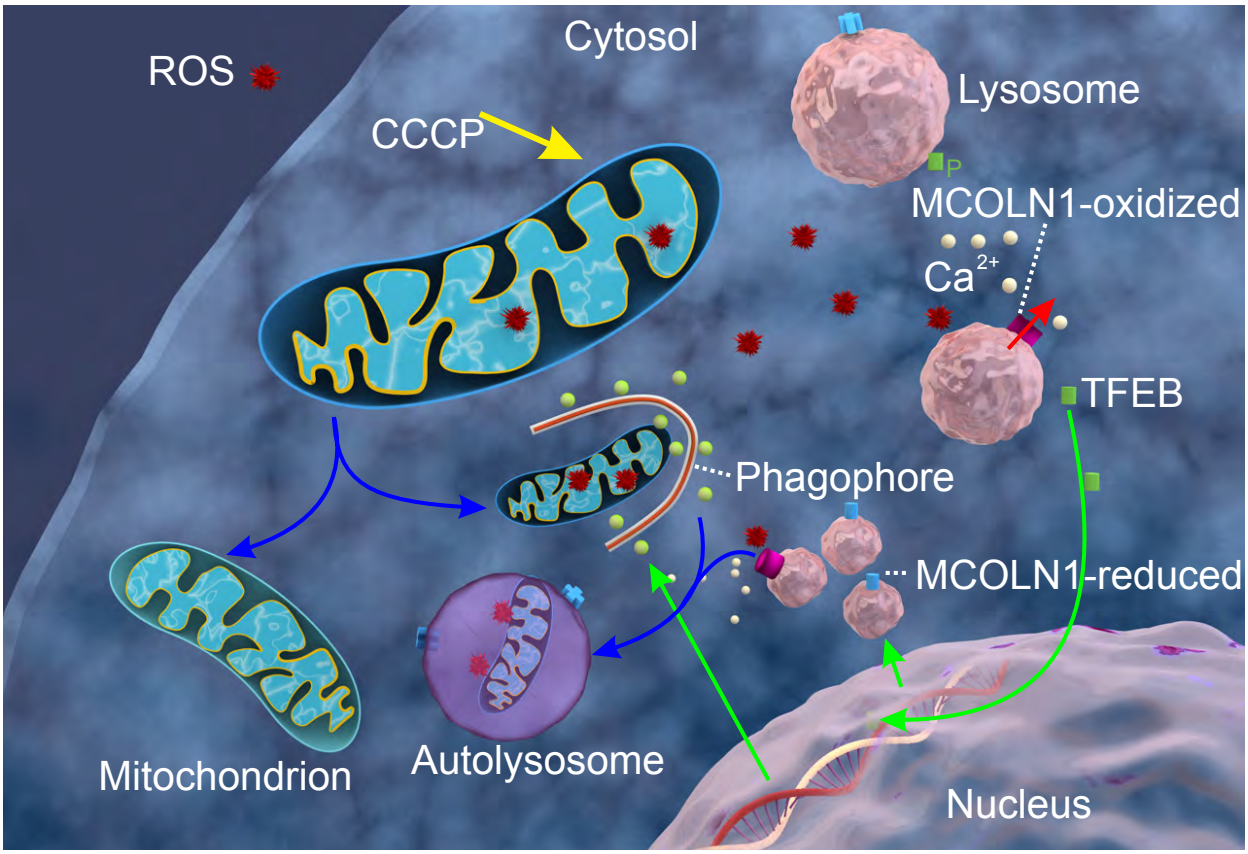


**Figure 2.9 A working model to illustrate the role of ML1 in ROS-induced TFEB activation and autophagy.** An increase in mitochondrial ROS (e.g. by CCCP-mediated mitochondrial depolarization) may activate ML1 channels on the perimeter membranes of lysosomes, inducing lysosomal $Ca^{2+}$ release of that activates calcineurin. Subsequently, $Ca^{2+}$-bound calcinurin dephosphorylates TFEB, which is otherwise kept in its phosphorylated form by the nutrient-sensitive lysosome-localized mTOR kinase (Settembre et al., 2012). Nucleus-localized TFEB then activates the transcription of a unique set of genes related to autophagy induction, autophagosome biogenesis, and lysosome biogenesis. Lysosomal $Ca^{2+}$ release may also directly promote lysosome reformation/biogenesis (Medina et al., 2015). Subsequently, autophagy is promoted to facilitate clearance of damaged mitochondria and removal of excessive ROS.

## Discussion

## 1. Summary of the study and significance

In the current study, we identified the missing links between ROS and autophagy: lysosomal $Ca^{2+}$, ML1, and TFEB (see **Fig. 2.9**). Our results suggest a model wherein an elevation of ROS levels (e.g., due to mitochondrial damage) leads to ML1 activation and lysosomal $Ca^{2+}$ release. Lysosomal $Ca^{2+}$, acting via calcineurin-mediated dephosphorylation (Medina et al., 2015), induces TFEB nuclear translocation, promoting both autophagosome biogenesis and lysosome biogenesis. Lysosomal $Ca^{2+}$ may also directly regulate lysosome biogenesis and autophagosome-lysosome fusion (Xu and Ren, 2015). The subsequent increase in autophagic flux may facilitate removal of damaged mitochondria and restoration of redox homeostasis. Hence, our work has revealed ML1 as a ROS sensor localized in lysosomes, triggering ROS-induced clearance of damaged mitochondria and ROS via autophagy. We have identified a novel negative feedback loop for cellular redox homeostasis. Since ROS dysregulation is involved in many pathological conditions, including LSDs, ischemia-reperfusion, MD, neurodegeneration, aging etc., ML1-mediated lysosomal clearance of ROS may be a potential mechanism underlying pathogenesis of these diseases, as well as a therapeutic target.

## 2. ML1 and mTOR regulate TFEB in lysosomal adaptation

As discussed in Chapter I, lysosome serves as a platform for cellular stress sensing and adaptation. ML1 and mTOR are the two lysosome-localized sensors that regulate TFEB, the effector protein regulating lysosomal gene transcription (Medina et al., 2015; Settembre et al., 2012). However, how the two molecules work together under different physiological conditions is under debate. Under oxidative stress, we found that lysosomal ML1 can be directly activated by oxidants, triggering TFEB nuclear translocation, and this process is independent of mTOR activity.

Yet, there are studies suggesting that mTOR may play a role in ROS regulation as well. For example, TSC (tuberous sclerosis complex) proteins have been shown to regulate Rheb on peroxisomes in response to ROS, thus suppress mTORC1 and induce autophagy (Zhang et al., 2013). But whether the pathway would trigger TFEB or lysosomal adaptation needs further studies. So far, ML1 seems to be the unique sensor for ROS localized on lysosomes to regulate lysosomal adaptation.

However, things are more complicated when it comes to starvation. As a well-established nutrient sensor, mTOR can be inhibited by depletion of amino acid, releasing the inhibitory effects on TFEB and inducing its nuclear translocation (Martina et al., 2012; Roczniak-Ferguson et al., 2012; Settembre et al., 2012). Yet, it has also been shown that lysosomal $Ca^{2+}$ release via ML1 was activated during starvation and is required for starvation-induced TFEB nuclear translocation (Medina et al., 2015). To be specific, the study found starvation-induced TFEB nuclear translocation is blocked by BAPTA-AM, but not EGTA-AM, suggesting that the local $Ca^{2+}$ release is important in this process (Medina et al., 2015). The group also found knockdown of ML1 and calcineurin subunit largely blocked starvation-induced TFEB nuclear translocation (Medina et al., 2015). Interestingly, mTOR inhibitor Torin 1-induced TFEB nuclear translocation was also blocked by BAPTA-AM or calcineurin knockdown (Medina et al., 2015). In this work, the authors proposed another pathway where starvation activates TFEB through lysosomal $Ca^{2+}$ release independently of mTOR. And even when mTOR is inhibited, lysosomal $Ca^{2+}$ release is still required for TFEB nuclear translocation (Medina et al., 2015). However, this study did not provide a mechanism for how nutrient starvation could induce lysosomal $Ca^{2+}$ release independent of mTOR.

Our data showed contradictory results. We did find BAPTA-AM, but not EGTA-AM, was able to block starvation-induced TFEB nuclear translocation (data not shown). However, by utilizing ML1 inhibitors and ML1 KO human fibroblasts available in the lab, we found starvation-induced TFEB cannot be blocked by genetic ablation or pharmacological inhibition of ML1. These data suggest that TFEB activation during starvation is $Ca^{2+}$-dependent, but not ML1-dependent. Indeed, the fact that BAPTA-AM but not EGTA-AM blocked starvation-induced TFEB activation only suggests that the $Ca^{2+}$ source and effector protein are very close, without any hint to the localization of these machineries. Thus, considering calcineurin is diffused in the cytoplasm and nucleus, any $Ca^{2+}$ source in the cell such as ER may contribute to TFEB activation (Medina et al., 2015; Usuda et al., 1996). More importantly, mTOR is reported to be regulated by $Ca^{2+}$ signaling (Gulati et al., 2008; Li et al., 2016a; Sun et al., 2018). Consistently, we also found Torin 1-induced TFEB nuclear translocation cannot be blocked by BAPTA-AM, ML1 KO or ML-SIs. Our data favor the explanation that under nutrient depletion, mTOR was the major pathway for regulation of TFEB. $Ca^{2+}$ was also required, but when mTOR was inhibited, starvation-induced TFEB nuclear translocation became indispensable of $Ca^{2+}$ chelating, suggesting mTOR may be a major downstream target for $Ca^{2+}$ signaling during starvation. We also found ML1 activity was not required for starvation-induced TFEB activation.

One possible explanation for this inconsistency is the time course of starvation. It is likely that mTOR is the fast sensor for TFEB nuclear translocation, and ML1 is activated at later stage. Indeed, our previous work has demonstrated ML1 as a downstream target for TFEB and is upregulated by mTOR inhibition, and following TFEB activation and lysosomal gene transcription under starvation (Wang et al., 2015b). Yet, our data have suggested that up to 6 hours of starvation,

ML-SIs cannot block starvation-induced TFEB nuclear translocation. More studies are needed to further demonstrate the inconsistency here.

**3. ROS regulate the autophagic-lysosomal pathway**

The connection between ROS and autophagy has been well documented (Li et al., 2015; Scherz-Shouval and Elazar, 2011). Several transcription factors, including NRF2 and FOXO3, are known to become active under oxidative stress conditions (Li et al., 2015). Recently, ATG4, a cytosolic negative regulator of LC3/ATG8, was identified as a direct ROS target that provides a rapid switch mechanism for autophagy induction (Scherz-Shouval et al., 2007). However, the direct ROS sensor regulating autophagy and lysosomal adaptation in response to oxidative stress remains largely unknown.

Our study showed ML1 is activated rapidly by exogenous oxidants in isolated lysosomes, or by drugs inducing endogenous oxidant release. ML1 activity is required in ROS-induced autophagosome formation, since blockage of the channel by ML-SIs or KO cells could completely block CCCP- and $H_2O_2$-induced autophagosome formation. Besides, since ML1 activates TFEB, a master regulator for autophagic and lysosomal genes, oxidants-induced ML1 activation also induced lysosomal biogenesis. Hence, ML1 serves as a coordinator of autophagosome formation and lysosome biogenesis to orchestrate autophagic flux in response to ROS. Besides, ROS-ML1 may regulate other aspects of lysosomal function. In MDs characterized by impairment of membrane repair, ML1 and lysosomal exocytosis are important players. It is possible that ROS-ML1 axis may regulate lysosomal exocytosis and membrane repair in MDs.

Although many studies have demonstrated ROS as an inducer for autophagy, ROS play complicated roles in regulation of autophagy and lysosomal function. In a recent study, inhibition

of NOX2, the major source of oxidants in muscles, prevented ROS production and promoted autophagy in *mdx* mice. The study also showed impaired autophagy and lysosomes in *mdx* mice, presumably caused by interrupted mTOR signaling and increased NOX2-ROS (Pal et al., 2014). Indeed, as discussed previously, low level, acute ROS production can serve as pro-survival signals for cell to trigger autophagy and lysosomal adaptation. But chronic, accumulated oxidative stress can be harmful to the cells. In genetic disorders like MD, ROS can be produced from very early stage of pathogenesis. Thus, the roles of ROS in specified pathophysiological conditions need to be carefully examined.

# CHAPTER III

## Activation of ML1 Ameliorates Duchenne Muscular Dystrophy in Mouse Models


### Abstract

Duchenne muscular dystrophy (DMD) is a devastating disease caused by mutations in dystrophin that compromise sarcolemma integrity, leaving muscles susceptible to contraction-induced damage. Currently, there is no treatment for DMD. Mutations in ML1, a lysosomal $Ca^{2+}$ channel required for lysosomal exocytosis, produce a DMD-like phenotype. Here, we show that transgenic overexpression or pharmacological activation of ML1 *in vivo* alleviates the dystrophic phenotype in *mdx* mice. At early acute necrosis stage in *mdx* mice, ML1 activation significantly ameliorates necrosis and central-nucleated fibers. In diaphragm, the only skeletal muscle in *mdx* mice shows progressive fibrotic phenotype mimicking patients, fibrosis and collagen levels were significantly decreased by ML1 channel overexpression. We also saw body weight decrease and dystrophy in the more severe utrophin$^{-/-}$;*mdx* mice were partially rescued by ML1 overexpression. Hence, the present work indicates that targeting lysosomal $Ca^{2+}$ channels can represent a promising approach to treating DMD and related muscle diseases.

## Introduction

Duchenne muscular dystrophy (DMD), an X-linked inherited muscle disease (Mercuri and Muntoni, 2013), is caused by loss-of-function mutations affecting dystrophin, a large cytoplasmic protein that connects the cytoskeleton with extracellular matrix proteins via the muscle membrane (sarcolemma) (Davies and Nowak, 2006; Rahimov and Kunkel, 2013). The fragile sarcolemma that makes human DMD muscles prone to contraction-induced muscle damage has been mimicked in the striated muscles of the *mdx* mouse, a murine model of DMD (Allen et al., 2016; Campbell, 1995; Stedman et al., 1991). Although gene therapy approaches, including CRISPR technology (Amoasii et al., 2017), have provided hope for a potential treatment approach for some specific variants of DMD, the existence of thousands of DMD-causing dystrophin mutations remains a major challenge (Mercuri and Muntoni, 2013). To develop a therapeutic approach that would be more broadly applicable to all forms of DMD, it is necessary to understand the common pathological mechanisms underlying the condition (Allen et al., 2016).

Muscle cells are especially sensitive to membrane damage, and recent studies have identified impairment of membrane repair capability as an important cause of muscular dystrophies (Bansal et al., 2003; Cai et al., 2009a; McNeil, 2009). For instance, we found recently that mice lacking ML1, a lysosomal $Ca^{2+}$ release channel required for lysosomal exocytosis (Dong et al., 2010a; Shen et al., 2012), display early-onset, progressive dystrophies similar to DMD (Cheng et al., 2014). When ML1 is pharmacologically inhibited or genetically inactivated, membrane resealing is impaired in skeletal muscles (Cheng et al., 2014). Hence, lysosomes may provide a major source of membranes for repairing damaged sarcolemma, and ML1 is essential for $Ca^{2+}$-dependent delivery of lysosomal membranes (i.e., lysosomal exocytosis) to damaged sites

(Cheng et al., 2014). Studies of other muscle diseases have also connected lysosomal dysfunction with muscle pathogenesis (Spampanato et al., 2013).

In the current proof-of-concept study, we examined whether upregulation of ML1, by genetic or pharmacological methods, is sufficient to increase lysosomal functions and sarcolemma repair. If so, ML1 may be a putative target for amelioration of muscle damage *in vivo*.

## Methods

**Study design.** The overall goal of this study is to determine the effect of ML1 upregulation on muscular dystrophy and membrane repair. All data presented here have been replicated in at least four mice or three biological replicates for *in vitro* experiments, with all histochemical staining data quantified by experimenters who are blind to genotypes/treatments. Based on pilot studies of ML1 upregulation on various pathologic hallmarks in mice, with a power of 0.8 and $P < 0.05$, we calculated a sample size of between 5 and 11 mice per group. Animals were randomly allocated into control and experimental groups.

**Mouse lines**. We purchased *mdx* (001801) and utrophin$^{+/-}$;*mdx* (014563) mice from Jackson Laboratories. We generated muscle cell-specific ML1-overexpressing (ML1 *ROSA-lSl*;MCK Cre or ML1$^{MCK}$) mice by crossing ROSA-loxSTOPlox-GCaMP3-ML1 (abbreviated ML1 *ROSA-lSl*) mice with a muscle cell-specific Cre line (MCK Cre) *(Sahoo et al., 2017)*. ML1$^{-/-}$ mice were kindly provided by Dr. Slaugenhaupt *(Cheng et al., 2014)*. All mice used in the study were backcrossed to the C57BL/6 genetic background. Mice were used under the University of Michigan's Institutional Animal Care & Use Committee's approval.

**Western blotting**. After lysing muscle tissues in ice-cold RIPA buffer with 1× protease inhibitor cocktail tablet (Roche), 20–40 μg of total protein aliquots were loaded into 4–12% Bis-Tris or 3–8% Tris-acetate sodium dodecyl sulfate-polyacrylamide gradient gels (Invitrogen) and then transferred to polyvinylidene fluoride membranes via iBlot 2 Gel Transfer Device (Life Technologies). The membranes were blocked in 5% (w/v) skim milk in PBS with 0.05% Tween20 for 1 h, and then incubated overnight in the blocking buffer at 4 °C. The primary antibodies used were: anti-ML1 (ACC-081, Alamone lab), anti-green fluorescent protein (GFP) (A6455, Invitrogen), anti-mouse Lamp1 (1D4B, DSHB), anti-human Lamp1 (H4A3, DSHB), anti-mouse TFEB (A303-673A, Bethyl), anti-human TFEB (4240, Cell Signaling), anti-LC3 (L8918, Sigma), anti-dystrophin (ab15277, Abcam), anti-utrophin (8A4, DSHB), anti-α-dystroglycan (sc-53987, Santa Cruz), and anti-GAPDH (glyceraldehyde 3-phosphate dehydrogenase)(MAB347, Millipore). Peroxidase-conjugated anti-rabbit, anti-mouse, or anti-rat secondary antibodies were applied at room temperature (RT) for 1 h, followed by Super-Signal West Pico Chemiluminescence Substrate (Thermo Scientific). Bands were quantitated in ImageJ software.

**Immunofluorescence**. Muscle tissues, harvested and frozen in 2-methylbutane pre-chilled in liquid nitrogen, were cryo-sectioned at 12 μm. After being washed with Tris buffered saline (TBS) + 0.025% Triton X, sections were blocked with 10% serum and 1% bovine serum albumin in TBS at RT for 2 h. Cell lines and isolated primary cells cultured on coverslips were washed with PBS, fixed in 4% paraformaldehyde, permeabilized in 0.3% Triton X in PBS, and blocked in 1% bovine serum albumin in PBS. Fixed cells and cryosections were then incubated at 4 °C overnight with primary antibodies targeting ML1, GFP, Lamp1, TFEB, dystrophin, or CD11b (M1/70.15.11.5.2, DSHB) at 1:50 or 1:200 solutions. Alexa Fluor secondary antibodies (Invitrogen) were then

applied for 1 h in the dark at RT followed by DAPI (4′,6-diamidino-2-phenylindole) counterstaining if necessary. Cells and tissue sections were imaged on a spinning disk confocal imaging system composed of an Olympus IX81 inverted microscope, 10×, 20× and 60× Olympus objectives, a CSU-X1 scanner (Yokogawa), an iXon EM-CCD camera (Andor), and MetaMorph Advanced Imaging acquisition software v.7.7.8.0 (Molecular Devices). Images analysis results were quantified in MetaMorph software.

**Primary muscle cell culture.** Murine myoblasts were harvested and cultured as previously described *(Springer et al., 2002)*. Briefly, skeletal muscles were isolated from postnatal day 0–3 pups and dissociated with 0.25% trypsin supplemented with 2 mg/mL collagenase (Sigma) at 37 °C. To remove fibroblasts, cells were preplated on a standard, non-tissue culture-coated Petri dish for 60–90 min. Muscle cells were then counted, seeded onto collagen-coated glass coverslips, and maintained at 37 °C under 5% $CO_2$ in F10 medium supplemented with 20% fetal bovine serum (FBS) and penicillin/streptomycin. To induce differentiation, myoblasts were grown to confluence before switching to Dulbecco's modification of Eagle medium (DMEM) containing 5% horse serum and penicillin/streptomycin. Electrophysiology, $Ca^{2+}$ imaging, and immunofluorescence labeling were performed after 3 d of differentiation induction to allow MCK-Cre expression.

**Whole-endolysosome electrophysiology**. Endolysosomal electrophysiology was performed on isolated endolysosomes from muscle cells treated with 1 μM vacuolin-1 to enlarge late endosomes and lysosomes *(Dong et al., 2008; Dong et al., 2010a)*. The bath (internal/cytoplasmic) solution contained 140 mM K-gluconate, 4 mM NaCl, 1 mM EGTA, 2 mM $Na_2$-ATP, 2 mM $MgCl_2$, 0.39 mM $CaCl_2$, 0.2 mM GTP, and 10 mM HEPES [pH adjusted with KOH to 7.2; the free $[Ca^{2+}]_i$ was estimated to be ~100 nM on Maxchelator software (http://maxchelator.stanford.edu/)]. The pipette

(luminal) solution consisted of a low-pH Tyrode's solution with 145 mM NaCl, 5 mM KCl, 2 mM $CaCl_2$, 1 mM $MgCl_2$, 10 mM HEPES, 10 mM MES, and 10 mM glucose (pH 4.6). A perfusion system was used to ensure efficient solution exchange. Data were collected with an Axopatch 2A patch clamp amplifier, Digidata 1440, and pClamp 10.0 software (Axon Instruments). Currents were digitized at 10 kHz and filtered at 2 kHz. All experiments were conducted at 21–23 °C, and all recordings were analyzed in pClamp 10.0 and Origin 8.0 (OriginLab, Northampton, MA).

**GCaMP3 $Ca^{2+}$ imaging.** $Ca^{2+}$ imaging was performed in $ML1^{MCK}$ and *mdx*;$ML1^{MCK}$ primary myotubes overexpressing GCaMP3-ML1 *(Sahoo et al., 2017)*. The fluorescence intensity at 488 nm ($F_{488}$) was recorded with the spinning disk confocal imaging system.

**Histochemical staining.** Frozen sections were warmed to RT and hydrated in double distilled (MilliQ) $H_2O$. Tissues were stained with H&E dyes (Fisher) for the nucleus and cytoplasm, respectively, followed by gradient washing in ethanol (70%, 90%, 100%) and xylene (100%). The stained sections were mounted in Permount medium (Fisher). Staining quantification was performed blindly following standardized operating procedures (SOP number: DMD_M.1.2.007). Necrotic myofibers, inflammatory cells and fibroblasts were all counted as necrotic area. Collagen content was assessed with a Masson's Trichrome Kit (Sigma). Area stained with blue color was quantified as fibrotic area.

**Muscle force measurement**. Mice were anesthetized by i.p. injection of Avertin (tribromoethanol, 250 mg/kg) and placed on a warmed platform to maintain body temperature. GAS muscle contractile properties were measured *in situ*, as described previously *(Larkin et al., 2011)*. Briefly, after the GAS was isolated from surrounding tissues, the distal tendon was secured to the lever arm of a servomotor (model 6650LR, Cambridge Technology). The knee and foot were clamped

to the platform. The muscle was activated by tibial nerve stimulation. With the muscle held at optimal length ($L_0$), 300-ms trains of stimulus pulses were applied at increasing frequencies until the maximum isometric tetanic force ($P_0$) was achieved. After the pre-stretch $P_0$ ($preP_0$) was recorded, we applied two stretches (12 s apart) of 30% of fiber length ($L_f$), which was estimated by multiplying $L_0$ by previously determined $L_f$-to-$L_0$ ratios. After a 1-min rest, post-stretch $P_0$ ($postP_0$) was obtained to determine the force deficit. To maintain muscle temperature and moisture, a warm saline drip (37 °C) was applied to the GAS continuously throughout the procedure. After the experiment, mice were euthanized, and muscles were removed and trimmed of their tendons. Physiological cross-sectional areas were determined by dividing muscle mass by the product of $L_f$ using a density of mammalian skeletal muscle of 1.06 g/cm$^3$. Specific $P_0$ ($SP_0$) refers to $P_0$ per cross-sectional area and the force deficit was calculated as 1 - $postP_0/preP_0$.

**Injection of small molecule compounds**. At P14, *mdx* mice were weighed and randomized into treatment groups. ML-SA compounds (dissolved in 10% DMSO, 40% PEG300, and 50% PBS), were administered to mice by i.p. injection. After 14 d of daily injection, the mice were subjected to various behavioral tests or sacrificed for histological and biochemical analyses. To induce cardiomyopathy in *mdx* mice, 0.5 mg/kg β-isoproterenol (Sigma) was injected subcutaneously 1 d before sacrificing *(Yue et al., 2004)*. ML-SA and ML-SI compounds were identified initially by $Ca^{2+}$-imaging-based high-throughput screening conducted at NIH/NCATS Chemical Genomics Center (https://pubchem.ncbi.nlm.nih.gov/bioassay/624414). ML-SA5 and CG002 are available upon request under MTA.

**Treadmill exercise**. Mice were trained on an Exer-6M treadmill (Columbus Instruments). Prior to running, they were acclimated to the treadmill chamber for 30 min. To induce damage, P28

mice ran on the treadmill with a 15° downgrade at 12–15 m/min for 30 min 1 d before being sacrificed for analysis (Radley-Crabb et al., 2012). To measure exhaustion time, the treadmill was set to a speed of 12–20 m/min.

**Statistical analysis**. Data are presented as the means ± standard errors of the mean (s.e.m.). Statistical comparisons were performed with analyses of variance (ANOVAs) and Turkey's *post hoc* tests or with paired and unpaired Student's t-tests where appropriate. A value $< 0.05$ was considered statistically significant.

## Results

### Verification of transgenic overexpression of ML1

To achieve muscle-specific overexpression of ML1 *in vivo*, we crossed a mouse line carrying a GCaMP3-ML1 transgene (ML1 *ROSA-lSl*) (Sahoo et al., 2017) with a Cre line driven by the muscle-specific creatine kinase promoter (MCK-Cre) (Bruning et al., 1998). The resultant ML1 *ROSA-lSl*;MCK-Cre (abbreviated as $ML1^{MCK}$) progeny were then crossed with *mdx* mice with a loss-of-function dystrophin mutation (Clarke et al., 1993), to generate *mdx*;$ML1^{MCK}$ mice (**Fig. 3.1A, B**). Western blotting and immunofluorescence analyses with anti-ML1 antibody revealed ML1 overexpression in both skeletal and cardiac muscle tissues of the *mdx*;$ML1^{MCK}$ mice; isolated primary myotubes were ML1-immunopositive, whereas non-muscle tissues showed no immunoreactivity (**Fig. 3.1C-F**).

Whole-lysosomal ML1 currents, activated by TRPML-specific synthetic agonists (ML-SA1, ML-SA5, and CG002) (Sahoo et al., 2017; Shen et al., 2012; Zhang et al., 2016), were 4–10

times larger in the ML1$^{MCK}$ myotubes than in wild-type (WT) controls (**Fig. 3.2A, B**). ML synthetic agonists induced robust glycyl-L-phenylalanine 2-naphthylamide –sensitive lysosomal $Ca^{2+}$ release (Sahoo et al., 2017) in ML1$^{MCK}$ myotubes, suggesting that genetically-overexpressed ML1 channels were functionally localized on the late endosomal and lysosomal membranes of muscle cells (**Fig. 3.2C-F**). Introducing ML1$^{MCK}$ into the ML1 knockout (KO) mice resulted in a complete rescue of the dystrophic phenotype (Cheng et al., 2014) (**Fig. 3.2G-I**). Hence, the ML1$^{MCK}$ mice were considered suitable for investigating the *in vivo* effects of ML1 overexpression on striated muscles.

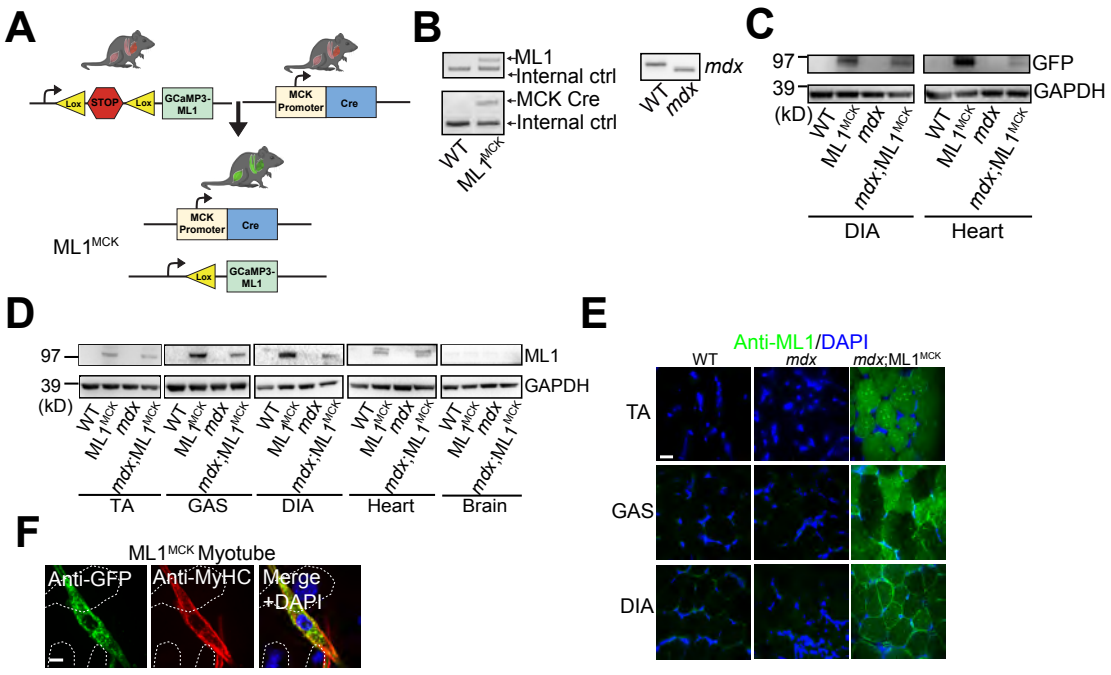


**Figure 3.1. Verification of ML1 overexpression in muscles.** (**A**) The GCaMP3-ML1 transgene was inserted into the ROSA26 locus with a *lox*STOP*lox* cassette. The transgenic mice were crossed with MCK Cre mice to achieve muscle-specific overexpression of ML1. (**B**) PCR genotyping of the *mdx* mutation, GCaMP3-ML1 transgene, and MCK Cre. (**C**) Western blotting analysis of GCaMP3-ML1 expression in ML1$^{MCK}$ DIA and cardiac muscle with anti-GFP antibody. (**D**) Western blotting with anti-ML1 antibody in brain and various skeletal muscle tissues, including GAS, TA, and DIA from WT, ML1 *ROSA-lSl*;MCK Cre (ML1$^{MCK}$), *mdx*, and *mdx*; ML1$^{MCK}$ mice.

GAPDH served as the loading control. (**E**) Immunofluorescence analysis of TA, GAS, and DIA cryo-sections from various transgenic mice. Scale bar = 10 μm. (**F**) Immunofluorescence analysis of primary myotubes isolated from ML1$^{MCK}$ mice. Scale bar = 10 μm. Panel B was generated by Yexin Yang from Xu lab.

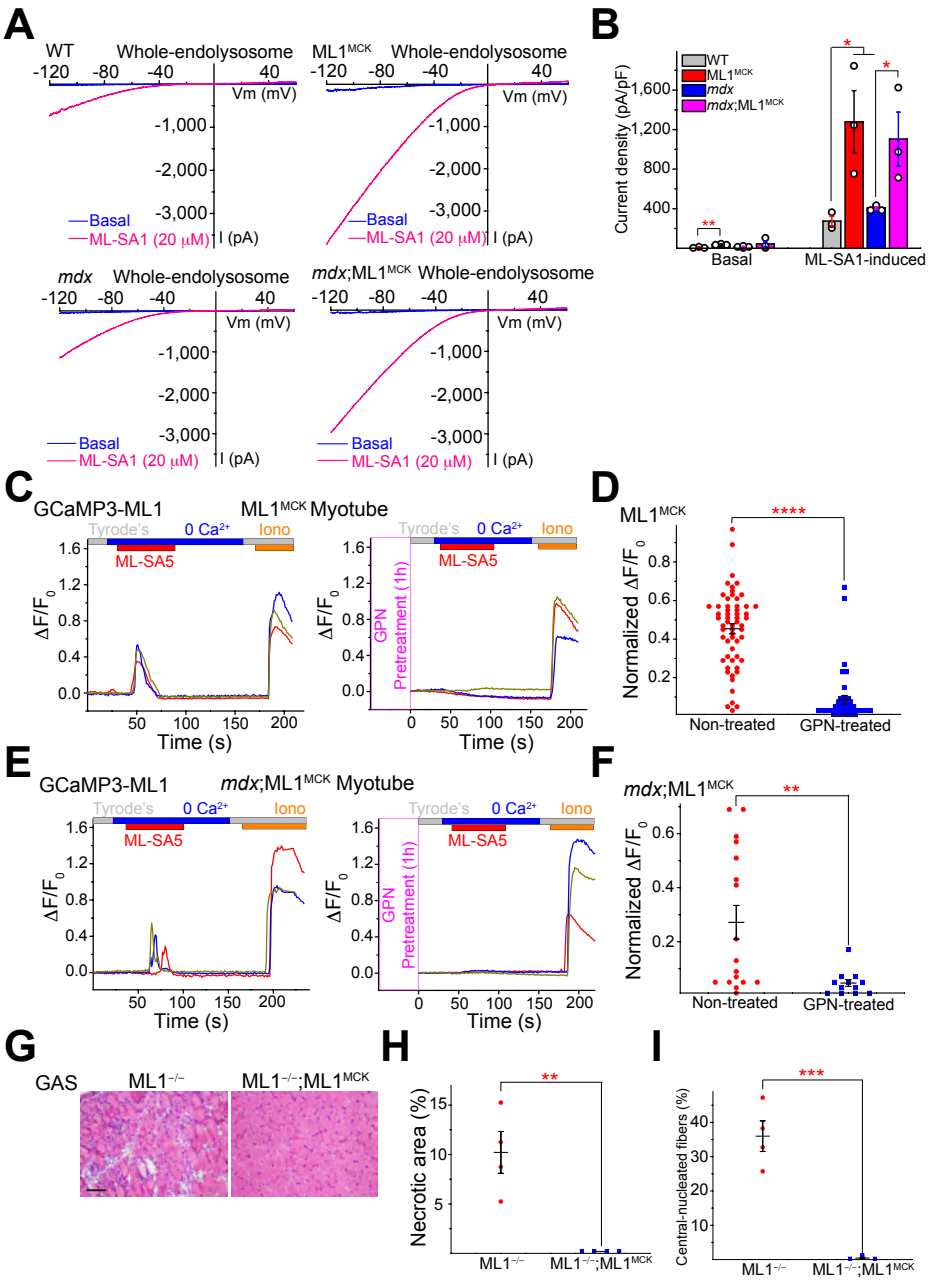


**Figure 3.2 Verification of ML1 activity.** (**A**) Whole-endolysosome ML1 currents activated by ML-SA1 (20 μM) in primary myotubes harvested from WT, *mdx*, ML1$^{MCK}$ and *mdx*;ML1$^{MCK}$ mice. (**B**) $I_{TRPML1}$ current densities of myotubes from **A**. Each open circle represents one cell/patch.

(**C**) ML-SA5-induced lysosomal $Ca^{2+}$ release, measured with GCaMP3 imaging, in primary myotubes isolated from $ML1^{MCK}$ mice. GPN (glycyl-L-phenylalanine 2-naphthylamide), a dipeptide causing osmotic lysis of lysosomes, was used as a negative (depleted lysosomal $Ca^{2+}$ stores) control. (**D**) Quantification of lysosomal $Ca^{2+}$ release in $ML1^{MCK}$ myotubes. N indicates the myotube number. (**E, F**) Lysosomal $Ca^{2+}$ release (**E**) and quantification (**F**) from *mdx*;$ML1^{MCK}$ myotubes. (**G**) Representative images showing H&E staining of GAS isolated from $ML1^{-/-}$ and $ML1^{-/-}$;$ML1^{MCK}$ mice. Scale bar = 100 μm. (**H, I**) Quantification of necrosis (**H**) and central-nucleation (**I**) in GAS sections from $ML1^{-/-}$ and $ML1^{-/-}$;$ML1^{MCK}$ mice. All data are means ± s.e.m.; *$p < 0.05$; **$p < 0.01$; ***$p < 0.001$; ****$p < 0.0001$. Panels A&B were generated by Dr. Xiaoli Zhang, and panels C&E were generated by Dr. Nirakar Sahoo from Xu lab.

**Transgenic overexpression of ML1 ameliorates MD in *mdx* mice**

*Mdx* mice exhibit early-onset muscular dystrophies, as evidenced by myofiber necrosis (myonecrosis) and degeneration/regeneration cycles, which were readily observed by postnatal day 14 (P14) (Straub et al., 1997). In 1-month-old *mdx*;$ML1^{MCK}$ mice, heamotoxylin and eosin (H&E) staining revealed that myonecrosis, quantified by the percentage of the necrotic area (i.e., necrotic myofibers, immune cells and fibroblasts) in whole cross-sections, was markedly reduced in tibialis anterior (TA) muscles compared with age-matched *mdx* mice, especially after downhill treadmill exercise (**Fig. 3.3A, B**). The number of centrally-nucleated fibers, caused by repeated myocyte degeneration and regeneration, was also significantly reduced in the *mdx*;$ML1^{MCK}$ muscles (**Fig. 3.3C**). Similar anti-dystrophic effects were seen in other skeletal muscles, including the gastrocnemius (GAS) and diaphragm (DIA) (**Fig. 3.3D-J**). Consistent with the histological results, physiological assays showed greater specific muscle force in *mdx* mice following $ML1^{MCK}$ overexpression (**Fig. 3.3K**).

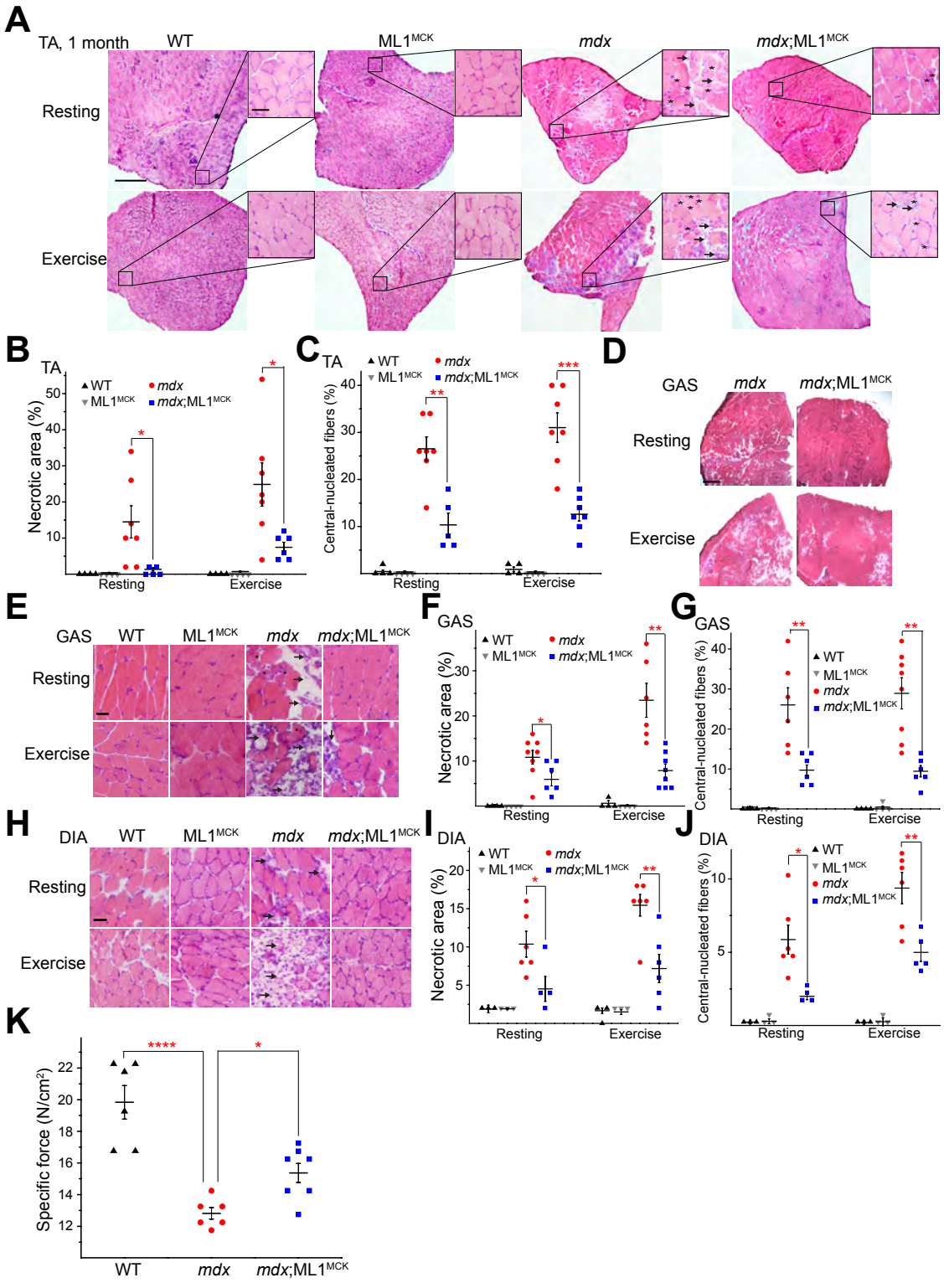
A
TA, 1 month
WT
ML1MCK
mdx
mdx;ML1MCK
Resting
Exercise
B
TA
Necrotic area (%)
WT
ML1MCK
mdx
mdx;ML1MCK
Resting
Exercise
C
TA
Central-nucleated fibers (%)
D
GAS
E
GAS
F
GAS
G
GAS
H
DIA
I
DIA
J
DIA
K
Specific force (N/cm²)

**Figure 3.3 Transgenic overexpression of ML1 ameliorates MD at early stage in *mdx* mice.** (**A**) H&E staining of TA sections from WT, ML1$^{MCK}$, *mdx*, and *mdx*;ML1$^{MCK}$ mice at 1 mo. old, before (rest) and after treadmill exercise. Arrows label necrotic areas and asterisks show central-nucleated myofibers. Scale bar = 500 μm or 50 μm (zoom-in images). (**B**) Percentage of necrotic area in TA muscles from various transgenic mice. Each datum (n indicates the number of the animal) represents the averaged result from at least five representative images randomly selected from at least three sections. Statistical analyses were performed by experimenters who were blind to animal genotypes. (**C**) Percentage of central-nucleated fibers in TA muscles from different transgenic mice. (**D, E**) H&E staining of GAS from *mdx* and *mdx*;ML1$^{MCK}$ mice under low (**D**) and high (**E**) magnification. Scale = 500 μm (**D**) or 50 μm (**E**). (**F, G**) Quantification of necrosis (**F**) and central-nucleation (**G**) of representative H&E stained images as shown in **F** and **G**. Each datum (n indicates the number of the animal) represents the averaged result from at least three representative images randomly selected from at least three sections. Statistical analyses were performed by experimenters who were blind to animal genotypes. (**H**) H&E staining of DIA. Scale = 50 μm. (**I, J**) Quantification of necrotic and central-nucleated fibers as shown in **H**. (**K**) Specific force test of GAS from multiple 1-mo.-old mice. Panel K was generated by Carol S. Davis from Dr. Susan V. Brooks lab.

In most skeletal muscles of *mdx* mice, the dystrophic phenotype did not appear to be progressive, perhaps due to compensatory expression of utrophin, a functional homolog of dystrophin (Grady et al., 1997). Dystrophy of the DIA in *mdx* mice, however, was progressive, as seen in human DMD (Stedman et al., 1991). Consistent with previous studies (Stedman et al., 1991), we observed massive necrosis and subsequent fibrous and adipose tissue replacement (i.e., fibrosis) in *mdx* DIA muscles (**Fig. 3.4A, B**). At all ages examined (1 mo., 4 mos., 10 mos.), myonecrosis and fibrosis were reduced significantly by ML1$^{MCK}$ overexpression (**Fig. 3.4A, B**). The content of collagen, a major component of fibrous scar tissue (Cheng et al., 2014), was also decreased by ML1$^{MCK}$ overexpression (**Fig. 3.4C, D**).

Relative to *mdx* mice, utrophin$^{-/-}$;*mdx* (dKO) mice have a much more severe and progressive muscular dystrophy that resembled human DMD (Grady et al., 1997). We also studied the effects of ML1$^{MCK}$ on utrophin$^{-/-}$;*mdx* mice. Both dystrophy and body weight loss characteristic of the utrophin$^{-/-}$;*mdx* phenotype (Grady et al., 1997) were improved by ML1-

overexpression (**Fig. 3.4E-G**). Together, these results suggest that transgenic overexpression of ML1 is sufficient to attenuate muscular dystrophy in DMD-like mouse models.

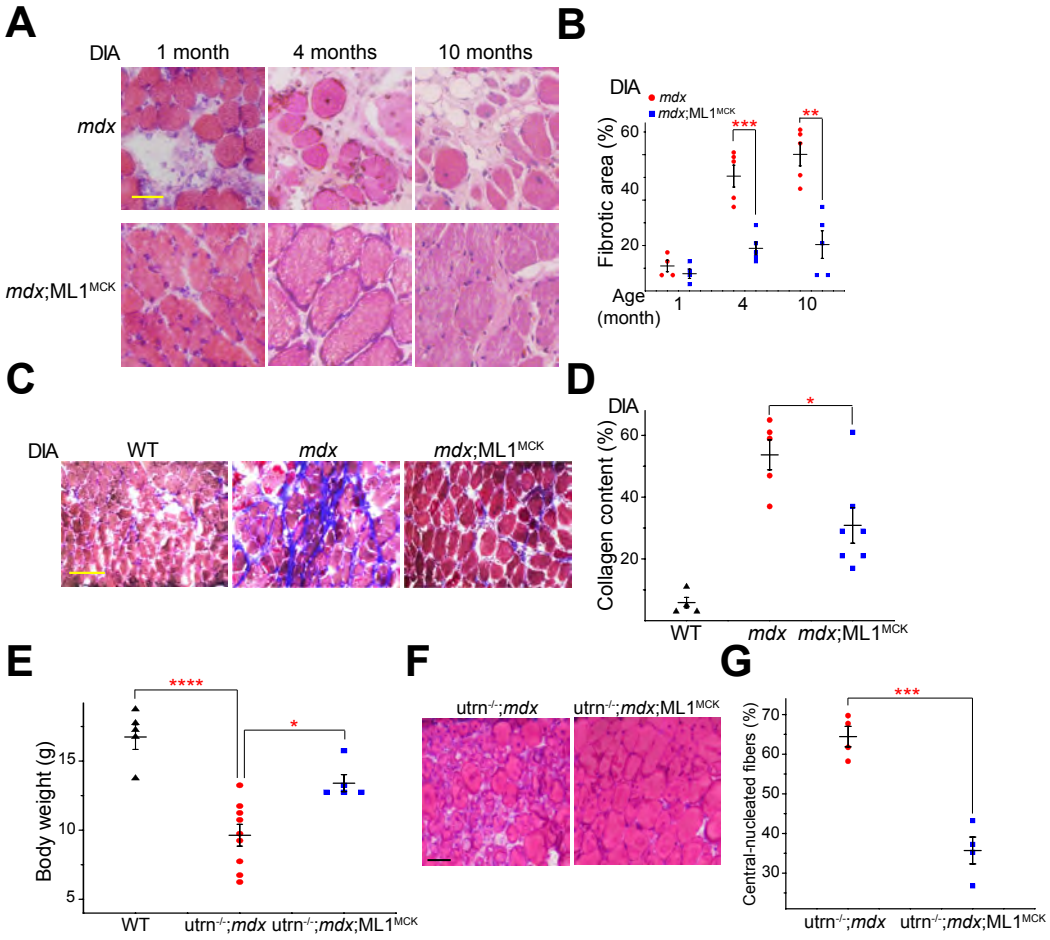


**Figure 3.4 Effects of ML1 overexpression in more severe MD models.** (**A**) H&E staining of DIA isolated from *mdx* and *mdx*;ML1$^{MCK}$ mice at 1 mo., 4 mos. and 10 mos. of age. Scale bar = 50 μm. (**B**) Age-dependent progressive fibrosis in DIA muscles isolated from *mdx* and *mdx*;ML1$^{MCK}$ mice. (**C**) Trichrome collagen staining of DIA from 4-mo.-old mice. Scale bar = 100 μm. (**D**) Quantification of results (n indicates the number of the animal) averaged from multiple randomly selected images as shown in **C**. (**E**) Body weight measurements at the age of 1 mo. (**F**) The effect of ML1 overexpression on central-nucleation of muscle isolated from utrophin$^{-/-}$; *mdx* (dKO) mice. (**G**) Quantification on central-nucleation of muscle isolated from utrophin$^{-/-}$; *mdx* (dKO) mice with or without ML1 overexpression. Scale = 50 μm. All data are means ± s.e.m.; *$p < 0.05$, **$p < 0.01$, ***$p < 0.001$, and ****$p < 0.0001$.

**Pharmacological activation of ML1 *in vivo* ameliorates MD in *mdx* mice**

Next, we tested whether small-molecule ML1 agonists have a muscle protective effect in *mdx* mice. Highly potent ML-SA compounds with $EC_{50}$ values in the nM range for endogenous ML1, namely ML-SA5 and CG002, exhibit good pharmacokinetic properties (Cmax > *in vitro* $EC_{50}$ at 2 mg/kg intraperitoneal injection) suitable for *in vivo* studies (**Fig. 3.6A**). *Mdx* mice received daily intraperitoneal (i.p.) injections of ML-SA5, starting at P14 and continuing for at least 2 weeks. Like the vehicle [10% DMSO+40% PEG+50% phosphate buffered saline (PBS)]-treated group, no pathological signs were evident following ML-SA injection. Both WT and *mdx* mice that received ML-SAs maintained normal body weights over the course of the experiment (**Fig. 3.7A, B**). However, at the i.p. dose of 2–5 mg/kg, daily ML-SA5-injection for two weeks decreased TA muscle necrosis by more than 70%, both at rest and after treadmill exercise (**Fig. 3.5A, B**). Centrally-nucleated fibers were also decreased in the ML-SA5-injected *mdx* mice (**Fig. 3.5A, C**). Similar rescue effects were also seen in the GAS and DIA (**Fig. 3.5D-I**), as well as in *mdx* mice that were i.p.-injected with the structurally-distinct ML1 agonist CG002 (**Fig. 3.6B-D**).

In contrast, i.p.-injection of ML-SI6, a potent ML1 inhibitor, worsened the dystrophic phenotype in *mdx* mice (**Fig. 3.8**). Furthermore, in ML1 KO mice that also exhibit a DMD-like phenotype such as necrosis and central nuclei (Cheng et al., 2014), no obvious ML-SA rescue effects were seen (**Fig. 3.7D-F**). Hence, the actions of ML synthetic agonists are likely to be mediated through ML1 (i.e., on-target). Besides, protein levels of DPC members such as utrophin and α-dystroglycan were not significantly changed upon ML-SA5 treatment, suggesting ML-SA may act independently of DPC proteins (**Fig. 3.9**). Finally, at the behavioral level, motor performance in a downhill treadmill test improved markedly following ML-SA injection in *mdx*

mice (**Fig. 3.5J, 3.6E**). Similar to the genetic overexpression studies, pharmacological activation of ML1 *in vivo* using small molecules was also muscle protective.

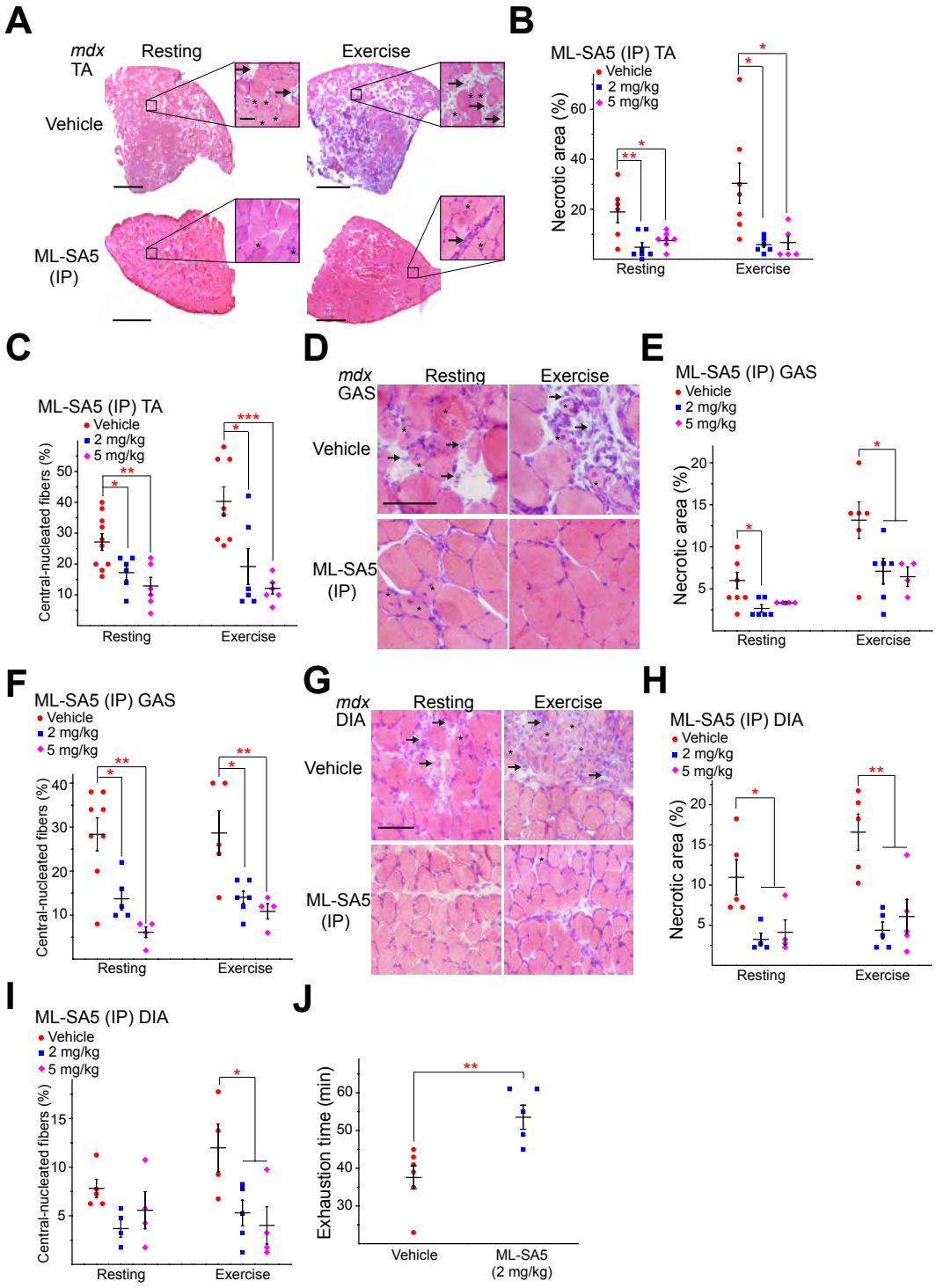

**Figure 3.5 ML1 agonist ML-SA5 injection improves MD in *mdx* mice.** (**A**) H&E staining of TA from *mdx* mice that received daily i.p. injection of ML-SA5 (2 mg/kg) for 14 d starting at P14. Arrows and asterisks indicate necrotic areas and central-nucleated fibers, respectively. Scale bar = 500 or 50 µm (zoom-in). (**B**) Percentages of necrotic area in ML-SA5-injected mice. Each datum (n indicates the number of the animal; ≥ 4) represents the averaged result from at least three representative images randomly selected from at least three sections. Statistical analyses were performed by experimenters who were blind to treatment conditions. (**C**) Percentage of centrally-nucleated fibers in ML-SA5-injected mice. (**D**) H&E staining of GAS from mice given daily i.p. injection of ML-SA5 (2 mg/kg) for 14 d. Scale bar = 50 µm. (**E, F**) Quantification of necrotic (**E**) and centrally-nucleated fibers (**F**) in ML-SA5-injected GAS. (**G-I**) H&E staining of DIA from ML-SA5-injected *mdx* mice. Scale bar = 50 µm. (**J**) Treadmill exhaustion time of *mdx* mice treated with ML-SA5 v*s.* vehicle control. N, number of tested animals. Experimenters were blind to the treatment conditions. All data are mean ± s.e.m.; **p* < 0.05, ***p* < 0.01, and ****p* < 0.001.

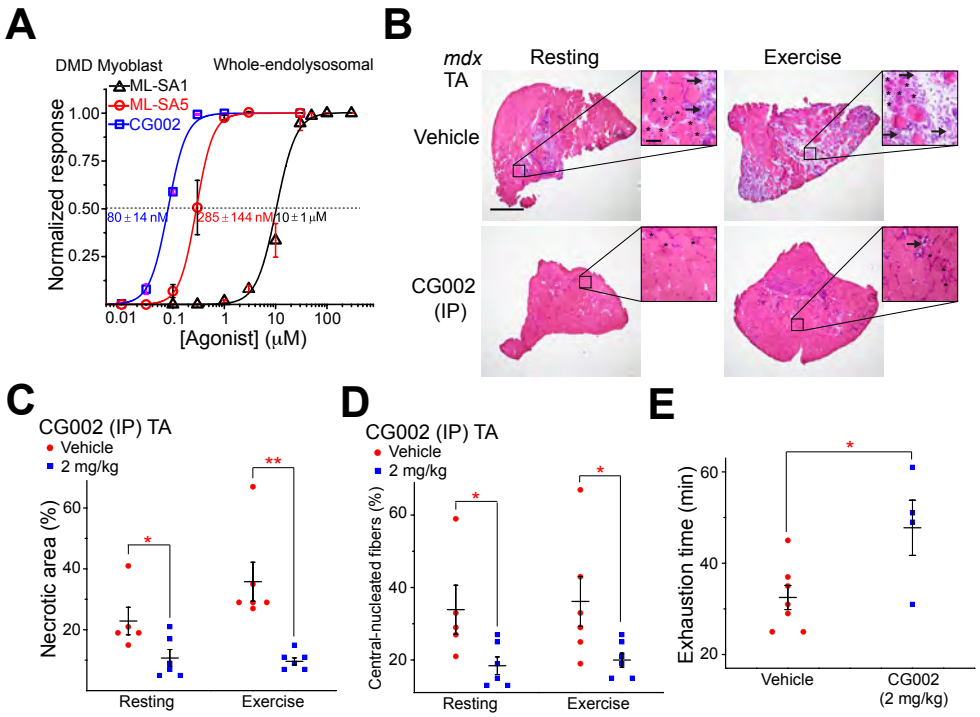


**Figure 3.6 Another structurally-unrelated ML1 agonist improves MD in *mdx* mice.** (**A**) ML-SA1, ML-SA5, and CG002 dose-dependently activated whole-endolysosomal ML1 currents in DMD myoblasts. (**B**) H&E staining of TA from *mdx* mice treated with CG002 (2 mg/kg, i.p. injection). Scale bar = 500 or 50 µm (zoom-in). (**C, D**) Effects of CG002 injection on myonecrosis and central nucleation. (**E**) Treadmill exhaustion time of *mdx* mice treated with CG002 *vs.* vehicle control. All data are means ± s.e.m.; **p* < 0.05 and ***p* < 0.01.

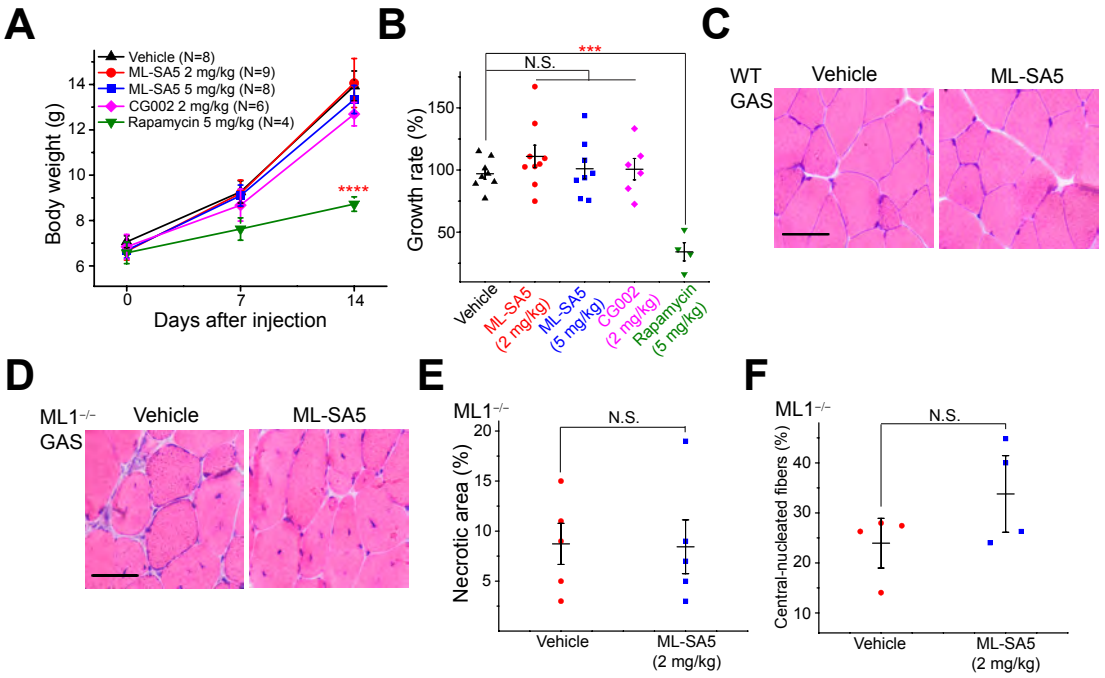


**Figure 3.7 No obvious toxicity and side-effects of ML1 agonists *in vivo*.** (**A, B**) Effects of i.p. injection of ML1 agonists and rapamycin on animal body weight. N indicates the number of tested animals in each group. Growth rate = (weight after injection – weight before injection) / weight before injection. (**C**) Effects of ML-SA5 (2 mg/kg) injection on muscle histology in WT mice. Scale bar = 50 μm. (**D-F**) Representative images (**D**) and quantification (**E, F**) of effects of ML-SA5 (2 mg/kg) injection on muscle histology in ML1$^{-/-}$ mice. Scale bar = 50 μm. All data are mean ± s.e.m.; ***$p < 0.001$, and ****$p < 0.0001$.

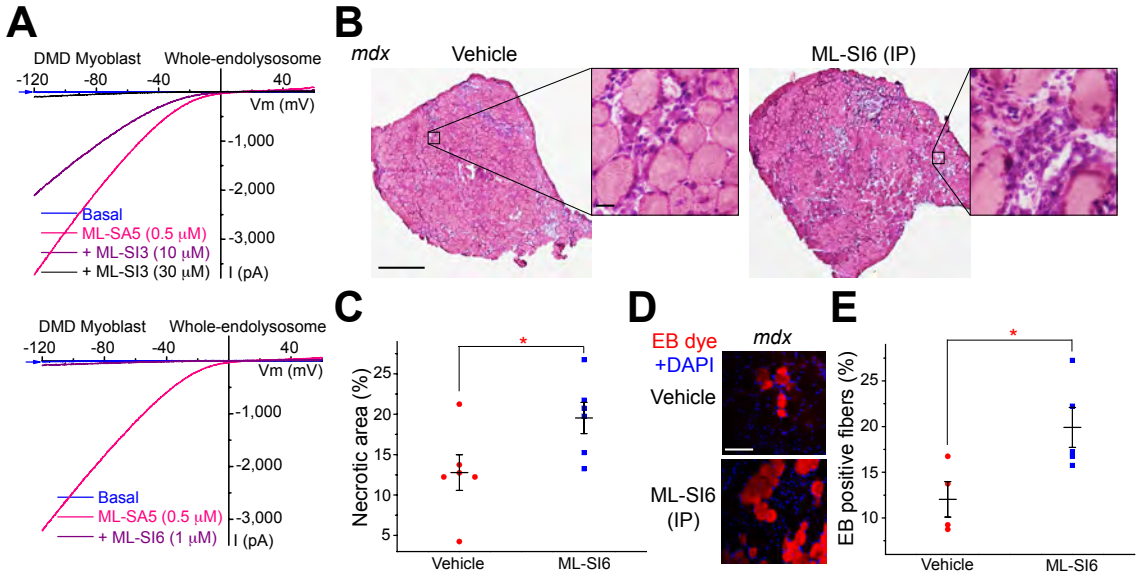

**Figure 3.8 Inhibition of ML1 activity exacerbates myopathology in *mdx* mice.** (**A**) ML-SA5 (0.5 μM)-activated whole-endolysosome ML1 currents were inhibited by synthetic inhibitors of ML1, ML-SI3 (10, 30 μM), and ML-SI6 (1 μM) in DMD myoblasts. (**B**) H&E staining of TA from *mdx* mice given daily i.p. injection of ML-SI6 (2 mg/kg) for 14 d. Scale = 500 μm or 20 μm (zoom in images). (**C**) Quantification of necrotic area of sections in **B**. (**D, E**) EB dye uptake in TA from ML-SI6-injected *mdx* mice. Scale = 100 μm. All data are means ± s.e.m.; **p* < 0.05.

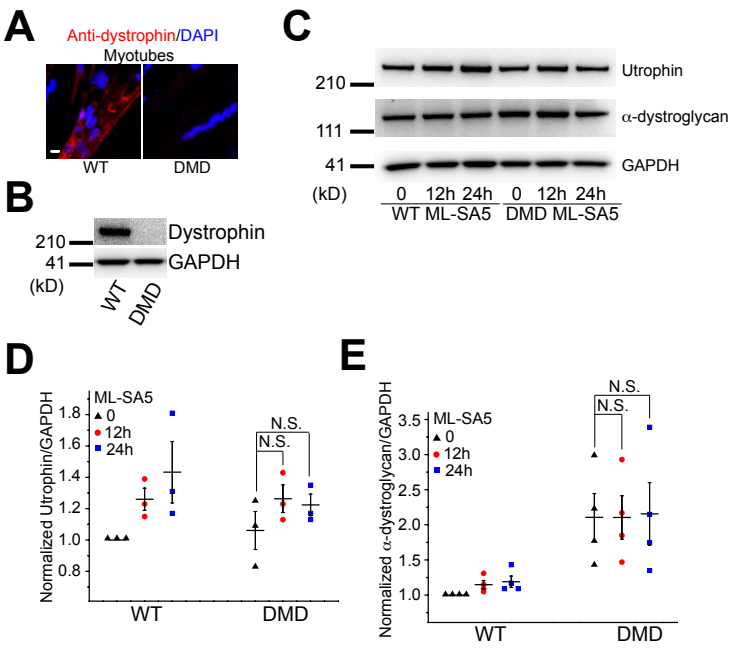


**Figure 3.9 ML1 agonists do not upregulate expression of α-dystroglycan complex components.** (**A**) Dystrophin immunolabeling in myotubes differentiated from immortalized WT and DMD human myoblasts. Scale bar = 10 μm. (**B**) Western blotting analysis of dystrophin expression in WT and DMD myoblasts. (**C-E**) Utrophin and α-dystroglycan protein levels in ML-SA5-treated WT and DMD myoblasts. Data are means ± s.e.m. Panel C was generated by Kaiyuan Tang.

## Discussion

### 1. Summary of the study and significance

ML1 deficiency causes a DMD-like muscle phenotype in both humans and rodents (Cheng et al., 2014). In the current study, we found that both genetic and pharmacological activation of

ML1 had muscle protective effects in *mdx* mice. At the early stage, the acute, severe necrosis in *mdx* mice was largely ameliorated with ML1 overexpression and agonist application. At later stages, progressive fibrosis in diaphragm was also improved by ML1 activation. Moreover, ML1 overexpression in the more severe utrophin$^{-/-}$;*mdx* mice also yielded protective effects. Last but not least, we showed structural-unrelated ML1 agonists could all improve muscle histology and these drugs did not show similar effects in ML1 KO mice, suggesting that the drugs are acting on target *in vivo*. Also, no obvious toxicity did we notice when injecting the compounds into WT mice. Together, our data revealed that activation of ML1, especially through the small molecule agonists, can be a potential therapeutic strategy for treating DMD.

**2. Clinical relevance of the study**

The current study suggests that activating lysosomal exocytosis by small molecule agonists for ML1 could ameliorate MD *in vivo*. Apparently, there are advantages of this strategy compared with gene therapies, including the more general targeting mechanism and easy application of drugs. However, caveats do exist when it comes to clinical relevance. The major drawback of the study lies in the *mdx* mouse model. As discussed in Chapter I, *mdx* mice exhibit much milder muscle phenotypes than DMD patients (McGreevy et al., 2015). Here I showed that ML1 overexpression and agonists ameliorated acute necrosis in *mdx* mice around 1 month old. Yet, necrosis seen in DMD patients is milder and chronic. Furthermore, the massive central-nucleated muscle fibers representing regeneration found in later stages in *mdx* mice are absent in patients. The muscle in *mdx* mice that best mimics progressive fibrosis in patients is the diaphragm muscle. We did see significant improvement of fibrosis and collagen deposition in ML1-overexpressed *mdx* diaphragm at later stages. However, after injecting compounds via intraperitoneal delivery for

longer time (~3 months), we noticed the vehicle could cause inflammation in diaphragm muscles (data not shown). It is likely that i.p. injection can cause accumulation of high concentration of drug close to the diaphragm, resulting in toxic responses. Therefore, drug formula and delivery routes need to be optimized if we want to look at later stages of drug response.

Due to limitations of *mdx* mouse model, we utilized the more severe utrophin$^{-/-}$;*mdx* double KO mice to investigate the effects of ML1 activation in MD models. Indeed, we saw a significant improvement of body weight by ML1 overexpression at 1 month old. However, we did not see dramatic increase of life spans in these mice by ML1 overexpression (data not shown). It is likely that ML1 activation is more effective in the early, less severe stage of the disease. In this scenario, the less severe utrophin$^{+/-}$;*mdx* mice can be used to test the effects of ML1 overexpression. It is also possible that ML1 may somehow influence the expression level of utrophin in *mdx* mice, resulting in the compensation of the lost dystrophin, thus knock out of utrophin would eliminate the rescue effects. To test this hypothesis, we need to look at the protein levels of utrophin and other DPC members in *mdx* and *mdx*;ML1$^{MCK}$ mice.

Except the mouse models, another caveat of the study is the lack of *in vivo* data of ML-SA compounds. Since no one has tried these compounds in *in vivo* experiments before, it would be very helpful to know the pharmacokinetics of the drugs. In addition, it would also be beneficial to know ML1 expression and activity, as well as the level of lysosomal exocytosis in muscles from DMD patients.

**3. ML1 and dystrophin/DPC in membrane repair**

In our previous study, we found the ML1 activity is necessary for lysosomal exocytosis, and the latter is important for membrane repair (Cheng et al., 2014). However, the links between

ML1/lysosomal exocytosis and dystrophin/DPC are still unclear. In ML1 KO mice, we did not see significant changes of dystrophin protein level (Cheng et al., 2014). In *mdx* differentiated myotubes, we only saw a mild increase in ML1 currents compared with WT. These data together suggest that ML1 may act on membrane repair in a separate pathway other than dystrophin. Indeed, ML-SA5 treatment led to mild but not statistically significant increase in utrophin levels in DMD myoblasts. And α-dystroglycan was not changed by ML-SA5 treatment. When we injected ML1 inhibitors into *mdx* mice, we saw exacerbation of MD in these mice. These data demonstrate that ML1 may act on another signaling pathway, but not directly on DPC. However, further studies are needed to dissect the possible connections between ML1/lysosome and DPC proteins in sarcolemmal repair.

# CHAPTER IV

## Activation of ML1 Facilitates Membrane Repair Through TFEB and Lysosomal Biogenesis


### Abstract

Failure of membrane repair is one of the early pathological changes in many MDs. Lysosomal $Ca^{2+}$ channel ML1 is required for lysosomal exocytosis, a process important for plasma membrane repair. Here, we are trying to dissect the mechanisms underlying the rescue effects we saw when activating ML1 in skeletal muscles. We found that increased sarcolemmal permeability in *mdx* mice, assayed by Evan's blue dye and serum CK level, was dramatically improved by ML1 overexpression or pharmacological activation. Muscle damage-repair assays also showed decreased muscle force deficit and faster membrane reseal in ML1-overexpressed *mdx* muscles upon mechanical stretch and laser injury, respectively. Since ML1 activation has been shown to trigger TFEB nuclear translocation and lysosomal biogenesis, we examined TFEB and lysosomal marker *in vivo*. Surprisingly, we found the lysosomal marker were increased, but not decreased, in early stage of *mdx* muscles, which is similar as what has been seen in LSDs. Overexpression of ML1 activated TFEB and corrected abnormal increase of lysosomal protein. By utilizing DMD myoblasts from patients, we confirmed that activation of ML1 could induce TFEB nuclear translocation and lysosomal biogenesis *in vitro*. More importantly, we also found that ML1 agonists prevented cell death induced by SLO toxin via TFEB. Finally, blocking lysosomal exocytosis inhibited this pro-survival effects of ML1 agonists. Together, our data suggested that

activation of lysosomal exocytosis via ML1-TFEB axis facilitates membrane repair and prevents cell death.

## Introduction

Impaired membrane repair is essential in pathogenesis of MDs (Allen et al., 2016). Lysosomal exocytosis has been proposed as an important machinery that the cell utilized to reseal damaged plasma membrane (Reddy et al., 2001). We found that genetical ablation or pharmacological inhibition of ML1 impaired lysosomal exocytosis, and ML1 KO mice also showed compromised sarcolemmal integrity and MD (Cheng et al., 2014). Besides, activation of ML1 has been found to induce lysosomal exocytosis (Samie et al., 2013).

TFEB is a master transcription factor for lysosomal genes (Sardiello et al., 2009). Overexpression of TFEB has been found to trigger lysosomal biogenesis and exocytosis (Medina et al., 2011; Palmieri et al., 2011). Our previous findings have revealed that activation of ML1 triggers TFEB nuclear translocation in a $Ca^{2+}$-dependent manner, inducing lysosomal biogenesis and promoting lysosomal function (Medina et al., 2015; Zhang et al., 2016). Here, by utilizing various membrane damage models, we have found activation of ML1 through genetical and pharmacological methods could facilitate membrane repair and promote cell survival via TFEB.

## Methods

**Uptake of EB dye**. Freshly prepared 1% EB dye (Sigma) w/v in PBS was injected i.p. at 10 ml/kg 1 d before tissue collection.

**Measurement of CK activity**. Venous tail blood was collected before and after treadmill exercise, and serum was separated by centrifugation. Serum CK activity was measured with a Creatine Kinase Activity Assay Kit (Abcam) following the manufacturer's instructions.

**Myofiber damage assay.** After mice were sacrificed, FDB muscles were removed surgically and then digested in 2 mg/mL type I collagenase (Sigma) at 37 °C for 60 min. After trituration and re-suspension in FluoroBrite DMEM solution (Thermo Fisher), single FDB fibers were mounted on a glass bottom dish precoated with Matrigel (Corning) and then stained with 5 μg/mL FM 4-64 dye (Thermo Fisher) immediately before imaging. A Leica SP5 inverted confocal microscope system with a multiphoton laser (laser power 2.3 W at wavelength 820 nm) was used to irradiate the fibers and take images. Fluorescence intensity at the injury site was measured by ImageJ software.

**Muscle cell line culture.** Immortalized human myoblast cell lines, including a WT line (ref. AB1079C38Q) and a DMD line (ref. AB1023DMD11Q: stop in exon 59), were provided by Dr. Vincent Mouly at the Institut de Myologie in France *(Mamchaoui et al., 2011)*. Myoblasts were grown in KMEM (1 volume of medium 199 + 4 volumes of DMEM, both from Thermo Fisher) supplemented with 20% FBS, fetuin (25 μg/mL, Sigma), insulin (5 μg/mL, Sigma), basic fibroblast growth factor (0.5 ng/mL, Thermo Fisher), human epidermal growth factor (5 ng/mL, Thermo Fisher), and dexamethasone (0.2 μg/mL, Sigma) in a humidified $CO_2$ incubator at 37 °C. Myoblasts were induced to differentiate into myotubes by switching to medium containing DMEM with 50 μg/mL gentamycin and 10 μg/mL insulin.

**RNA extraction and real time quantitative (qRT)-polymerase chain reaction (PCR) .** Total RNA was extracted from cultured human myoblasts with TRIzol (Invitrogen) and then purified with a Turbo DNA-free kit (Invitrogen). cDNA was then synthesized with a Superscript III RT kit (Invitrogen). We conducted qRT-PCR with PowerUp SYBR green 2X master mix (Invitrogen) and the following PCR primers *(Medina et al., 2015)*:

*HPRT*: forward (fw): 5’ -tggcgtcgtgattagtgatg-3’, reverse (rev): 5’ -aacacccttttccaaatcctca-3’;

*PGC1α*: fw: 5’ -catgcaaatcacaatcacagg-3’, rev: 5’ -ttgtggcttttgctgttgac-3’;

*MCOLN1*: fw: 5’ -gagtgggtgcgacaagtttc-3’, rev: 5’ -tgttctcttcccggaatgtc-3’;

*ATP6V0E1*: fw: 5’ -cattgtgatgagcgtgttctgg-3’, rev: 5’ -aactccccggttaggaccctta-3’;

*ATP6V1H*: fw: 5’ -ggaagtgtcagatgatcccca-3’, rev: 5’ -ccgtttgcctcgtggataat-3’;

*CTSF*: fw: 5’ -acagaggaggagttccgcacta-3’, rev: 5’ -gcttgcttcatcttgttgcca-3’;

*TFEB*: fw: 5’ -caaggccaatgacctggac-3’, rev: 5’ -agctccctggacttttgcag-3’;

*CTSD*: fw: 5’ -cttcgacaacctgatgcagc-3’, rev: 5’ -tacttggagtctgtgccacc-3’;

*PPP3CA*: fw: 5’ -gctgccctgatgaaccaac-3’, rev: 5’ -gcaggtggttctttgaatcgg-3’;

*DPP7*: fw: 5’ -gattcggaggaacctgagtg-3’, rev: 5’ -cggaagcaggatcttctgg-3’;

*CTSB*: fw: 5’ -agtggagaatggcacacccta-3’, rev: 5’ -aagagccattgtcacccca-3’;

*TPP1*: fw: 5’ -gatcccagctctcctcaatac-3’, rev: 5’ -gccatttttgcaccgtgtg-3’;

*NEU1*: fw: 5’ -tgaagtgtttgcccctggac-3’, rev: 5’ -aggcaccatgatcatcgctg-3’.

**Silencing RNA (siRNA) knockdown.** TFEB expression was transfected with siRNA oligonucleotides (5’-gaaaggagacgaagguucaacauca-3’) and Lipofectamine 2000 (both from Invitrogen). Cells were subjected to biochemical and cell biological analyses 72 h after transfection.

**Flow cytometry PI staining.** Cells were pretreated with various compounds, digested in accutase, and then washed with Tyrode’s solution supplemented with 20% FBS. After counting, cell membranes were damaged with SLO toxin (1 μg/ml, 10 min) at 37 °C. His-tagged SLO (carrying

a cysteine deletion that eliminates the need for thiol activation *(Idone et al., 2008)* was provided by R. Tweeten (University of Oklahoma, Norman, OK) and purified as described previously *(Cheng et al., 2014)*. SLO-treated cells were stained with 2 μg/ml PI (Thermo Fisher) for 5 min and analyzed by Attune NxT Acoustic Focusing Cytometer (Life Technologies). Total cell events were measured with Vybrant DyeCycle Violet stain (Invitrogen). At least 10,000 cells were used for each experimental group. Data were analyzed in Attune NxT software.

**Lamp1 surface labeling**. After 3 d of differentiation, immortalized human myotubes pretreated with ML-SAs were incubated with 0.5–1 μg/mL SLO at 37 °C for 30 min. Non-permeablized cells were labelled with anti-human Lamp1 (H4A3) antibody, which recognizes a luminal epitope, at 4 °C for 1 h. Cells were then fixed in 2% paraformaldehyde for 30 min, and incubated with Alexa-488 conjugated secondary antibody (Invitrogen) at RT for 1h.

## Results

### ML1 facilitates sarcolemma repair, thereby reducing skeletal and cardiac muscle damage in *mdx* mice

One of the major causes of MD is defective sarcolemma repair, and lysosomal exocytosis is a primary route for resealing damaged membranes (Cheng et al., 2015). Given the essential role of ML1 in lysosomal exocytosis and membrane resealing (Cheng et al., 2014), it is likely that ML1's muscle protective effects are mediated by sarcolemma repair. Muscle damage was experimentally induced *in vivo* with a short-term treadmill exercise protocol (Radley-Crabb et al., 2012) and confirmed with the entry of the membrane-impermeable Evans Blue (EB) dye (Cheng et al., 2014). The percentage of EB-positive fibers, which never exceeded 2% in WT muscles,

reached 9% at rest and 18% after treadmill exercise in *mdx* muscles (**Fig. 4.1A, B**). Notably, *mdx*;ML1$^{MCK}$ mice had less than 2% of EB-positive muscle fibers, even after treadmill exercise (**Fig. 4.1A, B**). EB uptake was also much reduced in ML-SA-treated *mdx* muscle (**Fig. 4.1D, E**). Cardiomyopathies are particularly evident in isoproterenol-challenged *mdx* mice (Yue et al., 2004). Notably, EB uptake in the heart tissue of *mdx* mice was much reduced by ML-SA injection (**Fig. 4.1G, H**). These results suggest that compromised membrane integrity in both skeletal and cardiac muscles can be improved by ML1 upregulation.

Serum creatine kinase (CK, a soluble cytoplasmic protein) level provides a systematic measurement of muscle membrane leakage and can serve as a biomarker for DMD (Cheng et al., 2014). ML1 overexpression and ML-SA i.p. injection decreased serum CK levels by more than 60% in *mdx* mice after exercise (**Fig. 4.1C**, **F**).

We performed an *ex vivo* muscle damage test, in which *in situ* force in GAS muscles were measured before and after mechanical stretch by blind experimenters (Radley-Crabb et al., 2012). The muscle force deficit seen in *mdx* mice was markedly decreased with ML1 overexpression (**Fig. 4.1I**), showing that ML1 expression has the potential to protect muscles from contraction-induced muscle damage *in vivo*. To study membrane repair *in vitro*, we used FM4-64 dye to detect membrane disruptions (Bansal et al., 2003) in single myofibers isolated from the flexor digitorum brevis (FDB) muscle (Bansal et al., 2003; Cai et al., 2009a). Upon laser irradiation, *mdx* fibers continued to take up FM dye at the injury sites for several minutes (**Fig. 4.1J, K**), whereas FM dye uptake was transient in ML1-overexpressed *mdx* muscle (**Fig. 4.1J, K**). These results suggest that ML1 activation facilitates membrane repair to reduce muscle damage in *mdx* mice.

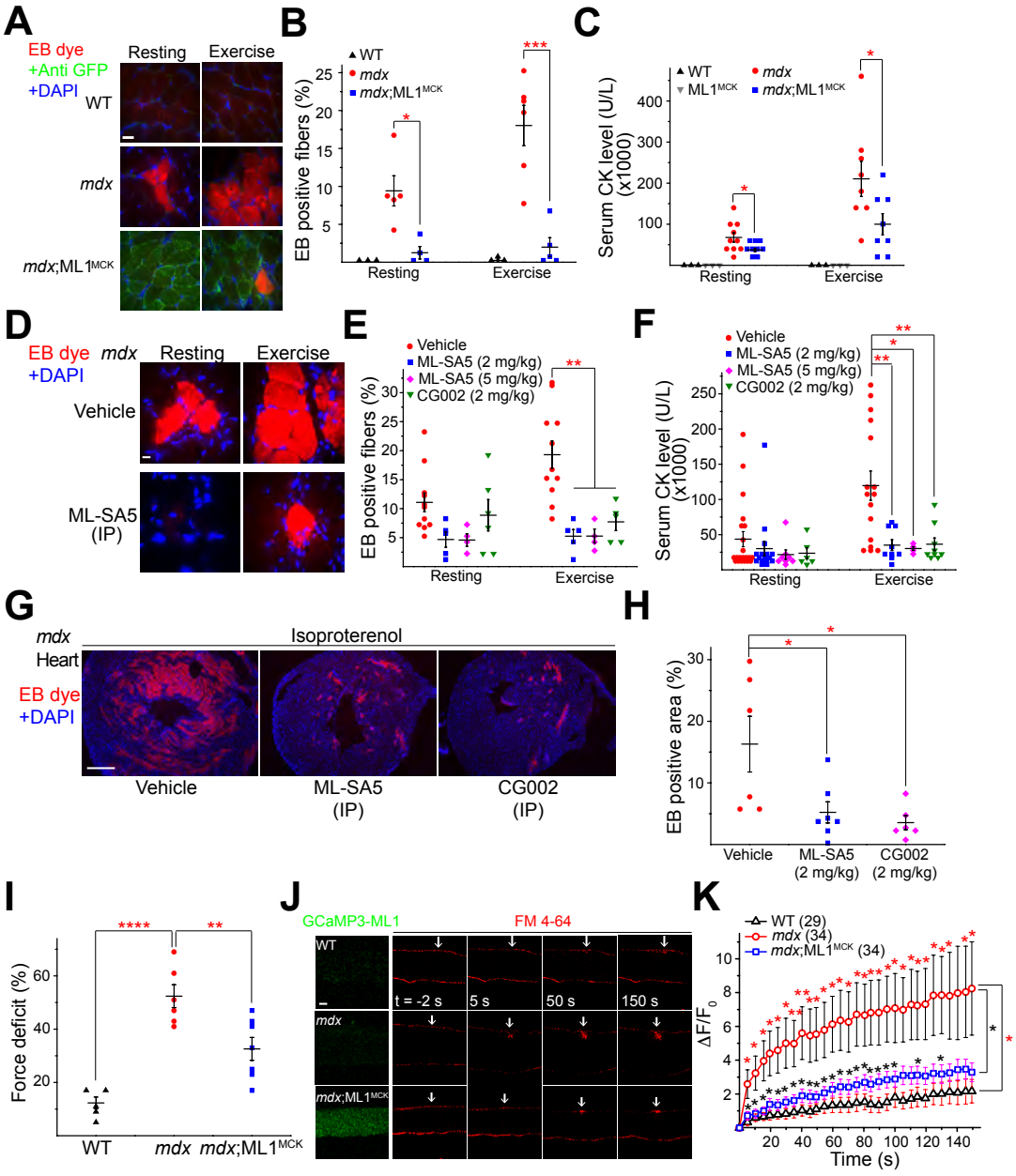


**Figure 4.1 ML1 activation facilitates membrane repair in *mdx* muscles.** (**A**) Representative images of EB dye uptake in GAS isolated from WT, *mdx*, and *mdx*;ML1$^{MCK}$ mice, before (rest) and after treadmill exercise. Scale bar = 10 μm. (**B**) Quantification of EB-positive fibers from panel a. Each datum (n, number of the animal) represents the averaged result from at least five representative images selected from at least three sections. (**C**) Serum CK levels in WT, ML1$^{MCK}$, *mdx*, and *mdx*;ML1$^{MCK}$ before and after treadmill exercise. Each datum represents the result from one animal. (**D**) EB dye uptake in GAS isolated from ML-SA5-treated *mdx* mice. Scale bar = 10 μm. (**E**) Quantification of EB dye uptake in GAS from ML-SA5- and CG002-treated *mdx* mice.

(**F**) Serum CK levels in ML-SA5- and CG002-treated *mdx* mice before and after treadmill exercise. (**G, H**) EB dye uptake in cardiac muscles isolated from ML-SA5 (2 mg/kg)- and CG002 (2 mg/kg)-injected *mdx* mice that were over-stimulated with β-isoproterenol to cause cardiac damage. Scale = 500 μm. (**I**) Muscle force deficit of mechanically-stretched GAS from 1-mo.-old mice. (**J**) Representative images of laser damage-induced FM dye accumulation in isolated FDB fibers. Arrows highlight damage sites. Scale = 20 μm. (**K**) Time-dependent laser damage-induced FM dye accumulation in FDB fibers isolated from WT, *mdx*, and *mdx*;ML1$^{MCK}$ mice. N indicates the number of the FDB fibers for each genotype. All data are means ± s.e.m.; $*p < 0.05$, $**p < 0.01$, and $***p < 0.001$. Panel G and I were generated by Wanwan He and Carol S. Davis respectively.

**Upregulation of ML1 in muscle activates TFEB and corrects lysosomal insufficiency**

Expression of lysosome-associated membrane protein 1 (Lamp1) is an indicator of lysosome function *in vivo*, such that Lamp1 upregulation accompanies lysosomal dysfunction or insufficiency (Xu and Ren, 2015). Aberrant Lamp1 expression has been reported in several *mdx* studies (Duguez et al., 2013; Pal et al., 2014). We found that Lamp1 levels were increased in *mdx* compared with WT mice in both GAS and DIA isolated from 1-month-old animals (**Fig. 4.2A-D**). In our immunofluorescence analysis, Lamp1 upregulation was apparent in muscle fibers and surrounding cells (e.g., infiltrated macrophages; **Fig. 4.2G**), suggesting that inflammation, which is known to be associated with necrosis (Tidball, 2005), may also contribute to Lamp1 upregulation. Collectively, these results suggest that there is lysosome insufficiency in the muscle tissues of *mdx* mice, and that lysosome biogenesis might have been weakly activated to compensate for the deficiency.

ML1 activation has been reported to increase lysosome biogenesis and Lamp1 levels through nuclear translocation of TFEB, a master regulator of lysosomal genes (Medina et al., 2015; Zhang et al., 2016). Intriguingly, Lamp1 expression was significantly lower in *mdx*;ML1$^{MCK}$ mice than in *mdx* mice (**Fig. 4.2A-D**). This seemingly puzzling result may be explained by ML1 expression boosting lysosome function and decreasing necrosis in muscle, obviating the need for

compensatory changes via the expression of lysosomal genes. In ML-SA-injected *mdx* mice, TFEB nuclear translocation was increased (**Fig. 4.3C, D**), but Lamp1 upregulation was suppressed (**Fig. 4.2E, F**). Hence, ML1 activation may further boost lysosome function to override lysosome insufficiency, yielding muscle protective effects. Similar scenarios have been reported in several lysosomal storage disorders (LSDs), in which TFEB activation has been found to increase lysosome biogenesis in WT cells while suppressing Lamp1 upregulation in LSD animal models (Spampanato et al., 2013; Xu and Ren, 2015).

To study the role of ML1 activation in lysosome biogenesis directly, we utilized DMD cells, an immortalized myoblast line developed from a DMD patient's muscle cells (**Fig. 4.4A, B**) (Sarathy et al., 2017). Only mild Lamp1 upregulation was observed in DMD myoblasts (**Fig. 4.4H**), suggesting that the lysosome insufficiency occurring in *mdx* mice might be caused by extensive *in vivo* muscle damage. Nanomolar concentrations of ML1 agonists were sufficient to induce striking nuclear translocation of TFEB (**Fig. 4.4C-E**) and the related protein TFE3 (**Fig. 4.5**). Consistently, expression of TFEB/TFE3 target genes, including those required for lysosome biogenesis and function, was elevated by ML-SA treatment (**Fig. 4.4F**). Notably, TFEB mRNA and protein expressions were significantly reduced in ML-SA-treated DMD cells (**Fig. 4.4F, G, I**), suggestive of feedback regulation. Hence, ML1 activation may lead to TFEB nuclear translocation, thereby increasing lysosome biogenesis, which in turn reduces lysosome stress and restores lysosome homeostasis.

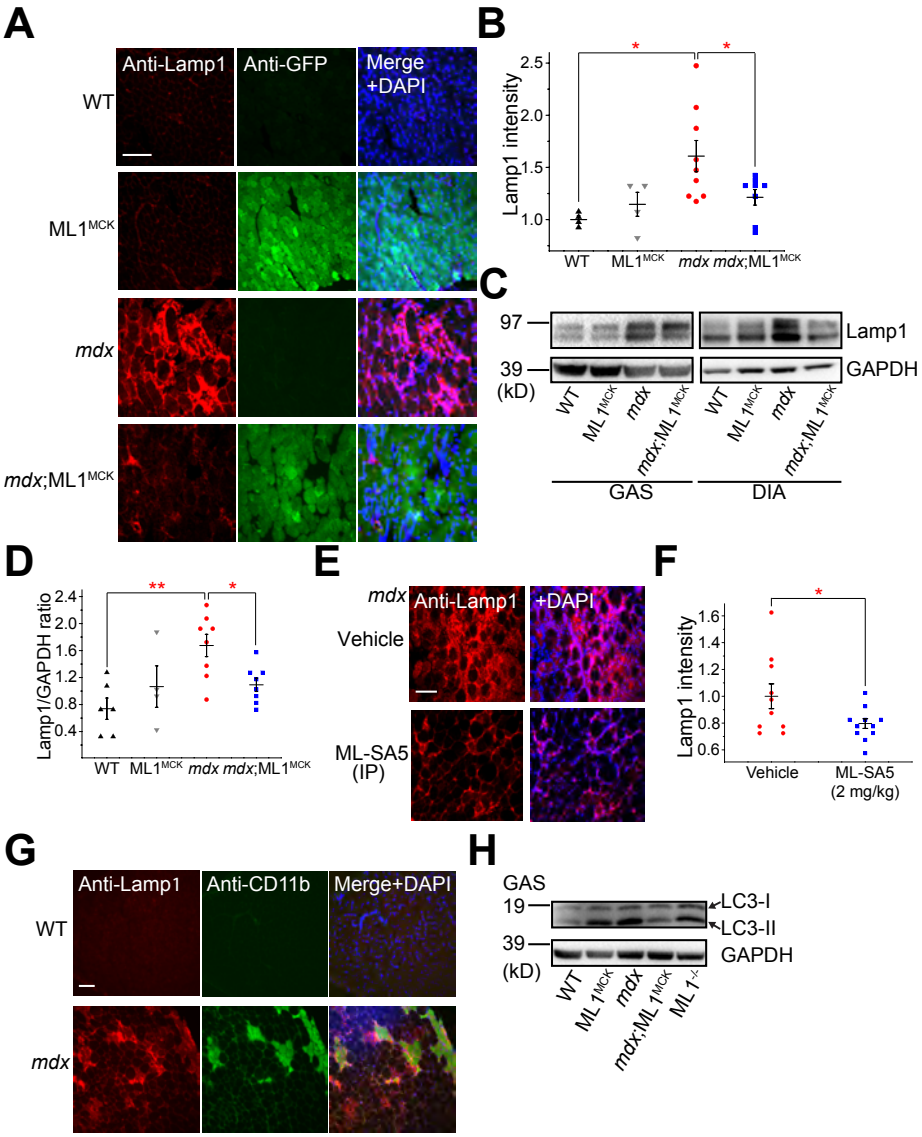


**Figure 4.2 Lysosomal insufficiency was corrected by ML1 activation.** (**A**) Lamp1 immunofluorescence staining of GAS from WT, ML1$^{MCK}$, and *mdx*, *mdx*;ML1$^{MCK}$ mice. Scale bar = 100 µm. (**B**) Quantitative analyses of images in **A**. For each datum representing each animal, at least five representative images from at least three sections were analyzed. (**C**) Western blotting analysis of Lamp1 protein expression in GAS and DIA. (**D**) Quantitation of western blotting results in panel **C**. For each datum representing each animal, at least five representative images from at least three sections were analyzed. (**E, F**) Lamp1 immunostaining in GAS from ML-SA5 (2 mg/kg)-treated *mdx* mice. Scale bar = 100 µm. (**G**) Lamp1 expression was high in CD11b-positive macrophages. Scale bar = 100 µm. (**H**) Western blotting analysis of LC3 protein levels in GAS from various transgenic mice. All data are means ± s.e.m.; $*p < 0.05$, $**p < 0.01$.

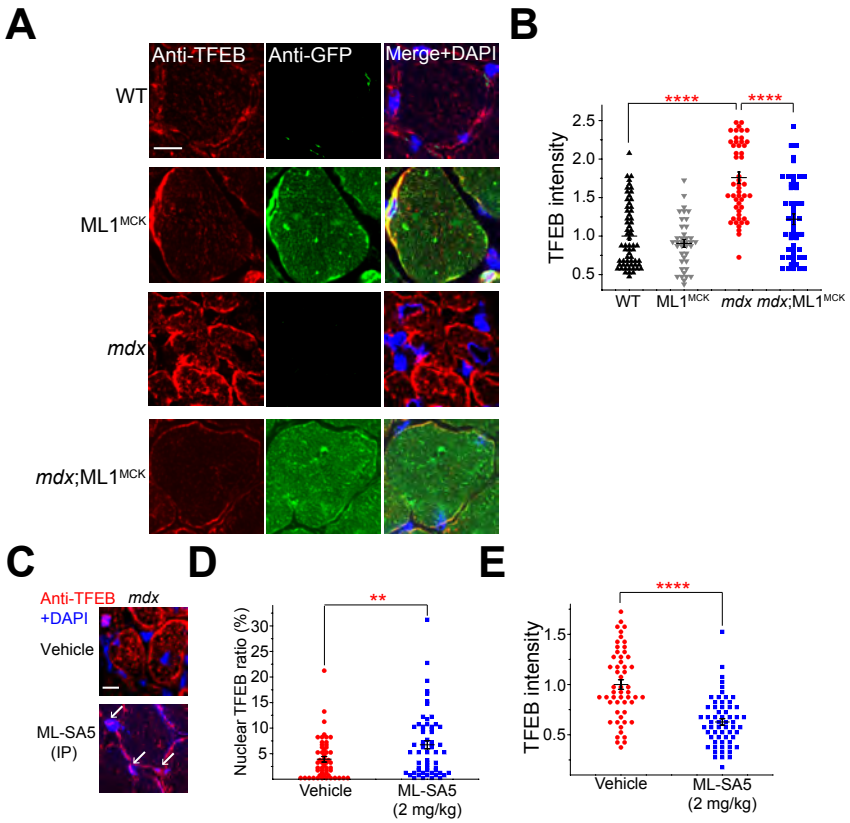


**Figure 4.3 ML1 overexpression and agonists activate TFEB *in vivo*.** (**A, B**) TFEB immunolabeling in GAS from WT, ML1$^{MCK}$, *mdx*, and *mdx*;ML1$^{MCK}$ mice. Scale bar = 10 μm. Each datum represents one muscle fiber in randomly selected images from at least four animals in each group. (**C**) TFEB immunolabeling in GAS from ML-SA5 treated mice. (**D**) Quantitative analysis of nuclear *vs.* total TFEB ratio from **C**. N indicates muscle fibers in randomly selected images from at least four muscles in each group. (**E**) Quantification for TFEB intensity. Each datum represents one muscle fiber in randomly selected images from at least four animals in each group. All data are means ± s.e.m.; $^{**}p < 0.01$, $^{****}p < 0.0001$.

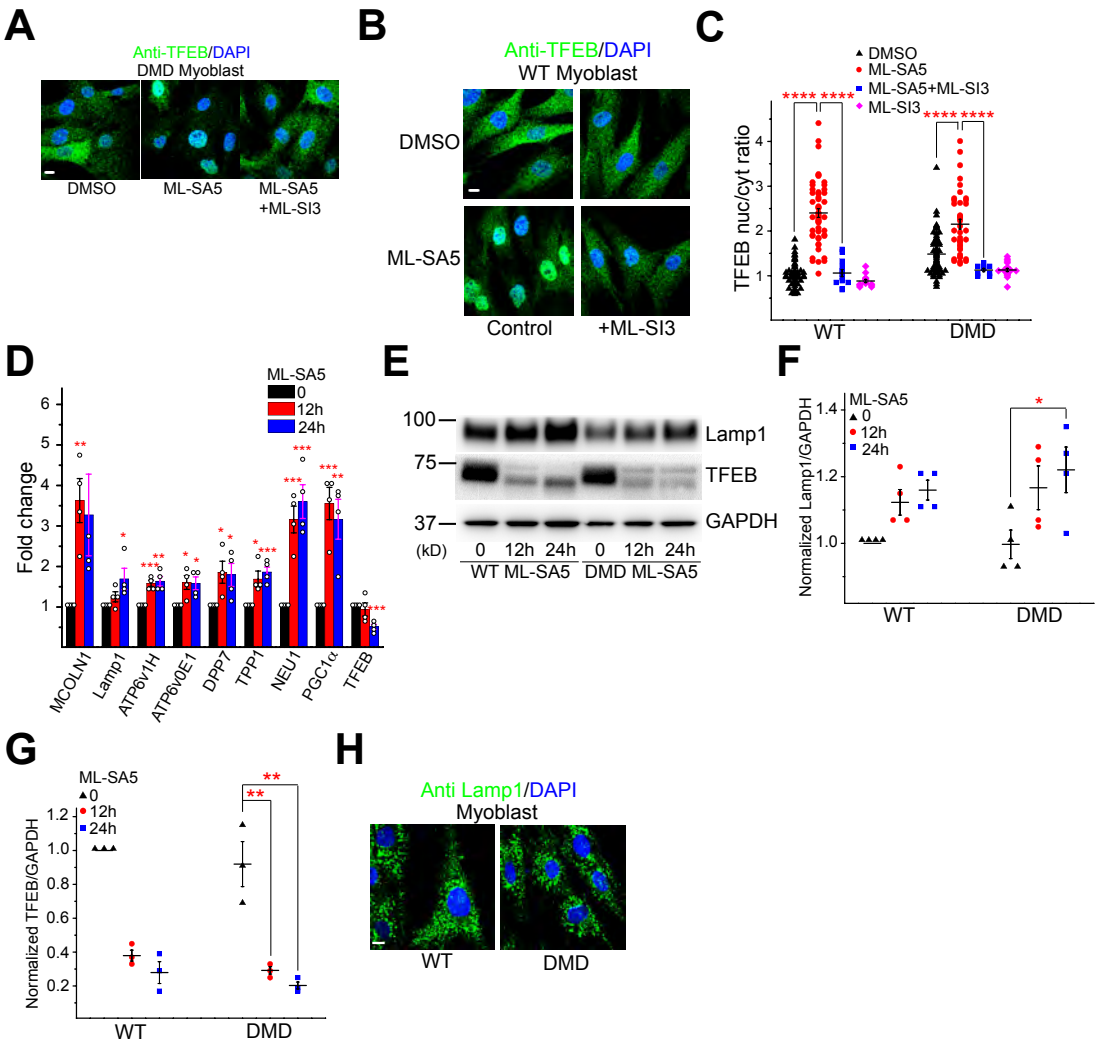


**Figure 4.4 ML1 agonists activate TFEB and lysosomal biogenesis in DMD myoblasts.** (**A**) The effects of ML-SA5 (0.5 μM for 1 h) on TFEB-nuclear translocation in the presence and absence of ML-SI3 (20 μM) in DMD cells. Scale bar = 10 μm. (**B, C**) TFEB immunolabeling of WT myoblasts upon ML-SA5 (0.5 μM) and ML-SI3 (20 μM) treatment. Scale = 10 μm. (**D**) mRNA expression levels of TFEB target genes determined by qPCR. HPRT was used as a control. (**E-G**) Lamp1 and TFEB protein levels in WT and DMD myoblasts were increased and decreased, respectively, upon ML-SA5 (0.5 μM) treatment for 12 h and 24 h. (**H**) Lamp1 immunolabeling in WT and DMD cells. Scale bar = 10 μm. All data are means ± s.e.m.; *$p < 0.05$, **$p < 0.01$, ***$p < 0.001$ and ****$p < 0.0001$. Panels D and E were generated by Zifan Zhao and Kaiyuan Tang, respectively.

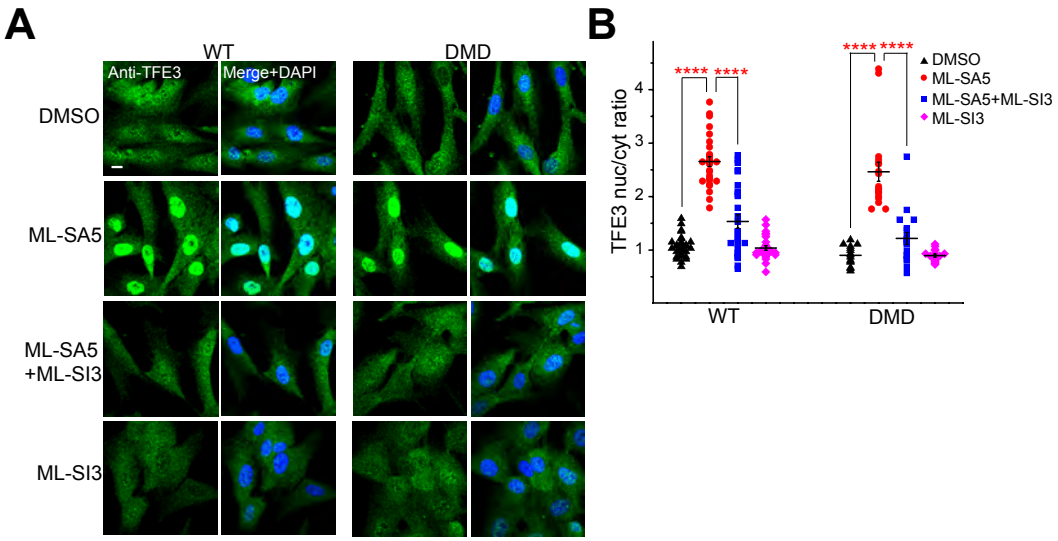


**Figure 4.5 Pharmacological activation of ML1 activates TFE3 in DMD myoblasts.** (**A, B**) TFE3 immunolabeling of WT and DMD myoblasts upon ML-SA5 (0.5 μM) and ML-SI3 (20 μM) treatment. Scale = 10 μm. Data are means ± s.e.m.; ****$p < 0.0001$.

**ML1 protects human DMD muscle cells from damage through TFEB and lysosomal exocytosis**

Whereas increased TFEB activation and lysosome biogenesis may amplify lysosomal trafficking events including lysosomal exocytosis (Medina et al., 2011), ML1 activation alone can trigger lysosomal exocytosis directly (Samie et al., 2013). Thus, ML1 activation may facilitate sarcolemma repair by increasing lysosomal exocytosis through both direct and indirect mechanisms (**Fig. 4.8**). Membrane damage [i.e., chemical injury caused by streptolysin O (SLO) toxin] triggers lysosomal exocytosis and membrane repair (Cheng et al., 2015). Propidium iodide (PI) staining is a common readout for membrane damage and cell viability (Idone et al., 2008). In DMD myoblasts and differentiated myotubes, both membrane damage and ML-SA treatment induced lysosomal exocytosis (**Fig. 4.7C, D**), suggesting that ML-SAs may trigger membrane

repair processes by mimicking a yet-to-be-identified damage signal. Consistent with this hypothesis, ML1 agonists and inhibitors decreased and increased, respectively, PI-positive cells following SLO treatment (**Fig. 4.6A, B**). The cytoprotective effects of ML-SAs were abolished by knock down of TFEB expression (**Fig. 4.6E-H**) or blockage of lysosomal exocytosis with dominant-negative Syt7 (**Fig. 4.7A, B**). Collectively, these results suggest that boosting ML1 activity may promote myocyte survival by reducing membrane damage (**Fig. 4.8**).

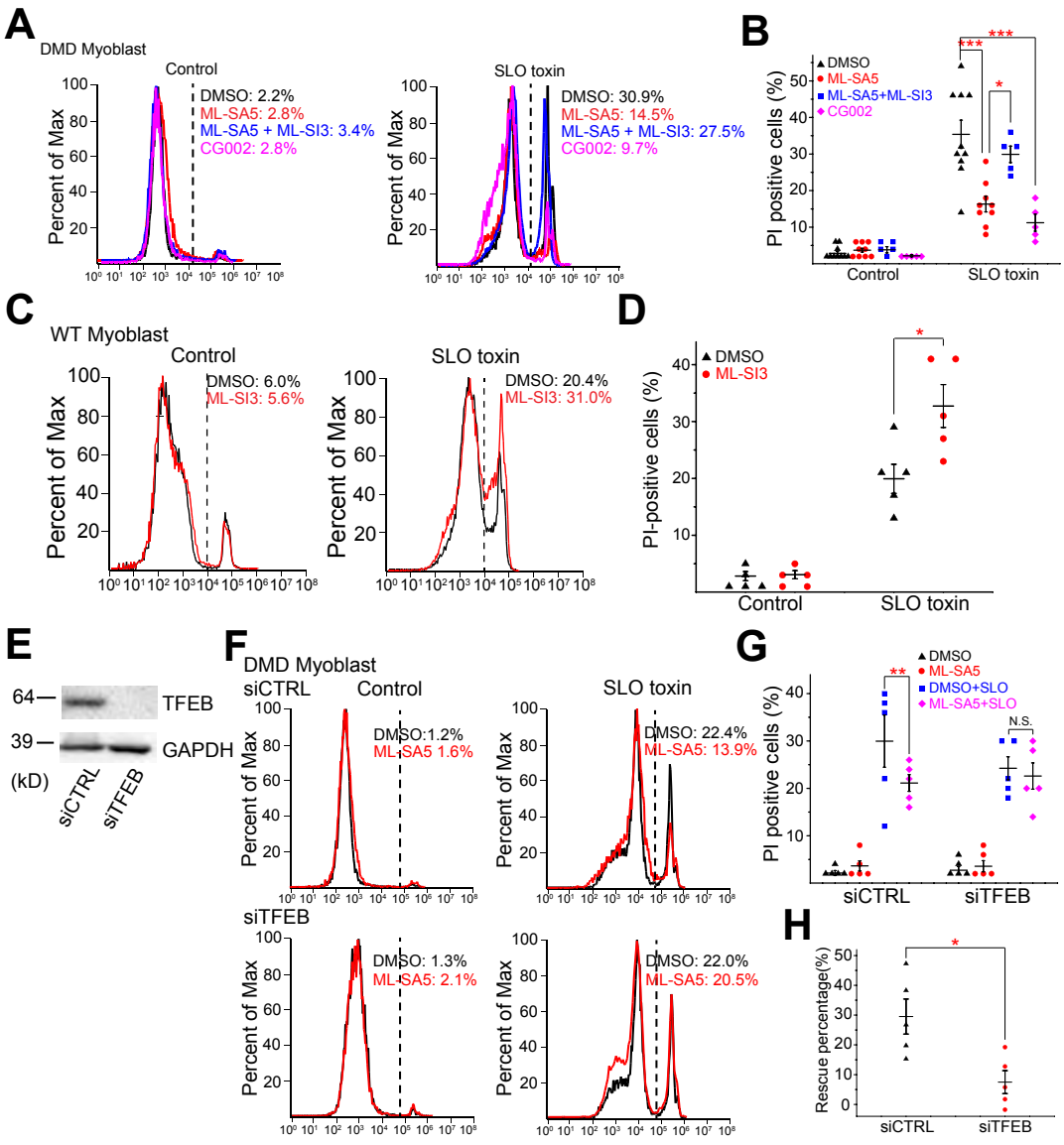

**Figure 4.6 ML1 agonist promotes cell survival via TFEB.** (**A**) Flow cytometric analysis of the viability of cultured muscle cells, assayed by PI staining following SLO toxin-induced membrane damage. Human DMD myoblasts were pre-treated with ML-SA5 (0.5 μM), CG002 (0.5 μM), and ML-SI3 (20 μM) for 7 h before being subjected to SLO toxin (0.5–1 μg/ml, 10 min) challenge. (**B**) Quantification of at least five independent repeats as shown in **A**. (**C, D**) PI-staining-based flow cytometry of the viability of cultured DMD myoblasts pretreated with ML-SI3 (20 μM) upon membrane damage by SLO toxin. (**E**) TFEB-specific siRNA decreased TFEB protein expression in DMD cells. (**F-H**) TFEB knockdown by siRNA blocked ML-SA5 effects on cell survival. All data are means ± s.e.m.; *$p < 0.05$, **$p < 0.01$, ***$p < 0.001$. Panel E was generated by Dr. Dan Li.

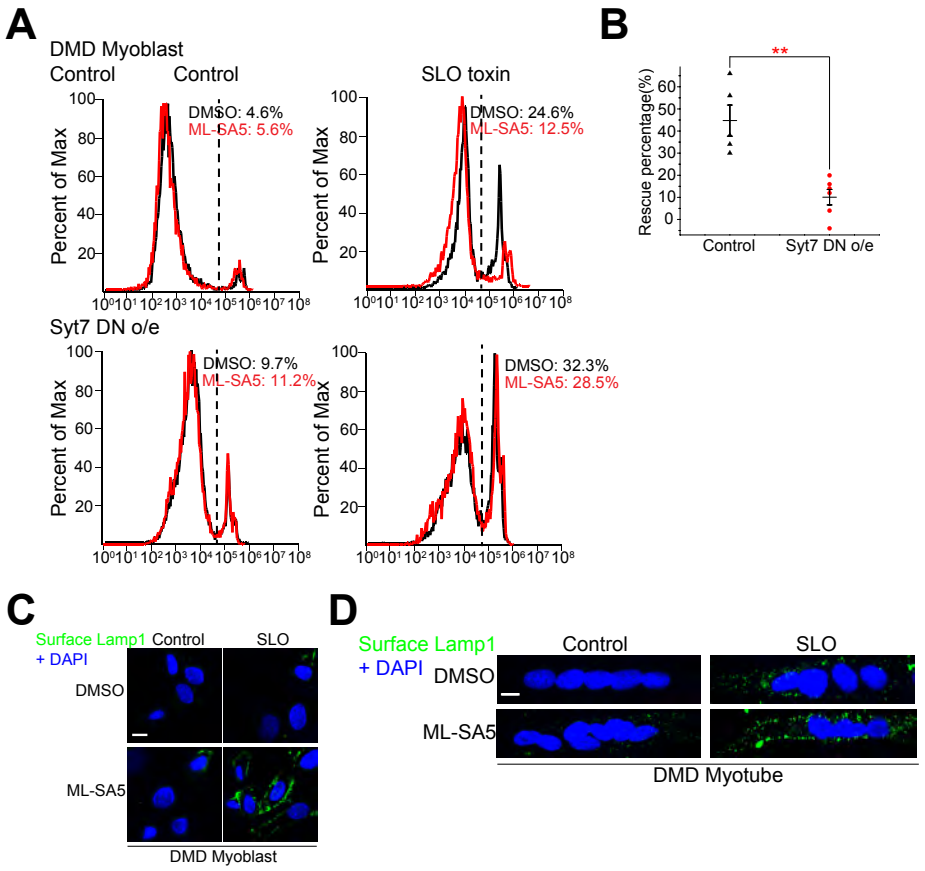


**Figure 4.7 Lysosomal exocytosis is required in ML-SA-induced cell survival.** (**A**) Flow cytometric analysis of DMD myoblasts transfected with a Syt-7 dominant-negative construct to block lysosomal exocytosis. (**B**) Quantitative analysis of **A**. (**C, D**) Lamp1 surface immunolabeling of DMD myoblasts (**C**) and differentiated myotubes (**D**) after ML-SA5 (0.5 μM) pretreatment and SLO (1 μg/mL, 30 min) challenge. Surface expression of Lamp1 was assayed with an anti-Lamp1 antibody that recognizes a luminal epitope in non-permeabilized cells. Scale = 10 μm. Data are means ± s.e.m.; **$p < 0.01$. Panels C&D were generated by Ce Wang in the Xu lab.

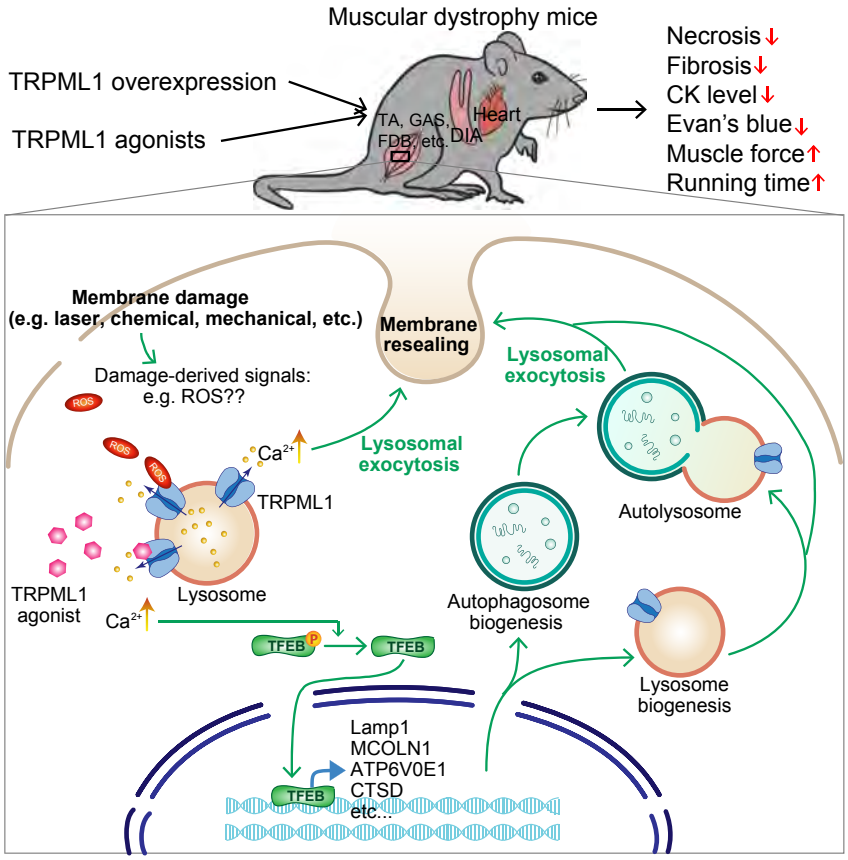


**Figure 4.8 Diagram demonstration of ML1 in lysosomal exocytosis and membrane repair.** Genetic or pharmacological upregulation of ML1 ameliorates muscle pathology *in vivo* through TFEB-dependent lysosome biogenesis, $Ca^{2+}$-dependent lysosomal exocytosis, and sarcolemma repair. Muscle damage may generate a yet-to-be-defined signal (e.g.,ROS) to activate ML1 channels on lysosome membranes. Subsequent lysosomal $Ca^{2+}$ release triggers $Ca^{2+}$-dependent lysosomal exocytosis and nuclear translocation of TFEB, which then activates transcription of a unique set of genes related to lysosome biogenesis. Subsequently, lysosome function is boosted and sarcolemma repair may be facilitated to reduce muscle damage in DMD cells *in vitro* and *in vivo*.

## Discussion

### 1. Summary of the study and significance

In the last chapter, the author presented that both genetic and pharmacological activation of ML1 had muscle protective effects in MD mice. Here, we showed that ML1 activation led to

TFEB nuclear translocation and increased lysosomal biogenesis, while increasing lysosomal trafficking (e.g., exocytosis), thereby facilitating sarcolemma repair to reduce muscle damage (**Fig. 4.8**). Hence, our proof-of-concept study has provided strong evidence that small-molecule ML1 agonists can be developed to treat DMD. Although DMD is not an LSD per se (Xu and Ren, 2015), the observed compensatory changes are suggestive of lysosome insufficiency. In both cases, augmenting ML1/TFEB-dependent lysosome biogenesis can alleviate lysosome insufficiency.

The simplest explanation for the presently observed muscle protective effect of ML1, in our view, would be facilitation of lysosomal exocytosis and membrane repair (**Fig. 4.8**). Consistent with this hypothesis, blockage of lysosomal exocytosis abolished ML1-dependent muscle protection. TFEB has been shown to be muscle protective in other studies (Spampanato et al., 2013). In LSDs, ML1 and TFEB form a positive feedback loop that promotes cellular clearance (Xu and Ren, 2015). It is possible that the same lysosome program may boost sarcolemma repair to reduce muscle damage in DMD and other muscle diseases. Hence, manipulating lysosome function with small molecules may have broad therapeutic potentials.

**2. Lysosome in MDs**

Muscle cells are terminally-differentiated. Being both metabolically and mechanically active, it requires cellular machineries to quickly turn over cell contents, as well as effectively repair damaged sarcolemma. Lysosomes can do both. Autophagy has been shown important for clearance of damaged cellular contents and maintenance of muscle mass (Sandri, 2010). Lysosomal exocytosis is found to be a major mechanism for mending damaged plasma membrane in cells. As I summarized in Chapter I and Table 1.1, some autophagic and lysosomal gene deficiency can directly lead to muscle pathologies. It is interesting to note that ATG gene

deficiency, which mediates early autophagosome initiation stage, causes muscle atrophy, while deficiency of lysosomal proteins like ML1 results in MD (**Table 1.1**). Consistently, ATG-deficient mice showed normal serum CK level, whereas ML1 KO mice and patients with Danon/Pompe/XEMA all have CK increase (Cheng et al., 2014; Malicdan and Nishino, 2012; Masiero et al., 2009). These findings suggest that lysosomes may regulate muscle physiology through different mechanisms.

How lysosomes are regulated in MD is under debate. In a study using secretome profile, Lamp1-positive vesicles were found enriched in secretomes from *mdx* myotubes. And these vesicles also accumulate inside of *mdx* myotubes. Consistently, immunostaining of muscle tissue has revealed increased Lamp1 in *mdx* mice (Duguez et al., 2013). However, in a recent study, ROS generated by NOX2 in *mdx* muscles were shown to impair lysosomal biogenesis, characterized by decreased Lamp1 levels (Pal et al., 2014). In our study, although variation exists between different muscles, in general, I found Lamp1 level was upregulated in *mdx* muscles at 1 month old. One possible explanation for these contradictory results is Lamp1 may be contributed by different cell types in muscles. This is especially relevant considering muscles are undergoing severe necrosis in *mdx* mice around 1 month old. Infiltrated inflammatory cells often have active lysosomes due to their digestive and secretory function. Consistently, I saw increased Lamp1 in the muscle tissue was highly co-localized with macrophage marker CD11b. When testing Lamp1 levels by Western blot, the band is representing the total level from Lamp1 in the whole tissue, which may be affected by the necrosis level in the muscle. Since the necrosis level is changed at different ages, it is possible that age can be affecting Lamp1 level in *mdx* mice. Furthermore, age may also affect

Lamp1 levels in muscle fibers due to different stages of pathogenesis. Thus, it is important to control the age of mice in studies and use staining method to specify the origin of Lamp1 proteins.

In previous studies, impaired autophagy in *mdx* mice has been shown by several studies. In these studies, LC3-II levels and GFP-LC3 puncta were decreased in *mdx* muscles and fibers. It is believed that interruption of mTOR signaling contributes to this aberrant autophagy level. However, I found LC3-II level was increased, but not decreased, in *mdx* muscles. It is possible that necrosis and age of the mice may affect LC3 similarly as Lamp1. Additionally, it is important to keep in mind that increase of LC3-II may be due to either increased autophagosome formation or decreased lysosomal degradation. Blocking lysosomal function can cause autophagosome accumulation and significantly increase LC3-II protein level (Klionsky et al., 2012). When designing experiments to examine autophagic flux, it is important to differentiate between these two possibilities.

When interpreting data of autophagy and lysosomal marker change in pathological conditions, caution needs to be taken when drawing conclusions on causality. Seeing increased lysosomal marker Lamp1 in MD does not mean increased Lamp1 level is contributing to the pathogenesis. In fact, it may be the consequences of disease development and compensation. What happens in LSDs is a best example, where mutations in lysosomal proteins caused lysosomal dysfunction, and cells are trying to generate more lysosomes to compensate, causing the storage phenotype. Consistently, methods used to boost lysosomal function and treat LSDs often decrease, but not increase, lysosome number/size in LSDs (Medina et al., 2011; Spampanato et al., 2013). Although the nature of LSDs and MDs are different, both diseases have more damaged cellular contents requiring lysosomal function. It is possible to see increased Lamp1 and lysosomes in MDs

in certain stages of the disease, therefore boosting lysosomal function may be a therapeutic target for treating MDs.

# CHAPTER V

## Discussion

### 1. Summary of the study and significance

Lysosomes are active organelles that regulate various cellular biological processes. In adaptation to cellular stress conditions, number, size, and function of lysosomes are adjusted to meet cellular needs (Sardiello et al., 2009). This lysosomal adaptation process is essential for stress responses of cells and organisms (Settembre and Ballabio, 2014). TFEB is the key molecule regulating lysosomal adaptation (Sardiello et al., 2009). Upon activation, TFEB translocates into the nucleus and initiates transcription of downstream lysosomal and autophagic genes (Sardiello et al., 2009). The lysosomal $Ca^{2+}$ channel ML1 turned out to be a major positive regulator of TFEB (Medina et al., 2015). Activation of ML1 triggers lysosomal $Ca^{2+}$ release, followed by TFEB nuclear translocation, and lysosome and autophagosome biogenesis (Medina et al., 2015). Hence, ML1, $Ca^{2+}$ release, and TFEB together form a pathway to regulate lysosomal adaptation and multiple aspects of lysosomal function including autophagy and lysosomal exocytosis (Medina et al., 2015; Medina et al., 2011). In this dissertation, I found that ML1 channels were directly activated by exogenous ROS as well as endogenous oxidative stress induced by mitochondrial damage. TFEB was then activated by $Ca^{2+}$ release through ML1, upregulating autophagic flux by generating more autophagosomes and lysosomes. This activation of the ML1-TFEB axis was essential for removal of excess ROS and damaged mitochondria (Chapter II). This study has shown

the physiological significance of ML1-TFEB pathway in regulation of mitophagy upon oxidative stress.

TFEB activation has been suggested to increase lysosomal exocytosis, a process important for the maintenance of muscle plasma membrane integrity, and ameliorate multiple LSDs including muscle diseases (Medina et al., 2011; Spampanato et al., 2013). Besides, ML1 deficient human and mice exhibit progressive muscular dystrophy (Cheng et al., 2014). By utilizing ML1 transgenic overexpression mouse lines and ML1 small molecule agonists available in the lab, I artificially activated ML1 *in vivo* and found that dystrophic pathologies were improved by ML1 activation (Chapter III). I also showed that upregulation of ML1 activated TFEB, corrected lysosomal insufficiency, and ameliorated sarcolemmal integrity. More importantly, ML1 agonists prevented muscle cell death induced by pore-forming toxins, and this process is TFEB- and lysosomal exocytosis-dependent (Chapter IV). This study has demonstrated that manipulation of ML1 activity and TFEB could be a potential therapeutic for muscular dystrophy as well as LSDs and lysosome-associated diseases.

## 2. Activation of ML1 in physiology and pathology

### 2.1 Endogenous ML1 modulators

Activation of ML1 by genetical overexpression or pharmacological agonists, especially *in vivo*, can be complicated, given that endogenous activators and inhibitors of ML1 may modulate the channel as well. In Chapter II, I showed that ROS could directly activate ML1. Interestingly, ROS are also active players in regulation of muscle physiology and pathology (Allen et al., 2016; Barbieri and Sestili, 2012). In muscle cells, ROS can be generated from several different sources (Barbieri and Sestili, 2012). Mitochondria are the predominant sources of ROS generation in most

cell types (Barbieri and Sestili, 2012). However, recent studies have shown that during contractile activity of muscle fibers, mitochondrial ROS production was not increased, while the cytosolic ROS underwent a 100% increase (Michaelson et al., 2010). This is possibly because mitochondria tend to generate more ROS under basal respiratory state compared to stimulated respiration (Di Meo and Venditti, 2001; Herrero and Barja, 1997). NOXs located within the sarcolemma and sarcoplasmic reticulum were proposed to be the major sources of ROS production in muscles (Piao et al., 2005; Powers and Jackson, 2008). Other sources of ROS generation include cytosolic xanthine oxidase (XO) generating superoxide anion, and phospholipase A2 (PLA2), a $Ca^{2+}$-dependent enzyme increasing NOXs activity and promoting mitochondrial ROS production (Gomez-Cabrera et al., 2005; Petrof et al., 1993).

ROS production in muscles is known to be regulated by contractile activities and inflammation (Barbieri and Sestili, 2012). During aerobic exercise, superoxide production is increased by 50 to 100 folds (Kanter, 1994; Urso and Clarkson, 2003). NOXs are considered to be the major sources of ROS during contraction (Piao et al., 2005). NOX2 is believed to be activated by stretch, possibly through microtubule-dependent mechanisms, and contribute to muscle damage and weakness in dystrophic *mdx* muscles (Khairallah et al., 2012). PLA2 activity in DMD muscles is also 10 times greater than in controls (Lindahl et al., 1995). Besides, inflammation and subsequent cytokine release lead to more ROS generation, likely through mitochondria and enzymes like NOX and XO (Barbieri and Sestili, 2012; Langen et al., 2004).

Due to sarcolemmal damage and infiltration of inflammatory cells, ROS levels in DMD muscles are significantly higher (Allen et al., 2016; Barbieri and Sestili, 2012). With muscle-specific ML1 overexpression, it is likely that cytosolic ROS increase could readily activate ML1

and lysosomal $Ca^{2+}$ release, triggering lysosomal exocytosis as well as the TFEB signaling pathway. However, things are more controversial when it comes to ML-SA-injected mice. Co-application of ROS with ML-SA to cultured cells did not yield synergistic effects on ML1 currents (data not shown). It is possible that ROS may directly oxidize the channel and cause structural changes so ML-SAs can no longer bind. It is also likely that ML-SAs can be modulated by oxidation. However, these results do not necessarily suggest what happens *in vivo*. The concentration of ML-SAs finally reached in muscle cells is probably much lower than what we dumped into the solution when doing patch clamp. Moreover, compared with highly active, short-lived ROS, ML-SA5 and CG002 are sticky drugs which are hard to be washed out. Thus, how ROS and ML-SAs may work together to modulate ML1 channels *in vivo* still needs to be elucidated.

Apart from ROS, $PI(3,5)P_2$, $PI(4,5)P_2$ and sphingomyelins also modulate ML1 channels (Xu and Ren, 2015). The regulatory mechanisms for these lipids in muscles under physiological and pathological conditions are not clear. It was reported that insulin treatment increased $PI(3,5)P_2$ in cardiomyocytes, activating ryanodine receptor, $Ca^{2+}$ release, and muscle contraction (Touchberry et al., 2010). Co-application of $PI(3,5)P_2$ and ML-SAs had synergistic effects on ML1 activation (Shen et al., 2012), and cryo-EM structure showed separate binding sites for $PI(3,5)P_2$ and ML-SA1 (Chen et al., 2017; Li et al., 2017; Schmiege et al., 2017). In ML-SA-injected mice, it is possible that endogenous $PI(3,5)P_2$ also contributed to ML1 and downstream signaling activation. Endogenous inhibitors for ML1 are also important since constant activation of ML1 channels is apparently toxic to cells (Dong et al., 2009). More importantly, $PI(4,5)P_2$ and

sphingomyelins are predominantly localized to plasma membrane, so ML1 activity can be inhibited after lysosomal exocytosis (Xu and Ren, 2015).

**2.2 ML-SAs: mechanisms, pharmacodynamics, pharmacokinetics, and side effects**

Based on our data, the most straightforward explanation for ML-SAs' effects on muscular dystrophy in *mdx* mice is ML-SA injection induced TFEB nuclear translocation and lysosomal biogenesis, preparing more lysosomes to repair sarcolemmal damage caused in daily exercises. However, it is also possible that ML-SA treatment may promote muscle cell survival via other TFEB-independent mechanisms such as vesicle trafficking. Further studies are needed to dissect the mechanisms of ML-SA's effects *in vivo*. Besides, I did not notice dose-dependence for ML-SA, likely due to variations within groups. An alternate explanation would be the therapeutic window for dosage of ML-SA is small and 2 mg/kg treatment already reaches the peak of biological effects. To address these questions, more characterization of pharmacodynamics needs to be done. A major drawback of this study is the lack of data on pharmacokinetics. It would be very helpful to know how fast ML-SAs are absorbed, how long they can last *in vivo*, and the distribution of these drugs in different organs. This is not only relevant for determination of dosage and dissection of drug mechanisms, but also important for analyzing side effects of these drugs. Since ML1 and lysosomes have multiple roles in regulating various physiological processes and tissues, more studies should be performed to characterize side effects of ML-SAs.

## REFERENCES


Aartsma-Rus, A., and Krieg, A.M. (2017). FDA Approves Eteplirsen for Duchenne Muscular Dystrophy: The Next Chapter in the Eteplirsen Saga. Nucleic acid therapeutics *27*, 1-3.

Allen, D.G., Whitehead, N.P., and Froehner, S.C. (2016). Absence of Dystrophin Disrupts Skeletal Muscle Signaling: Roles of Ca2+, Reactive Oxygen Species, and Nitric Oxide in the Development of Muscular Dystrophy. Physiol Rev *96*, 253-305.

Amoasii, L., Hildyard, J.C.W., Li, H., Sanchez-Ortiz, E., Mireault, A., Caballero, D., Harron, R., Stathopoulou, T.-R., Massey, C., and Shelton, J.M. (2018). Gene editing restores dystrophin expression in a canine model of Duchenne muscular dystrophy. Science *362*, 86-91.

Amoasii, L., Long, C., Li, H., Mireault, A.A., Shelton, J.M., Sanchez-Ortiz, E., McAnally, J.R., Bhattacharyya, S., Schmidt, F., Grimm, D*., et al.* (2017). Single-cut genome editing restores dystrophin expression in a new mouse model of muscular dystrophy. Sci Transl Med *9*.

Anderson, L.V.B., Davison, K., Moss, J.A., Young, C., Cullen, M.J., Walsh, J., Johnson, M.A., Bashir, R., Britton, S., and Keers, S. (1999). Dysferlin is a plasma membrane protein and is expressed early in human development. Human molecular genetics *8*, 855-861.

Andrews, N.W. (2017). Detection of Lysosomal Exocytosis by Surface Exposure of Lamp1 Luminal Epitopes. Methods Mol Biol *1594*, 205-211.

Bach, G., Zeevi, D.A., Frumkin, A., and Kogot-Levin, A. (2010). Mucolipidosis type IV and the mucolipins. Biochem Soc Trans *38*, 1432-1435.

Bahro, M., and Pfeifer, U. (1987). Short-term stimulation by propranolol and verapamil of cardiac cellular autophagy. Journal of molecular and cellular cardiology *19*, 1169-1178.

Bansal, D., Miyake, K., Vogel, S.S., Groh, S., Chen, C.C., Williamson, R., McNeil, P.L., and Campbell, K.P. (2003). Defective membrane repair in dysferlin-deficient muscular dystrophy. Nature *423*, 168-172.

Barbieri, E., and Sestili, P. (2012). Reactive oxygen species in skeletal muscle signaling. Journal of signal transduction *2012*.

Bargal, R., Avidan, N., Ben-Asher, E., Olender, Z., Zeigler, M., Frumkin, A., Raas-Rothschild, A., Glusman, G., Lancet, D., and Bach, G. (2000). Identification of the gene causing mucolipidosis type IV. Nature genetics *26*, 118.

Barnham, K.J., Masters, C.L., and Bush, A.I. (2004). Neurodegenerative diseases and oxidative stress. Nat Rev Drug Discov *3*, 205-214.

Beastrom, N., Lu, H., Macke, A., Canan, B.D., Johnson, E.K., Penton, C.M., Kaspar, B.K., Rodino-Klapac, L.R., Zhou, L., and Janssen, P.M.L. (2011). Mdx5Cv mice manifest more severe muscle dysfunction and diaphragm force deficits than do mdx mice. The American journal of pathology *179*, 2464-2474.

Benard, G., Bellance, N., James, D., Parrone, P., Fernandez, H., Letellier, T., and Rossignol, R. (2007). Mitochondrial bioenergetics and structural network organization. J Cell Sci *120*, 838-848.

Bibee, K.P., Cheng, Y.-J., Ching, J.K., Marsh, J.N., Li, A.J., Keeling, R.M., Connolly, A.M., Golumbek, P.T., Myerson, J.W., and Hu, G. (2014). Rapamycin nanoparticles target defective autophagy in muscular dystrophy to enhance both strength and cardiac function. The FASEB Journal *28*, 2047-2061.

Blake, D.J., Weir, A., Newey, S.E., and Davies, K.E. (2002). Function and genetics of dystrophin and dystrophin-related proteins in muscle. Physiological reviews *82*, 291-329.

Bodine, S.C., Latres, E., Baumhueter, S., Lai, V.K.M., Nunez, L., Clarke, B.A., Poueymirou, W.T., Panaro, F.J., Na, E., and Dharmarajan, K. (2001). Identification of ubiquitin ligases required for skeletal muscle atrophy. Science *294*, 1704-1708.

Bogeski, I., and Niemeyer, B.A. (2014). Redox regulation of ion channels. Antioxid Redox Signal *21*, 859-862.

Bonaldo, P., and Sandri, M. (2013). Cellular and molecular mechanisms of muscle atrophy. Dis Model Mech *6*, 25-39.

Bouché, V., Espinosa, A.P., Leone, L., Sardiello, M., Ballabio, A., and Botas, J. (2016). Drosophila Mitf regulates the V-ATPase and the lysosomal-autophagic pathway. Autophagy *12*, 484-498.

Boudewyn, L.C., and Walkley, S.U. (2018). Current concepts in the neuropathogenesis of mucolipidosis type IV. Journal of neurochemistry.

Brady, R.O. (2006). Enzyme replacement for lysosomal diseases. Annu Rev Med *57*, 283-296.

Brancaccio, P., Maffulli, N., and Limongelli, F.M. (2007). Creatine kinase monitoring in sport medicine. British medical bulletin *81*, 209-230.

Bruning, J.C., Michael, M.D., Winnay, J.N., Hayashi, T., Horsch, D., Accili, D., Goodyear, L.J., and Kahn, C.R. (1998). A muscle-specific insulin receptor knockout exhibits features of the metabolic syndrome of NIDDM without altering glucose tolerance. Mol Cell *2*, 559-569.

Bulfield, G., Siller, W.G., Wight, P.A., and Moore, K.J. (1984). X chromosome-linked muscular dystrophy (mdx) in the mouse. Proceedings of the National Academy of Sciences *81*, 1189-1192.

Bushby, K., Finkel, R., Birnkrant, D.J., Case, L.E., Clemens, P.R., Cripe, L., Kaul, A., Kinnett, K., McDonald, C., and Pandya, S. (2010). Diagnosis and management of Duchenne muscular dystrophy, part 1: diagnosis, and pharmacological and psychosocial management. The Lancet Neurology *9*, 77-93.

Cai, C., Masumiya, H., Weisleder, N., Matsuda, N., Nishi, M., Hwang, M., Ko, J.K., Lin, P., Thornton, A., Zhao, X.*, et al.* (2009a). MG53 nucleates assembly of cell membrane repair machinery. Nat Cell Biol *11*, 56-64.

Cai, C., Weisleder, N., Ko, J.K., Komazaki, S., Sunada, Y., Nishi, M., Takeshima, H., and Ma, J. (2009b). Membrane repair defects in muscular dystrophy are linked to altered interaction between MG53, caveolin-3, and dysferlin. J Biol Chem *284*, 15894-15902.

Call, J.A., Voelker, K.A., Wolff, A.V., McMillan, R.P., Evans, N.P., Hulver, M.W., Talmadge, R.J., and Grange, R.W. (2008). Endurance capacity in maturing mdx mice is markedly enhanced by combined voluntary wheel running and green tea extract. Journal of applied physiology.

Campbell, K.P. (1995). Three muscular dystrophies: loss of cytoskeleton-extracellular matrix linkage. Cell *80*, 675-679.

Cang, C., Zhou, Y., Navarro, B., Seo, Y.-j., Aranda, K., Shi, L., Battaglia-Hsu, S., Nissim, I., Clapham, D.E., and Ren, D. (2013). mTOR regulates lysosomal ATP-sensitive two-pore Na+ channels to adapt to metabolic state. Cell *152*, 778-790.

Castellano, B.M., Thelen, A.M., Moldavski, O., Feltes, M., van der Welle, R.E.N., Mydock-McGrane, L., Jiang, X., van Eijkeren, R.J., Davis, O.B., Louie, S.M.*, et al.* (2017). Lysosomal cholesterol activates mTORC1 via an SLC38A9–Niemann-Pick C1 signaling complex. Science *355*, 1306.

Cerny, J., Feng, Y., Yu, A., Miyake, K., Borgonovo, B., Klumperman, J., Meldolesi, J., McNeil, P.L., and Kirchhausen, T. (2004). The small chemical vacuolin-1 inhibits Ca(2+)-dependent lysosomal exocytosis but not cell resealing. EMBO Rep *5*, 883-888.

Chakrabarti, S., Kobayashi, K.S., Flavell, R.A., Marks, C.B., Miyake, K., Liston, D.R., Fowler, K.T., Gorelick, F.S., and Andrews, N.W. (2003). Impaired membrane resealing and autoimmune myositis in synaptotagmin VII-deficient mice. J Cell Biol *162*, 543-549.

Chapman, V.M., Miller, D.R., Armstrong, D., and Caskey, C.T. (1989). Recovery of induced mutations for X chromosome-linked muscular dystrophy in mice. Proceedings of the National Academy of Sciences *86*, 1292-1296.

Chen, C.S., Bach, G., and Pagano, R.E. (1998). Abnormal transport along the lysosomal pathway in mucolipidosis, type IV disease. Proc Natl Acad Sci U S A *95*, 6373-6378.

Chen, Q., She, J., Zeng, W., Guo, J., Xu, H., Bai, X.C., and Jiang, Y. (2017). Structure of mammalian endolysosomal TRPML1 channel in nanodiscs. Nature *550*, 415-418.

Cheng, X., Shen, D., Samie, M., and Xu, H. (2010). Mucolipins: Intracellular TRPML1-3 channels. FEBS Lett *584*, 2013-2021.

Cheng, X., Zhang, X., Gao, Q., Ali Samie, M., Azar, M., Tsang, W.L., Dong, L., Sahoo, N., Li, X., Zhuo, Y.*, et al.* (2014). The intracellular Ca(2)(+) channel MCOLN1 is required for sarcolemma repair to prevent muscular dystrophy. Nat Med *20*, 1187-1192.

Cheng, X., Zhang, X., Yu, L., and Xu, H. (2015). Calcium signaling in membrane repair. Semin Cell Dev Biol *45*, 24-31.

Chien, Y.-H., Lee, N.-C., Huang, H.-J., Thurberg, B.L., Tsai, F.-J., and Hwu, W.-L. (2011). Later-onset Pompe disease: early detection and early treatment initiation enabled by newborn screening. The Journal of pediatrics *158*, 1023-1027.

Chua, J.P., Reddy, S.L., Merry, D.E., Adachi, H., Katsuno, M., Sobue, G., Robins, D.M., and Lieberman, A.P. (2013). Transcriptional activation of TFEB/ZKSCAN3 target genes underlies enhanced autophagy in spinobulbar muscular atrophy. Human molecular genetics *23*, 1376-1386.

Chuang, H.H., and Lin, S. (2009). Oxidative challenges sensitize the capsaicin receptor by covalent cysteine modification. Proc Natl Acad Sci U S A *106*, 20097-20102.

Clapham, D.E. (2007). Calcium signaling. Cell *131*, 1047-1058.

Clarke, M.S., Khakee, R., and McNeil, P.L. (1993). Loss of cytoplasmic basic fibroblast growth factor from physiologically wounded myofibers of normal and dystrophic muscle. J Cell Sci *106 ( Pt 1)*, 121-133.

Colvin, R.A., Means, T.K., Diefenbach, T.J., Moita, L.F., Friday, R.P., Sever, S., Campanella, G.S.V., Abrazinski, T., Manice, L.A., and Moita, C. (2010). Synaptotagmin-mediated vesicle fusion regulates cell migration. Nature immunology *11*, 495.

Cooper, S.T., and McNeil, P.L. (2015). Membrane repair: mechanisms and pathophysiology. Physiological reviews *95*, 1205-1240.

Cresswell, P. (1994). Assembly, transport, and function of MHC class II molecules. Annu Rev Immunol *12*, 259-293.

Curcio-Morelli, C., Charles, F.A., Micsenyi, M.C., Cao, Y., Venugopal, B., Browning, M.F., Dobrenis, K., Cotman, S.L., Walkley, S.U., and Slaugenhaupt, S.A. (2010). Macroautophagy is defective in mucolipin-1-deficient mouse neurons. Neurobiol Dis *40*, 370-377.

Czibener, C., Sherer, N.M., Becker, S.M., Pypaert, M., Hui, E., Chapman, E.R., Mothes, W., and Andrews, N.W. (2006). Ca2+ and synaptotagmin VII-dependent delivery of lysosomal membrane to nascent phagosomes. J Cell Biol *174*, 997-1007.

Davies, K.E., and Nowak, K.J. (2006). Molecular mechanisms of muscular dystrophies: old and new players. Nat Rev Mol Cell Biol *7*, 762-773.

Davis, D.B., Delmonte, A.J., Ly, C.T., and McNally, E.M. (2000). Myoferlin, a candidate gene and potential modifier of muscular dystrophy. Human molecular genetics *9*, 217-226.

De Duve, C. (2005). The lysosome turns fifty. Nature cell biology *7*, 847.

De Palma, C., Morisi, F., Cheli, S., Pambianco, S., Cappello, V., Vezzoli, M., Rovere-Querini, P., Moggio, M., Ripolone, M., and Francolini, M. (2012). Autophagy as a new therapeutic target in Duchenne muscular dystrophy. Cell death & disease *3*, e418.

De Palma, C., Perrotta, C., Pellegrino, P., Clementi, E., and Cervia, D. (2014). Skeletal muscle homeostasis in duchenne muscular dystrophy: modulating autophagy as a promising therapeutic strategy. Frontiers in aging neuroscience *6*, 188.

Deconinck, A.E., Rafael, J.A., Skinner, J.A., Brown, S.C., Potter, A.C., Metzinger, L., Watt, D.J., Dickson, J.G., Tinsley, J.M., and Davies, K.E. (1997). Utrophin-dystrophin-deficient mice as a model for Duchenne muscular dystrophy. Cell *90*, 717-727.

Decressac, M., Mattsson, B., Weikop, P., Lundblad, M., Jakobsson, J., and Bjorklund, A. (2013). TFEB-mediated autophagy rescues midbrain dopamine neurons from alpha-synuclein toxicity. Proc Natl Acad Sci U S A *110*, E1817-1826.

Deng, H., Xiu, X., and Jankovic, J. (2015). Genetic convergence of Parkinson's disease and lysosomal storage disorders. Mol Neurobiol *51*, 1554-1568.

Di Meo, S., and Venditti, P. (2001). Mitochondria in exercise-induced oxidative stress. Neurosignals *10*, 125-140.

Di Palma, F., Belyantseva, I.A., Kim, H.J., Vogt, T.F., Kachar, B., and Noben-Trauth, K. (2002). Mutations in Mcoln3 associated with deafness and pigmentation defects in varitint-waddler (Va) mice. Proceedings of the National Academy of Sciences *99*, 14994-14999.

Dong, X.P., Cheng, X., Mills, E., Delling, M., Wang, F., Kurz, T., and Xu, H. (2008). The type IV mucolipidosis-associated protein TRPML1 is an endolysosomal iron release channel. Nature *455*, 992-996.

Dong, X.P., Shen, D., Wang, X., Dawson, T., Li, X., Zhang, Q., Cheng, X., Zhang, Y., Weisman, L.S., Delling, M.*, et al.* (2010a). PI(3,5)P(2) Controls Membrane Traffic by Direct Activation of Mucolipin Ca Release Channels in the Endolysosome. Nat Commun *1*.

Dong, X.P., Shen, D., Wang, X., Dawson, T., Li, X., Zhang, Q., Cheng, X., Zhang, Y., Weisman, L.S., Delling, M.*, et al.* (2010b). PI(3,5)P(2) controls membrane trafficking by direct activation of mucolipin Ca(2+) release channels in the endolysosome. Nat Commun *1*, 38.

Dong, X.P., Wang, X., Shen, D., Chen, S., Liu, M., Wang, Y., Mills, E., Cheng, X., Delling, M., and Xu, H. (2009). Activating mutations of the TRPML1 channel revealed by proline-scanning mutagenesis. J Biol Chem *284*, 32040-32052.

Dou, Y., Wu, H.J., Li, H.Q., Qin, S., Wang, Y.E., Li, J., Lou, H.F., Chen, Z., Li, X.M., Luo, Q.M.*, et al.* (2012). Microglial migration mediated by ATP-induced ATP release from lysosomes. Cell Res *22*, 1022-1033.

Dudley, R.W.R., Danialou, G., Govindaraju, K., Lands, L., Eidelman, D.E., and Petrof, B.J. (2006). Sarcolemmal damage in dystrophin deficiency is modulated by synergistic interactions between mechanical and oxidative/nitrosative stresses. The American journal of pathology *168*, 1276-1287.

Duguez, S., Duddy, W., Johnston, H., Laine, J., Le Bihan, M.C., Brown, K.J., Bigot, A., Hathout, Y., Butler-Browne, G., and Partridge, T. (2013). Dystrophin deficiency leads to disturbance of LAMP1-vesicle-associated protein secretion. Cell Mol Life Sci *70*, 2159-2174.

Durbeej, M., and Campbell, K.P. (2002). Muscular dystrophies involving the dystrophin-glycoprotein complex: an overview of current mouse models. Curr Opin Genet Dev *12*, 349-361.

Ebashi, S., and Endo, M. (1968). Calcium and muscle contraction. Progress in biophysics and molecular biology *18*, 123-183.

Ebato, C., Uchida, T., Arakawa, M., Komatsu, M., Ueno, T., Komiya, K., Azuma, K., Hirose, T., Tanaka, K., Kominami, E.*, et al.* (2008). Autophagy is important in islet homeostasis and compensatory increase of beta cell mass in response to high-fat diet. Cell Metab *8*, 325-332.

Efeyan, A., Zoncu, R., Chang, S., Gumper, I., Snitkin, H., Wolfson, R.L., Kirak, O., Sabatini, D.D., and Sabatini, D.M. (2013). Regulation of mTORC1 by the Rag GTPases is necessary for neonatal autophagy and survival. Nature *493*, 679.

Efeyan, A., Zoncu, R., and Sabatini, D.M. (2012). Amino acids and mTORC1: from lysosomes to disease. Trends Mol Med *18*, 524-533.

Eichelsdoerfer, J.L., Evans, J.A., Slaugenhaupt, S.A., and Cuajungco, M.P. (2010). Zinc dyshomeostasis is linked with the loss of mucolipidosis IV-associated TRPML1 ion channel. J Biol Chem *285*, 34304-34308.

Elbaz-Alon, Y., Rosenfeld-Gur, E., Shinder, V., Futerman, A.H., Geiger, T., and Schuldiner, M. (2014). A dynamic interface between vacuoles and mitochondria in yeast. Dev Cell *30*, 95-102.

Eskelinen, E.L., Schmidt, C.K., Neu, S., Willenborg, M., Fuertes, G., Salvador, N., Tanaka, Y., Lullmann-Rauch, R., Hartmann, D., Heeren, J.*, et al.* (2004). Disturbed cholesterol traffic but normal proteolytic function in LAMP-1/LAMP-2 double-deficient fibroblasts. Mol Biol Cell *15*, 3132-3145.

Evesson, F.J., Peat, R.A., Lek, A., Brilot, F., Lo, H.P., Dale, R.C., Parton, R.G., North, K.N., and Cooper, S.T. (2010). Reduced plasma membrane expression of dysferlin mutants is attributed to accelerated endocytosis via a syntaxin-4-associated pathway. Journal of Biological Chemistry *285*, 28529-28539.

Falkenburger, B.H., Jensen, J.B., Dickson, E.J., Suh, B.C., and Hille, B. (2010). Phosphoinositides: lipid regulators of membrane proteins. J Physiol *588*, 3179-3185.

Franco Jr, A., and Lansman, J.B. (1990). Calcium entry through stretch-inactivated ion channels in mdx myotubes. Nature *344*, 670.

Franco-Obregón, A., and Lansman, J.B. (2002). Changes in mechanosensitive channel gating following mechanical stimulation in skeletal muscle myotubes from the mdx mouse. The Journal of physiology *539*, 391-407.

Fritz, T., Niederreiter, L., Adolph, T., Blumberg, R.S., and Kaser, A. (2011). Crohn's disease: NOD2, autophagy and ER stress converge. Gut *60*, 1580-1588.

Futerman, A.H., and Van Meer, G. (2004). The cell biology of lysosomal storage disorders. Nature reviews Molecular cell biology *5*, 554.

Galluzzi, L., Pietrocola, F., Levine, B., and Kroemer, G. (2014). Metabolic control of autophagy. Cell *159*, 1263-1276.

Gamstorp, I., Gustavson, K.H., Hellström, O., and Nordgren, B. (1986). A trial of selenium and vitamin E in boys with muscular dystrophy. Journal of child neurology *1*, 211-214.

Gervásio, O.L., Whitehead, N.P., Yeung, E.W., Phillips, W.D., and Allen, D.G. (2008). TRPC1 binds to caveolin-3 and is regulated by Src kinase–role in Duchenne muscular dystrophy. Journal of cell science *121*, 2246-2255.

Gomez-Cabrera, M.C., Borrás, C., Pallardó, F.V., Sastre, J., Ji, L.L., and Viña, J. (2005). Decreasing xanthine oxidase-mediated oxidative stress prevents useful cellular adaptations to exercise in rats. The Journal of physiology *567*, 113-120.

Goonasekera, S.A., Lam, C.K., Millay, D.P., Sargent, M.A., Hajjar, R.J., Kranias, E.G., and Molkentin, J.D. (2011). Mitigation of muscular dystrophy in mice by SERCA overexpression in skeletal muscle. The Journal of clinical investigation *121*, 1044-1052.

Gowers, W.R. (1879). Pseudo-hyppertrophic Muscular Paralysis (JA Churchill).

Grady, R.M., Grange, R.W., Lau, K.S., Maimone, M.M., Nichol, M.C., Stull, J.T., and Sanes, J.R. (1999). Role for α-dystrobrevin in the pathogenesis of dystrophin-dependent muscular dystrophies. Nature cell biology *1*, 215.

Grady, R.M., Teng, H., Nichol, M.C., Cunningham, J.C., Wilkinson, R.S., and Sanes, J.R. (1997). Skeletal and cardiac myopathies in mice lacking utrophin and dystrophin: a model for Duchenne muscular dystrophy. Cell *90*, 729-738.

Grumati, P., Coletto, L., Sabatelli, P., Cescon, M., Angelin, A., Bertaggia, E., Blaauw, B., Urciuolo, A., Tiepolo, T., and Merlini, L. (2010). Autophagy is defective in collagen VI muscular dystrophies, and its reactivation rescues myofiber degeneration. Nature medicine *16*, 1313.

Guglieri, M., Straub, V., Bushby, K., and Lochmüller, H. (2008). Limb–girdle muscular dystrophies. Current opinion in neurology *21*, 576-584.

Gulati, P., Gaspers, L.D., Dann, S.G., Joaquin, M., Nobukuni, T., Natt, F., Kozma, S.C., Thomas, A.P., and Thomas, G. (2008). Amino acids activate mTOR complex 1 via Ca2+/CaM signaling to hVps34. Cell Metab *7*, 456-465.

Haenggi, T., and Fritschy, J.M. (2006). Role of dystrophin and utrophin for assembly and function of the dystrophin glycoprotein complex in non-muscle tissue. Cellular and Molecular Life Sciences CMLS *63*, 1614-1631.

Hamer, P.W., McGeachie, J.M., Davies, M.J., and Grounds, M.D. (2002). Evans Blue Dye as an in vivo marker of myofibre damage: optimising parameters for detecting initial myofibre membrane permeability. Journal of anatomy *200*, 69-79.

Han, R., and Campbell, K.P. (2007). Dysferlin and muscle membrane repair. Curr Opin Cell Biol *19*, 409-416.

Han, R., Rader, E.P., Levy, J.R., Bansal, D., and Campbell, K.P. (2011). Dystrophin deficiency exacerbates skeletal muscle pathology in dysferlin-null mice. Skelet Muscle *1*, 35.

Head, S.I. (2010). Branched fibres in old dystrophic mdx muscle are associated with mechanical weakening of the sarcolemma, abnormal Ca2+ transients and a breakdown of Ca2+ homeostasis during fatigue. Experimental Physiology *95*, 641-656.

Herrero, A., and Barja, G. (1997). ADP-regulation of mitochondrial free radical production is different with complex I-or complex II-linked substrates: implications for the exercise paradox and brain hypermetabolism. Journal of bioenergetics and biomembranes *29*, 241-249.

Hers, H.G. (1963). α-Glucosidase deficiency in generalized glycogen-storage disease (Pompe's disease). Biochemical Journal *86*, 11.

Hirschi, M., Herzik, M.A., Jr., Wie, J., Suo, Y., Borschel, W.F., Ren, D., Lander, G.C., and Lee, S.Y. (2017). Cryo-electron microscopy structure of the lysosomal calcium-permeable channel TRPML3. Nature *550*, 411-414.

Hoffman, E.P., Brown Jr, R.H., and Kunkel, L.M. (1987). Dystrophin: the protein product of the Duchenne muscular dystrophy locus. Cell *51*, 919-928.

Hoffman, J.F. (1992). On red blood cells, hemolysis and resealed ghosts. In The Use of Resealed Erythrocytes as Carriers and Bioreactors (Springer), pp. 1-15.

Hosokawa, N., Hara, T., Kaizuka, T., Kishi, C., Takamura, A., Miura, Y., Iemura, S.-i., Natsume, T., Takehana, K., and Yamada, N. (2009). Nutrient-dependent mTORC1 association with the ULK1–Atg13–FIP200 complex required for autophagy. Molecular biology of the cell *20*, 1981-1991.

Howard, A.C., McNeil, A.K., and McNeil, P.L. (2011). Promotion of plasma membrane repair by vitamin E. Nat Commun *2*, 597.

Huotari, J., and Helenius, A. (2011). Endosome maturation. The EMBO journal *30*, 3481-3500.

Hurley, J.H., and Young, L.N. (2017). Mechanisms of autophagy initiation. Annual review of biochemistry *86*, 225-244.

Idone, V., Tam, C., Goss, J.W., Toomre, D., Pypaert, M., and Andrews, N.W. (2008). Repair of injured plasma membrane by rapid Ca2+-dependent endocytosis. J Cell Biol *180*, 905-914.

Ishida, Y., Nayak, S., Mindell, J.A., and Grabe, M. (2013). A model of lysosomal pH regulation. J Gen Physiol *141*, 705-720.

Jahn, R., and Scheller, R.H. (2006). SNAREs--engines for membrane fusion. Nat Rev Mol Cell Biol *7*, 631-643.

Jaiswal, J.K., Andrews, N.W., and Simon, S.M. (2002). Membrane proximal lysosomes are the major vesicles responsible for calcium-dependent exocytosis in nonsecretory cells. J Cell Biol *159*, 625-635.

Jaiswal, J.K., Chakrabarti, S., Andrews, N.W., and Simon, S.M. (2004). Synaptotagmin VII restricts fusion pore expansion during lysosomal exocytosis. PLoS biology *2*, e233.

Jimenez, A.J., Maiuri, P., Lafaurie-Janvore, J., Divoux, S., Piel, M., and Perez, F. (2014). ESCRT machinery is required for plasma membrane repair. Science *343*, 1247136.

Kalatzis, V., Cherqui, S., Antignac, C., and Gasnier, B. (2001). Cystinosin, the protein defective in cystinosis, is a H(+)-driven lysosomal cystine transporter. Embo j *20*, 5940-5949.

Kanter, M.M. (1994). Free radicals, exercise, and antioxidant supplementation. International journal of sport nutrition *4*, 205-220.

Khairallah, R.J., Shi, G., Sbrana, F., Prosser, B.L., Borroto, C., Mazaitis, M.J., Hoffman, E.P., Mahurkar, A., Sachs, F., and Sun, Y. (2012). Microtubules underlie dysfunction in duchenne muscular dystrophy. Sci Signal *5*, ra56-ra56.

Kilpatrick, K., Zeng, Y., Hancock, T., and Segatori, L. (2015). Genetic and chemical activation of TFEB mediates clearance of aggregated alpha-synuclein. PLoS One *10*, e0120819.

Kim, E., Goraksha-Hicks, P., Li, L., Neufeld, T.P., and Guan, K.-L. (2008). Regulation of TORC1 by Rag GTPases in nutrient response. Nature cell biology *10*, 935.

Kim, J., Kundu, M., Viollet, B., and Guan, K.L. (2011). AMPK and mTOR regulate autophagy through direct phosphorylation of Ulk1. Nat Cell Biol *13*, 132-141.

Kim, J.-H., Kwak, H.-B., Thompson, L.V., and Lawler, J.M. (2013). Contribution of oxidative stress to pathology in diaphragm and limb muscles with Duchenne muscular dystrophy. Journal of muscle research and cell motility *34*, 1-13.

Kirkegaard, T., and Jäättelä, M. (2009). Lysosomal involvement in cell death and cancer. Biochimica et Biophysica Acta (BBA)-Molecular Cell Research *1793*, 746-754.

Kiselyov, K., Chen, J., Rbaibi, Y., Oberdick, D., Tjon-Kon-Sang, S., Shcheynikov, N., Muallem, S., and Soyombo, A. (2005). TRP-ML1 is a lysosomal monovalent cation channel that undergoes proteolytic cleavage. Journal of Biological Chemistry *280*, 43218-43223.

Kitada, T., Asakawa, S., Hattori, N., Matsumine, H., Yamamura, Y., Minoshima, S., Yokochi, M., Mizuno, Y., and Shimizu, N. (1998). Mutations in the parkin gene cause autosomal recessive juvenile parkinsonism. nature *392*, 605.

Klionsky, D.J., Abdalla, F.C., Abeliovich, H., Abraham, R.T., Acevedo-Arozena, A., Adeli, K., Agholme, L., Agnello, M., Agostinis, P., Aguirre-Ghiso, J.A.*, et al.* (2012). Guidelines for the use and interpretation of assays for monitoring autophagy. Autophagy *8*, 445-544.

Klionsky, D.J., Cregg, J.M., Dunn, W.A., Jr., Emr, S.D., Sakai, Y., Sandoval, I.V., Sibirny, A., Subramani, S., Thumm, M., Veenhuis, M.*, et al.* (2003). A unified nomenclature for yeast autophagy-related genes. In Dev Cell (United States), pp. 539-545.

Komatsu, M., Waguri, S., Ueno, T., Iwata, J., Murata, S., Tanida, I., Ezaki, J., Mizushima, N., Ohsumi, Y., Uchiyama, Y.*, et al.* (2005). Impairment of starvation-induced and constitutive autophagy in Atg7-deficient mice. J Cell Biol *169*, 425-434.

Korolchuk, V.I., Saiki, S., Lichtenberg, M., Siddiqi, F.H., Roberts, E.A., Imarisio, S., Jahreiss, L., Sarkar, S., Futter, M., and Menzies, F.M. (2011). Lysosomal positioning coordinates cellular nutrient responses. Nature cell biology *13*, 453.

Kozai, D., Ogawa, N., and Mori, Y. (2014). Redox regulation of transient receptor potential channels. Antioxid Redox Signal *21*, 971-986.

Kroemer, G., and Levine, B. (2008). Autophagic cell death: the story of a misnomer. In Nat Rev Mol Cell Biol (England), pp. 1004-1010.

Kroemer, G., Marino, G., and Levine, B. (2010). Autophagy and the integrated stress response. Mol Cell *40*, 280-293.

Kuma, A., Hatano, M., Matsui, M., Yamamoto, A., Nakaya, H., Yoshimori, T., Ohsumi, Y., Tokuhisa, T., and Mizushima, N. (2004). The role of autophagy during the early neonatal starvation period. Nature *432*, 1032.

Kunkel, L.M. (1986). Analysis of deletions in DNA from patients with Becker and Duchenne muscular dystrophy. Nature *322*, 73.

Kunkel, L.M., Monaco, A.P., Middlesworth, W., Ochs, H.D., and Latt, S.A. (1985). Specific cloning of DNA fragments absent from the DNA of a male patient with an X chromosome deletion. Proceedings of the National Academy of Sciences *82*, 4778-4782.

Langen, R.C., Van Der Velden, J.L., Schols, A.M., Kelders, M.C., Wouters, E.F., and Janssen-Heininger, Y.M. (2004). Tumor necrosis factor-alpha inhibits myogenic differentiation through MyoD protein destabilization. The FASEB Journal *18*, 227-237.

Larkin, L.M., Davis, C.S., Sims-Robinson, C., Kostrominova, T.Y., Remmen, H.V., Richardson, A., Feldman, E.L., and Brooks, S.V. (2011). Skeletal muscle weakness due to deficiency of CuZn-superoxide dismutase is associated with loss of functional innervation. Am J Physiol Regul Integr Comp Physiol *301*, R1400-1407.

Lek, A., Evesson, F.J., Lemckert, F.A., Redpath, G.M., Lueders, A.K., Turnbull, L., Whitchurch, C.B., North, K.N., and Cooper, S.T. (2013). Calpains, cleaved mini-dysferlinC72, and L-type channels underpin calcium-dependent muscle membrane repair. J Neurosci *33*, 5085-5094.

Levine, B., and Yuan, J. (2005). Autophagy in cell death: an innocent convict? J Clin Invest *115*, 2679-2688.

Li, L., Tan, J., Miao, Y., Lei, P., and Zhang, Q. (2015). ROS and Autophagy: Interactions and Molecular Regulatory Mechanisms. Cell Mol Neurobiol *35*, 615-621.

Li, M., Zhang, W.K., Benvin, N.M., Zhou, X., Su, D., Li, H., Wang, S., Michailidis, I.E., Tong, L., Li, X*., et al.* (2017). Structural basis of dual Ca(2+)/pH regulation of the endolysosomal TRPML1 channel. Nat Struct Mol Biol *24*, 205-213.

Li, P., Gu, M., and Xu, H. (2018). Lysosomal ion channels as decoders of cellular signals. Trends in biochemical sciences.

Li, R.J., Xu, J., Fu, C., Zhang, J., Zheng, Y.G., Jia, H., and Liu, J.O. (2016a). Regulation of mTORC1 by lysosomal calcium and calmodulin. Elife *5*.

Li, X., Rydzewski, N., Hider, A., Zhang, X., Yang, J., Wang, W., Gao, Q., Cheng, X., and Xu, H. (2016b). A molecular mechanism to regulate lysosome motility for lysosome positioning and tubulation. Nat Cell Biol *18*, 404-417.

Li, X., Wang, X., Zhang, X., Zhao, M., Tsang, W.L., Zhang, Y., Yau, R.G., Weisman, L.S., and Xu, H. (2013). Genetically encoded fluorescent probe to visualize intracellular phosphatidylinositol 3,5-bisphosphate localization and dynamics. Proc Natl Acad Sci U S A *110*, 21165-21170.

Li, Y., Xu, M., Ding, X., Yan, C., Song, Z., Chen, L., Huang, X., Wang, X., Jian, Y., Tang, G.*, et al.* (2016c). Protein kinase C controls lysosome biogenesis independently of mTORC1. Nat Cell Biol *18*, 1065-1077.

Lie, P.P.Y., and Nixon, R.A. (2019). Lysosome trafficking and signaling in health and neurodegenerative diseases. Neurobiol Dis *122*, 94-105.

Lindahl, M., Backman, E., Henriksson, K.G., Gorospe, J.R., and Hoffman, E.P. (1995). Phospholipase A2 activity in dystrophinopathies. Neuromuscular Disorders *5*, 193-199.

Liu, Y., Zhou, Y., and Zhu, K. (2012). Inhibition of glioma cell lysosome exocytosis inhibits glioma invasion. PloS one *7*, e45910.

Lloyd-Evans, E., Morgan, A.J., He, X., Smith, D.A., Elliot-Smith, E., Sillence, D.J., Churchill, G.C., Schuchman, E.H., Galione, A., and Platt, F.M. (2008). Niemann-Pick disease type C1 is a sphingosine storage disease that causes deregulation of lysosomal calcium. Nat Med *14*, 1247-1255.

Lloyd-Evans, E., Waller-Evans, H., Peterneva, K., and Platt, F.M. (2010). Endolysosomal calcium regulation and disease (Portland Press Limited).

Lubke, T., Lobel, P., and Sleat, D.E. (2009). Proteomics of the lysosome. Biochim Biophys Acta *1793*, 625-635.

Luzio, J.P., Bright, N.A., and Pryor, P.R. (2007a). The role of calcium and other ions in sorting and delivery in the late endocytic pathway. Biochem Soc Trans *35*, 1088-1091.

Luzio, J.P., Pryor, P.R., and Bright, N.A. (2007b). Lysosomes: fusion and function. Nat Rev Mol Cell Biol *8*, 622-632.

Machado, E., White-Gilbertson, S., van de Vlekkert, D., Janke, L., Moshiach, S., Campos, Y., Finkelstein, D., Gomero, E., Mosca, R., and Qiu, X. (2015). Regulated lysosomal exocytosis mediates cancer progression. Science advances *1*, e1500603.

Malicdan, M.C., and Nishino, I. (2012). Autophagy in lysosomal myopathies. Brain Pathol *22*, 82-88.

Malicdan, M.C., Noguchi, S., Nonaka, I., Saftig, P., and Nishino, I. (2008). Lysosomal myopathies: an excessive build-up in autophagosomes is too much to handle. Neuromuscular Disorders *18*, 521-529.

Mamchaoui, K., Trollet, C., Bigot, A., Negroni, E., Chaouch, S., Wolff, A., Kandalla, P.K., Marie, S., Di Santo, J., St Guily, J.L.*, et al.* (2011). Immortalized pathological human myoblasts: towards a universal tool for the study of neuromuscular disorders. Skeletal Muscle *1*, 34.

Mansueto, G., Armani, A., Viscomi, C., D'Orsi, L., De Cegli, R., Polishchuk, E.V., Lamperti, C., Di Meo, I., Romanello, V., and Marchet, S. (2017). Transcription factor EB controls metabolic flexibility during exercise. Cell metabolism *25*, 182-196.

Mariño, G., Salvador-Montoliu, N., Fueyo, A., Knecht, E., Mizushima, N., and López-Otín, C. (2007). Tissue-specific autophagy alterations and increased tumorigenesis in mice deficient in Atg4C/autophagin-3. Journal of Biological Chemistry *282*, 18573-18583.

Martina, J.A., Chen, Y., Gucek, M., and Puertollano, R. (2012). MTORC1 functions as a transcriptional regulator of autophagy by preventing nuclear transport of TFEB. Autophagy *8*, 903-914.

Martinez, I., Chakrabarti, S., Hellevik, T., Morehead, J., Fowler, K., and Andrews, N.W. (2000). Synaptotagmin VII regulates Ca(2+)-dependent exocytosis of lysosomes in fibroblasts. J Cell Biol *148*, 1141-1149.

Masiero, E., Agatea, L., Mammucari, C., Blaauw, B., Loro, E., Komatsu, M., Metzger, D., Reggiani, C., Schiaffino, S., and Sandri, M. (2009). Autophagy is required to maintain muscle mass. Cell Metab *10*, 507-515.

Mathews, K.D., and Moore, S.A. (2003). Limb-girdle muscular dystrophy. Current neurology and neuroscience reports *3*, 78-85.

Matsui, Y., Takagi, H., Qu, X., Abdellatif, M., Sakoda, H., Asano, T., Levine, B., and Sadoshima, J. (2007). Distinct roles of autophagy in the heart during ischemia and reperfusion: roles of AMP-activated protein kinase and Beclin 1 in mediating autophagy. Circulation research *100*, 914-922.

Matsumura, K., Ervasti, J.M., Ohlendieck, K., Kahl, S.D., and Campbell, K.P. (1992). Association of dystrophin-related protein with dystrophin-associated proteins in mdx mouse muscle. Nature *360*, 588.

Matsuo, M., Togawa, M., Hirabaru, K., Mochinaga, S., Narita, A., Adachi, M., Egashira, M., Irie, T., and Ohno, K. (2013). Effects of cyclodextrin in two patients with Niemann–Pick type C disease. Molecular genetics and metabolism *108*, 76-81.

Mc Donald, J.M., and Krainc, D. (2017). Lysosomal Proteins as a Therapeutic Target in Neurodegeneration. Annu Rev Med *68*, 445-458.

McCartney, A.J., Zhang, Y., and Weisman, L.S. (2014). Phosphatidylinositol 3, 5-bisphosphate: low abundance, high significance. BioEssays *36*, 52-64.

McGreevy, J.W., Hakim, C.H., McIntosh, M.A., and Duan, D. (2015). Animal models of Duchenne muscular dystrophy: from basic mechanisms to gene therapy. Disease models & mechanisms *8*, 195-213.

McNeil, P. (2009). Membrane repair redux: redox of MG53. Nat Cell Biol *11*, 7-9.

McNeil, P.L., and Kirchhausen, T. (2005). An emergency response team for membrane repair. Nat Rev Mol Cell Biol *6*, 499-505.

Medina, D.L., Di Paola, S., Peluso, I., Armani, A., De Stefani, D., Venditti, R., Montefusco, S., Scotto-Rosato, A., Prezioso, C., Forrester, A.*, et al.* (2015). Lysosomal calcium signalling regulates autophagy through calcineurin and TFEB. Nat Cell Biol *17*, 288-299.

Medina, D.L., Fraldi, A., Bouche, V., Annunziata, F., Mansueto, G., Spampanato, C., Puri, C., Pignata, A., Martina, J.A., Sardiello, M.*, et al.* (2011). Transcriptional activation of lysosomal exocytosis promotes cellular clearance. Dev Cell *21*, 421-430.

Meikle, P.J., Hopwood, J.J., Clague, A.E., and Carey, W.F. (1999). Prevalence of lysosomal storage disorders. Jama *281*, 249-254.

Mendell, J.R., Rodino-Klapac, L.R., Sahenk, Z., Roush, K., Bird, L., Lowes, L.P., Alfano, L., Gomez, A.M., Lewis, S., and Kota, J. (2013). Eteplirsen for the treatment of Duchenne muscular dystrophy. Annals of neurology *74*, 637-647.

Mercuri, E., and Muntoni, F. (2012). The ever-expanding spectrum of congenital muscular dystrophies. Annals of neurology *72*, 9-17.

Mercuri, E., and Muntoni, F. (2013). Muscular dystrophies. Lancet *381*, 845-860.

Michaelson, L.P., Shi, G., Ward, C.W., and Rodney, G.G. (2010). Mitochondrial redox potential during contraction in single intact muscle fibers. Muscle & nerve *42*, 522-529.

Mindell, J.A. (2012). Lysosomal acidification mechanisms. Annu Rev Physiol *74*, 69-86.

Mizushima, N., and Komatsu, M. (2011). Autophagy: renovation of cells and tissues. Cell *147*, 728-741.

Mizushima, N., Yamamoto, A., Matsui, M., Yoshimori, T., and Ohsumi, Y. (2004). In vivo analysis of autophagy in response to nutrient starvation using transgenic mice expressing a fluorescent autophagosome marker. Molecular biology of the cell *15*, 1101-1111.

Moens, P., Baatsen, P., and Maréchal, G. (1993). Increased susceptibility of EDL muscles from mdx mice to damage induced by contractions with stretch. Journal of Muscle Research & Cell Motility *14*, 446-451.

Mofarrahi, M., Brandes, R.P., Gorlach, A., Hanze, J., Terada, L.S., Quinn, M.T., Mayaki, D., Petrof, B., and Hussain, S.N.A. (2008). Regulation of proliferation of skeletal muscle precursor cells by NADPH oxidase. Antioxidants & redox signaling *10*, 559-574.

Morgan, A.J., Davis, L.C., and Galione, A. (2015). Imaging approaches to measuring lysosomal calcium. Methods Cell Biol *126*, 159-195.

Mostov, K., and Werb, Z. (1997). Journey across the osteoclast. Science *276*, 219-220.

Mrakovic, A., Kay, J.G., Furuya, W., Brumell, J.H., and Botelho, R.J. (2012). Rab7 and Arl8 GTPases are necessary for lysosome tubulation in macrophages. Traffic *13*, 1667-1679.

Murrow, L., and Debnath, J. (2013). Autophagy as a stress-response and quality-control mechanism: implications for cell injury and human disease. Annu Rev Pathol *8*, 105-137.

Nakai, A., Yamaguchi, O., Takeda, T., Higuchi, Y., Hikoso, S., Taniike, M., Omiya, S., Mizote, I., Matsumura, Y., Asahi, M.*, et al.* (2007). The role of autophagy in cardiomyocytes in the basal state and in response to hemodynamic stress. Nat Med *13*, 619-624.

Narendra, D., Tanaka, A., Suen, D.F., and Youle, R.J. (2008). Parkin is recruited selectively to impaired mitochondria and promotes their autophagy. J Cell Biol *183*, 795-803.

Nelson, C.E., Hakim, C.H., Ousterout, D.G., Thakore, P.I., Moreb, E.A., Rivera, R.M.C., Madhavan, S., Pan, X., Ran, F.A., and Yan, W.X. (2016). In vivo genome editing improves muscle function in a mouse model of Duchenne muscular dystrophy. Science *351*, 403-407.

Neufeld, E.F. (1991). Lysosomal storage diseases. Annual review of biochemistry *60*, 257-280.

Nishikawa, T., Edelstein, D., Du, X.L., Yamagishi, S., Matsumura, T., Kaneda, Y., Yorek, M.A., Beebe, D., Oates, P.J., Hammes, H.P.*, et al.* (2000). Normalizing mitochondrial superoxide production blocks three pathways of hyperglycaemic damage. Nature *404*, 787-790.

Nishino, I., Fu, J., Tanji, K., Yamada, T., Shimojo, S., Koori, T., Mora, M., Riggs, J.E., Oh, S.J., Koga, Y.*, et al.* (2000). Primary LAMP-2 deficiency causes X-linked vacuolar cardiomyopathy and myopathy (Danon disease). Nature *406*, 906-910.

Nixon, R.A. (2004). Niemann-Pick Type C disease and Alzheimer's disease: the APP-endosome connection fattens up. The American journal of pathology *164*, 757-761.

Nixon, R.A. (2013). The role of autophagy in neurodegenerative disease. Nature medicine *19*, 983.

Nuss, J.E., Amaning, J.K., Bailey, C.E., DeFord, J.H., Dimayuga, V.L., Rabek, J.P., and Papaconstantinou, J. (2009). Oxidative modification and aggregation of creatine kinase from aged mouse skeletal muscle. Aging (Albany NY) *1*, 557.

Pal, R., Palmieri, M., Loehr, J.A., Li, S., Abo-Zahrah, R., Monroe, T.O., Thakur, P.B., Sardiello, M., and Rodney, G.G. (2014). Src-dependent impairment of autophagy by oxidative stress in a mouse model of Duchenne muscular dystrophy. Nat Commun *5*, 4425.

Palmieri, M., Impey, S., Kang, H., di Ronza, A., Pelz, C., Sardiello, M., and Ballabio, A. (2011). Characterization of the CLEAR network reveals an integrated control of cellular clearance pathways. Hum Mol Genet *20*, 3852-3866.

Parenti, G., Andria, G., and Ballabio, A. (2015). Lysosomal storage diseases: from pathophysiology to therapy. Annu Rev Med *66*, 471-486.

Parkinson-Lawrence, E.J., Shandala, T., Prodoehl, M., Plew, R., Borlace, G.N., and Brooks, D.A. (2010). Lysosomal storage disease: revealing lysosomal function and physiology. Physiology *25*, 102-115.

Pastore, N., Ballabio, A., and Brunetti-Pierri, N. (2013a). Autophagy master regulator TFEB induces clearance of toxic SERPINA1/α-1-antitrypsin polymers. Autophagy *9*, 1094-1096.

Pastore, N., Blomenkamp, K., Annunziata, F., Piccolo, P., Mithbaokar, P., Sepe, R.M., Vetrini, F., Palmer, D., Ng, P., and Polishchuk, E. (2013b). Gene transfer of master autophagy regulator TFEB results in clearance of toxic protein and correction of hepatic disease in alpha-1-anti-trypsin deficiency. EMBO molecular medicine *5*, 397-412.

Pauly, M., Daussin, F., Burelle, Y., Li, T., Godin, R., Fauconnier, J., Koechlin-Ramonatxo, C., Hugon, G., Lacampagne, A., and Coisy-Quivy, M. (2012). AMPK activation stimulates autophagy and ameliorates muscular dystrophy in the mdx mouse diaphragm. The American journal of pathology *181*, 583-592.

Peter, A.K., Marshall, J.L., and Crosbie, R.H. (2008). Sarcospan reduces dystrophic pathology: stabilization of the utrophin–glycoprotein complex. The Journal of cell biology *183*, 419-427.

Petrof, B.J., Shrager, J.B., Stedman, H.H., Kelly, A.M., and Sweeney, H.L. (1993). Dystrophin protects the sarcolemma from stresses developed during muscle contraction. Proceedings of the National Academy of Sciences *90*, 3710-3714.

Piao, Y.J., Seo, Y.H., Hong, F., Kim, J.H., Kim, Y.-J., Kang, M.H., Kim, B.S., Jo, S.A., Jo, I., and Jue, D.-M. (2005). Nox 2 stimulates muscle differentiation via NF-κB/iNOS pathway. Free Radical Biology and Medicine *38*, 989-1001.

Polito, V.A., Li, H., Martini-Stoica, H., Wang, B., Yang, L., Xu, Y., Swartzlander, D.B., Palmieri, M., di Ronza, A., Lee, V.M.*, et al.* (2014). Selective clearance of aberrant tau proteins and rescue of neurotoxicity by transcription factor EB. EMBO Mol Med *6*, 1142-1160.

Powers, S.K., and Jackson, M.J. (2008). Exercise-induced oxidative stress: cellular mechanisms and impact on muscle force production. Physiological reviews *88*, 1243-1276.

Prior, T.W., and Bridgeman, S.J. (2005). Experience and strategy for the molecular testing of Duchenne muscular dystrophy. The Journal of Molecular Diagnostics *7*, 317-326.

Proux-Gillardeaux, V., Raposo, G., Irinopoulou, T., and Galli, T. (2007). Expression of the Longin domain of TI-VAMP impairs lysosomal secretion and epithelial cell migration. Biology of the Cell *99*, 261-271.

Pryor, P.R., Mullock, B.M., Bright, N.A., Gray, S.R., and Luzio, J.P. (2000). The role of intraorganellar Ca(2+) in late endosome-lysosome heterotypic fusion and in the reformation of lysosomes from hybrid organelles. J Cell Biol *149*, 1053-1062.

Pryor, P.R., Reimann, F., Gribble, F.M., and Luzio, J.P. (2006). Mucolipin-1 Is a Lysosomal Membrane Protein Required for Intracellular Lactosylceramide Traffic. Traffic *7*, 1388-1398.

Puertollano, R., and Kiselyov, K. (2009). TRPMLs: in sickness and in health. Am J Physiol Renal Physiol *296*, F1245-1254.

Radley-Crabb, H., Terrill, J., Shavlakadze, T., Tonkin, J., Arthur, P., and Grounds, M. (2012). A single 30 min treadmill exercise session is suitable for 'proof-of concept studies' in adult mdx mice: a comparison of the early consequences of two different treadmill protocols. Neuromuscul Disord *22*, 170-182.

Rahimov, F., and Kunkel, L.M. (2013). The cell biology of disease: cellular and molecular mechanisms underlying muscular dystrophy. J Cell Biol *201*, 499-510.

Rainero, E., and Norman, J.C. (2013). Late endosomal and lysosomal trafficking during integrin-mediated cell migration and invasion: cell matrix receptors are trafficked through the late endosomal pathway in a way that dictates how cells migrate. Bioessays *35*, 523-532.

Ramachandran, N., Munteanu, I., Wang, P., Ruggieri, A., Rilstone, J.J., Israelian, N., Naranian, T., Paroutis, P., Guo, R., and Ren, Z.-P. (2013). VMA21 deficiency prevents vacuolar ATPase assembly and causes autophagic vacuolar myopathy. Acta neuropathologica *125*, 439-457.

Rando, T.A. (2002). Oxidative stress and the pathogenesis of muscular dystrophies. American journal of physical medicine & rehabilitation *81*, S175-S186.

Rao, S.K., Huynh, C., Proux-Gillardeaux, V., Galli, T., and Andrews, N.W. (2004). Identification of SNAREs involved in synaptotagmin VII-regulated lysosomal exocytosis. Journal of Biological Chemistry *279*, 20471-20479.

Rautou, P.-E., Mansouri, A., Lebrec, D., Durand, F., Valla, D., and Moreau, R. (2010). Autophagy in liver diseases. Journal of hepatology *53*, 1123-1134.

Rebsamen, M., Pochini, L., Stasyk, T., de Araújo, M.E.G., Galluccio, M., Kandasamy, R.K., Snijder, B., Fauster, A., Rudashevskaya, E.L., and Bruckner, M. (2015). SLC38A9 is a

component of the lysosomal amino acid sensing machinery that controls mTORC1. Nature *519*, 477.

Reddy, A., Caler, E.V., and Andrews, N.W. (2001). Plasma membrane repair is mediated by Ca(2+)-regulated exocytosis of lysosomes. Cell *106*, 157-169.

Rega, L.R., Polishchuk, E., Montefusco, S., Napolitano, G., Tozzi, G., Zhang, J., Bellomo, F., Taranta, A., Pastore, A., Polishchuk, R.*, et al.* (2016). Activation of the transcription factor EB rescues lysosomal abnormalities in cystinotic kidney cells. Kidney Int *89*, 862-873.

Roczniak-Ferguson, A., Petit, C.S., Froehlich, F., Qian, S., Ky, J., Angarola, B., Walther, T.C., and Ferguson, S.M. (2012). The transcription factor TFEB links mTORC1 signaling to transcriptional control of lysosome homeostasis. Sci Signal *5*, ra42.

Rodriguez, A., Webster, P., Ortego, J., and Andrews, N.W. (1997). Lysosomes behave as Ca2+-regulated exocytic vesicles in fibroblasts and epithelial cells. J Cell Biol *137*, 93-104.

Rong, Y., McPhee, C.K., Deng, S., Huang, L., Chen, L., Liu, M., Tracy, K., Baehrecke, E.H., Yu, L., and Lenardo, M.J. (2011). Spinster is required for autophagic lysosome reformation and mTOR reactivation following starvation. Proceedings of the National Academy of Sciences *108*, 7826-7831.

Ruivo, R., Anne, C., Sagne, C., and Gasnier, B. (2009). Molecular and cellular basis of lysosomal transmembrane protein dysfunction. Biochim Biophys Acta *1793*, 636-649.

Saftig, P., and Klumperman, J. (2009). Lysosome biogenesis and lysosomal membrane proteins: trafficking meets function. Nat Rev Mol Cell Biol *10*, 623-635.

Sahoo, N., Gu, M., Zhang, X., Raval, N., Yang, J., Bekier, M., Calvo, R., Patnaik, S., Wang, W., King, G.*, et al.* (2017). Gastric Acid Secretion from Parietal Cells Is Mediated by a Ca(2+) Efflux Channel in the Tubulovesicle. Dev Cell *41*, 262-273 e266.

Samie, M., Wang, X., Zhang, X., Goschka, A., Li, X., Cheng, X., Gregg, E., Azar, M., Zhuo, Y., Garrity, A.G.*, et al.* (2013). A TRP channel in the lysosome regulates large particle phagocytosis via focal exocytosis. Dev Cell *26*, 511-524.

Samie, M.A., and Xu, H. (2014). Lysosomal exocytosis and lipid storage disorders. J Lipid Res *55*, 995-1009.

Sancak, Y., Bar-Peled, L., Zoncu, R., Markhard, A.L., Nada, S., and Sabatini, D.M. (2010). Ragulator-Rag complex targets mTORC1 to the lysosomal surface and is necessary for its activation by amino acids. Cell *141*, 290-303.

Sancak, Y., Peterson, T.R., Shaul, Y.D., Lindquist, R.A., Thoreen, C.C., Bar-Peled, L., and Sabatini, D.M. (2008). The Rag GTPases bind raptor and mediate amino acid signaling to mTORC1. Science *320*, 1496-1501.

Sandri, M. (2010). Autophagy in skeletal muscle. FEBS letters *584*, 1411-1416.

Sarathy, A., Wuebbles, R.D., Fontelonga, T.M., Tarchione, A.R., Mathews Griner, L.A., Heredia, D.J., Nunes, A.M., Duan, S., Brewer, P.D., Van Ry, T.*, et al.* (2017). SU9516 Increases alpha7beta1 Integrin and Ameliorates Disease Progression in the mdx Mouse Model of Duchenne Muscular Dystrophy. Mol Ther *25*, 1395-1407.

Sardiello, M., Palmieri, M., di Ronza, A., Medina, D.L., Valenza, M., Gennarino, V.A., Di Malta, C., Donaudy, F., Embrione, V., Polishchuk, R.S.*, et al.* (2009). A gene network regulating lysosomal biogenesis and function. Science *325*, 473-477.

Scheffer, L.L., Sreetama, S.C., Sharma, N., Medikayala, S., Brown, K.J., Defour, A., and Jaiswal, J.K. (2014). Mechanism of Ca 2+-triggered ESCRT assembly and regulation of cell membrane repair. Nature communications *5*, 5646.

Scherz-Shouval, R., and Elazar, Z. (2011). Regulation of autophagy by ROS: physiology and pathology. Trends Biochem Sci *36*, 30-38.

Scherz-Shouval, R., Shvets, E., Fass, E., Shorer, H., Gil, L., and Elazar, Z. (2007). Reactive oxygen species are essential for autophagy and specifically regulate the activity of Atg4. EMBO J *26*, 1749-1760.

Schessl, J., Zou, Y., and Bönnemann, C.G. Congenital muscular dystrophies and the extracellular matrix (Elsevier).

Schmiege, P., Fine, M., Blobel, G., and Li, X. (2017). Human TRPML1 channel structures in open and closed conformations. Nature *550*, 366-370.

Schroder, B., Wrocklage, C., Pan, C., Jager, R., Kosters, B., Schafer, H., Elsasser, H.P., Mann, M., and Hasilik, A. (2007). Integral and associated lysosomal membrane proteins. Traffic *8*, 1676-1686.

Schwake, M., Schroder, B., and Saftig, P. (2013). Lysosomal membrane proteins and their central role in physiology. Traffic *14*, 739-748.

Schweitzer, J.K., Krivda, J.P., and D'Souza-Schorey, C. (2009). Neurodegeneration in Niemann-Pick Type C disease and Huntington's disease: impact of defects in membrane trafficking. Curr Drug Targets *10*, 653-665.

Settembre, C., and Ballabio, A. (2014). Lysosomal adaptation: how the lysosome responds to external cues. Cold Spring Harb Perspect Biol *6*.

Settembre, C., De Cegli, R., Mansueto, G., Saha, P.K., Vetrini, F., Visvikis, O., Huynh, T., Carissimo, A., Palmer, D., Klisch, T.J.*, et al.* (2013a). TFEB controls cellular lipid metabolism through a starvation-induced autoregulatory loop. Nat Cell Biol *15*, 647-658.

Settembre, C., Di Malta, C., Polito, V.A., Garcia Arencibia, M., Vetrini, F., Erdin, S., Erdin, S.U., Huynh, T., Medina, D., Colella, P.*, et al.* (2011). TFEB links autophagy to lysosomal biogenesis. Science *332*, 1429-1433.

Settembre, C., Fraldi, A., Medina, D.L., and Ballabio, A. (2013b). Signals from the lysosome: a control centre for cellular clearance and energy metabolism. Nat Rev Mol Cell Biol *14*, 283-296.

Settembre, C., Zoncu, R., Medina, D.L., Vetrini, F., Erdin, S., Huynh, T., Ferron, M., Karsenty, G., Vellard, M.C., Facchinetti, V.*, et al.* (2012). A lysosome-to-nucleus signalling mechanism senses and regulates the lysosome via mTOR and TFEB. Embo j *31*, 1095-1108.

Shea, L., and Raben, N. (2009). Autophagy in skeletal muscle: implications for Pompe disease. Int J Clin Pharmacol Ther *47 Suppl 1*, S42-47.

Shen, D., Wang, X., Li, X., Zhang, X., Yao, Z., Dibble, S., Dong, X.P., Yu, T., Lieberman, A.P., Showalter, H.D.*, et al.* (2012). Lipid storage disorders block lysosomal trafficking by inhibiting a TRP channel and lysosomal calcium release. Nat Commun *3*, 731.

Shen, H.M., and Mizushima, N. (2014). At the end of the autophagic road: an emerging understanding of lysosomal functions in autophagy. Trends Biochem Sci *39*, 61-71.

Shkryl, V.M., Martins, A.S., Ullrich, N.D., Nowycky, M.C., Niggli, E., and Shirokova, N. (2009). Reciprocal amplification of ROS and Ca 2+ signals in stressed mdx dystrophic skeletal muscle fibers. Pflügers Archiv-European Journal of Physiology *458*, 915-928.

Sicinski, P., Geng, Y., Ryder-Cook, A.S., Barnard, E.A., Darlison, M.G., and Barnard, P.J. (1989). The molecular basis of muscular dystrophy in the mdx mouse: a point mutation. Science *244*, 1578-1580.

Slaugenhaupt, S.A. (2002). The molecular basis of mucolipidosis type IV. Curr Mol Med *2*, 445-450.

Smiley, S.T., Reers, M., Mottola-Hartshorn, C., Lin, M., Chen, A., Smith, T.W., Steele, G.D., Jr., and Chen, L.B. (1991). Intracellular heterogeneity in mitochondrial membrane potentials revealed by a J-aggregate-forming lipophilic cation JC-1. Proc Natl Acad Sci U S A *88*, 3671-3675.

Song, W., Wang, F., Savini, M., Ake, A., di Ronza, A., Sardiello, M., and Segatori, L. (2013). TFEB regulates lysosomal proteostasis. Hum Mol Genet *22*, 1994-2009.

Spampanato, C., Feeney, E., Li, L., Cardone, M., Lim, J.A., Annunziata, F., Zare, H., Polishchuk, R., Puertollano, R., Parenti, G.*, et al.* (2013). Transcription factor EB (TFEB) is a new therapeutic target for Pompe disease. EMBO Mol Med *5*, 691-706.

Spencer, M.J., Croall, D.E., and Tidball, J.G. (1995). Calpains are activated in necrotic fibers from mdx dystrophic mice. Journal of Biological Chemistry *270*, 10909-10914.

Springer, M.L., Rando, T.A., and Blau, H.M. (2002). Gene delivery to muscle. Curr Protoc Hum Genet *Chapter 13*, Unit13 14.

Stedman, H.H., Sweeney, H.L., Shrager, J.B., Maguire, H.C., Panettieri, R.A., Petrof, B., Narusawa, M., Leferovich, J.M., Sladky, J.T., and Kelly, A.M. (1991). The mdx mouse diaphragm reproduces the degenerative changes of Duchenne muscular dystrophy. Nature *352*, 536-539.

Straub, V., and Campbell, K.P. (1997). Muscular dystrophies and the dystrophin-glycoprotein complex. Current opinion in neurology *10*, 168-175.

Straub, V., Rafael, J.A., Chamberlain, J.S., and Campbell, K.P. (1997). Animal models for muscular dystrophy show different patterns of sarcolemmal disruption. J Cell Biol *139*, 375-385.

Sudhof, T.C. (2013). Neurotransmitter release: the last millisecond in the life of a synaptic vesicle. Neuron *80*, 675-690.

Sugie, K., Noguchi, S., Kozuka, Y., Arikawa-Hirasawa, E., Tanaka, M., Yan, C., Saftig, P., von Figura, K., Hirano, M., and Ueno, S. (2005). Autophagic vacuoles with sarcolemmal features delineate Danon disease and related myopathies. Journal of Neuropathology & Experimental Neurology *64*, 513-522.

Sun, X., Yang, Y., Zhong, X.Z., Cao, Q., Zhu, X.H., Zhu, X., and Dong, X.P. (2018). A negative feedback regulation of MTORC1 activity by the lysosomal Ca(2+) channel MCOLN1 (mucolipin 1) using a CALM (calmodulin)-dependent mechanism. Autophagy *14*, 38-52.

Suzuki, T., Nakagawa, M., Yoshikawa, A., Sasagawa, N., Yoshimori, T., Ohsumi, Y., Nishino, I., Ishiura, S., and Nonaka, I. (2002). The first molecular evidence that autophagy relates rimmed vacuole formation in chloroquine myopathy. The Journal of Biochemistry *131*, 647-651.

Tam, C., Idone, V., Devlin, C., Fernandes, M.C., Flannery, A., He, X., Schuchman, E., Tabas, I., and Andrews, N.W. (2010). Exocytosis of acid sphingomyelinase by wounded cells promotes endocytosis and plasma membrane repair. The Journal of cell biology *189*, 1027-1038.

Tanaka, Y., Guhde, G., Suter, A., Eskelinen, E.L., Hartmann, D., Lullmann-Rauch, R., Janssen, P.M., Blanz, J., von Figura, K., and Saftig, P. (2000). Accumulation of autophagic vacuoles and cardiomyopathy in LAMP-2-deficient mice. Nature *406*, 902-906.

Terasaki, M., Miyake, K., and McNeil, P.L. (1997). Large plasma membrane disruptions are rapidly resealed by Ca2+-dependent vesicle–vesicle fusion events. The Journal of cell biology *139*, 63-74.

Terman, A., and Brunk, U.T. (2005). Autophagy in cardiac myocyte homeostasis, aging, and pathology. Cardiovascular research *68*, 355-365.

Thompson, E.G., Schaheen, L., Dang, H., and Fares, H. (2007). Lysosomal trafficking functions of mucolipin-1 in murine macrophages. BMC Cell Biol *8*, 54.

Tidball, J.G. (2005). Inflammatory processes in muscle injury and repair. Am J Physiol Regul Integr Comp Physiol *288*, R345-353.

Tiede, S., Storch, S., Lübke, T., Henrissat, B., Bargal, R., Raas-Rothschild, A., and Braulke, T. (2005). Mucolipidosis II is caused by mutations in GNPTA encoding the α/β GlcNAc-1-phosphotransferase. Nature medicine *11*, 1109.

Tinsley, J., Deconinck, N., Fisher, R., Kahn, D., Phelps, S., Gillis, J.-M., and Davies, K. (1998). Expression of full-length utrophin prevents muscular dystrophy in mdx mice. Nature medicine *4*, 1441.

Tognon, E., Kobia, F., Busi, I., Fumagalli, A., De Masi, F., and Vaccari, T. (2016). Control of lysosomal biogenesis and Notch-dependent tissue patterning by components of the TFEB-V-ATPase axis in Drosophila melanogaster. Autophagy *12*, 499-514.

Touchberry, C.D., Bales, I.K., Stone, J.K., Rohrberg, T.J., Parelkar, N.K., Nguyen, T., Fuentes, O., Liu, X., Qu, C.-K., and Andresen, J.J. (2010). Phosphatidylinositol 3, 5-bisphosphate (PI (3, 5) P2) potentiates cardiac contractility via activation of the ryanodine receptor. Journal of Biological Chemistry *285*, 40312-40321.

Treusch, S., Knuth, S., Slaugenhaupt, S.A., Goldin, E., Grant, B.D., and Fares, H. (2004). Caenorhabditis elegans functional orthologue of human protein h-mucolipin-1 is required for lysosome biogenesis. Proceedings of the National Academy of Sciences of the United States of America *101*, 4483.

Tsunemi, T., Ashe, T.D., Morrison, B.E., Soriano, K.R., Au, J., Roque, R.A., Lazarowski, E.R., Damian, V.A., Masliah, E., and La Spada, A.R. (2012). PGC-1alpha rescues Huntington's disease proteotoxicity by preventing oxidative stress and promoting TFEB function. Sci Transl Med *4*, 142ra197.

Turner, P.R., Westwood, T., Regen, C.M., and Steinhardt, R.A. (1988). Increased protein degradation results from elevated free calcium levels found in muscle from mdx mice. Nature *335*, 735.

Underwood, B.R., Imarisio, S., Fleming, A., Rose, C., Krishna, G., Heard, P., Quick, M., Korolchuk, V.I., Renna, M., Sarkar, S.*, et al.* (2010). Antioxidants can inhibit basal autophagy and enhance neurodegeneration in models of polyglutamine disease. Hum Mol Genet *19*, 3413-3429.

Urso, M.L., and Clarkson, P.M. (2003). Oxidative stress, exercise, and antioxidant supplementation. Toxicology *189*, 41-54.

Usuda, N., Arai, H., Sasaki, H., Hanai, T., Nagata, T., Muramatsu, T., Kincaid, R.L., and Higuchi, S. (1996). Differential subcellular localization of neural isoforms of the catalytic subunit of calmodulin-dependent protein phosphatase (calcineurin) in central nervous system neurons: immunohistochemistry on formalin-fixed paraffin sections employing antigen retrieval by microwave irradiation. Journal of Histochemistry & Cytochemistry *44*, 13-18.

Valente, E.M., Abou-Sleiman, P.M., Caputo, V., Muqit, M.M.K., Harvey, K., Gispert, S., Ali, Z., Del Turco, D., Bentivoglio, A.R., and Healy, D.G. (2004). Hereditary early-onset Parkinson's disease caused by mutations in PINK1. Science *304*, 1158-1160.

Van Deutekom, J.C.T., and Van Ommen, G.-J.B. (2003). Advances in Duchenne muscular dystrophy gene therapy. Nature Reviews Genetics *4*, 774.

Vandebrouck, C., Duport, G., Cognard, C., and Raymond, G. (2001). Cationic channels in normal and dystrophic human myotubes. Neuromuscular Disorders *11*, 72-79.

Vanier, M.T. (2010). Niemann-Pick disease type C. Orphanet journal of rare diseases *5*, 16.

Venkatachalam, K., Long, A.A., Elsaesser, R., Nikolaeva, D., Broadie, K., and Montell, C. (2008). Motor deficit in a Drosophila model of mucolipidosis type IV due to defective clearance of apoptotic cells. Cell *135*, 838-851.

Venugopal, B., Browning, M.F., Curcio-Morelli, C., Varro, A., Michaud, N., Nanthakumar, N., Walkley, S.U., Pickel, J., and Slaugenhaupt, S.A. (2007). Neurologic, gastric, and opthalmologic pathologies in a murine model of mucolipidosis type IV. Am J Hum Genet *81*, 1070-1083.

Vergarajauregui, S., Connelly, P.S., Daniels, M.P., and Puertollano, R. (2008). Autophagic dysfunction in mucolipidosis type IV patients. Hum Mol Genet *17*, 2723-2737.

Vergarajauregui, S., Martina, J.A., and Puertollano, R. (2009). Identification of the penta-EF-hand protein ALG-2 as a Ca2+-dependent interactor of mucolipin-1. J Biol Chem *284*, 36357-36366.

Vergarajauregui, S., and Puertollano, R. (2006a). Two di-leucine motifs regulate trafficking of mucolipin-1 to lysosomes. Traffic *7*, 337-353.

Vergarajauregui, S., and Puertollano, R. (2006b). Two di-leucine motifs regulate trafficking of mucolipin-1 to lysosomes. Traffic *7*, 337-353.

Vicinanza, M., Korolchuk, V.I., Ashkenazi, A., Puri, C., Menzies, F.M., Clarke, J.H., and Rubinsztein, D.C. (2015). PI(5)P regulates autophagosome biogenesis. Mol Cell *57*, 219-234.

Waddell, L.B., Lemckert, F.A., Zheng, X.F., Tran, J., Evesson, F.J., Hawkes, J.M., Lek, A., Street, N.E., Lin, P., and Clarke, N.F. (2011). Dysferlin, annexin A1, and mitsugumin 53 are upregulated in muscular dystrophy and localize to longitudinal tubules of the T-system with stretch. Journal of Neuropathology & Experimental Neurology *70*, 302-313.

Wang, S., Tsun, Z.Y., Wolfson, R.L., Shen, K., Wyant, G.A., Plovanich, M.E., Yuan, E.D., Jones, T.D., Chantranupong, L., Comb, W.*, et al.* (2015a). Metabolism. Lysosomal amino acid transporter SLC38A9 signals arginine sufficiency to mTORC1. Science *347*, 188-194.

Wang, W., Gao, Q., Yang, M., Zhang, X., Yu, L., Lawas, M., Li, X., Bryant-Genevier, M., Southall, N.T., Marugan, J.*, et al.* (2015b). Up-regulation of lysosomal TRPML1 channels is essential for lysosomal adaptation to nutrient starvation. Proc Natl Acad Sci U S A *112*, E1373-1381.

Wang, X., Zhang, X., Dong, X.P., Samie, M., Li, X., Cheng, X., Goschka, A., Shen, D., Zhou, Y., Harlow, J.*, et al.* (2012a). TPC proteins are phosphoinositide- activated sodium-selective ion channels in endosomes and lysosomes. Cell *151*, 372-383.

Wang, Y., Nartiss, Y., Steipe, B., McQuibban, G.A., and Kim, P.K. (2012b). ROS-induced mitochondrial depolarization initiates PARK2/PARKIN-dependent mitochondrial degradation by autophagy. Autophagy *8*, 1462-1476.

Ward, S., O'Donnell, P., Fernandez, S., and Vite, C.H. (2010). 2-hydroxypropyl-β-cyclodextrin raises hearing threshold in normal cats and in cats with Niemann-Pick type C disease. Pediatric research *68*, 52.

Watkins, S.C., Hoffman, E.P., Slayter, H.S., and Kunkel, L.M. (1988). Immunoelectron microscopic localization of dystrophin in myofibres. Nature *333*, 863.

Weisleder, N., Takeshima, H., and Ma, J. (2008). Immuno-proteomic approach to excitation–contraction coupling in skeletal and cardiac muscle: molecular insights revealed by the mitsugumins. Cell calcium *43*, 1-8.

Weisleder, N., Takizawa, N., Lin, P., Wang, X., Cao, C., Zhang, Y., Tan, T., Ferrante, C., Zhu, H., Chen, P.J.*, et al.* (2012). Recombinant MG53 protein modulates therapeutic cell membrane repair in treatment of muscular dystrophy. Sci Transl Med *4*, 139ra185.

Whitehead, N.P., Pham, C., Gervasio, O.L., and Allen, D.G. (2008). N-Acetylcysteine ameliorates skeletal muscle pathophysiology in mdx mice. The Journal of physiology *586*, 2003-2014.

Whitehead, N.P., Streamer, M., Lusambili, L.I., Sachs, F., and Allen, D.G. (2006). Streptomycin reduces stretch-induced membrane permeability in muscles from mdx mice. Neuromuscular Disorders *16*, 845-854.

Whitehead, N.P., Yeung, E.W., Froehner, S.C., and Allen, D.G. (2010). Skeletal muscle NADPH oxidase is increased and triggers stretch-induced damage in the mdx mouse. PloS one *5*, e15354.

Wong, C.O., Li, R., Montell, C., and Venkatachalam, K. (2012). Drosophila TRPML is required for TORC1 activation. Curr Biol *22*, 1616-1621.

Wu, X., Steigelman, K.A., Bonten, E., Hu, H., He, W., Ren, T., Zuo, J., and d'Azzo, A. (2010). Vacuolization and alterations of lysosomal membrane proteins in cochlear marginal cells contribute to hearing loss in neuraminidase 1-deficient mice. Biochim Biophys Acta *1802*, 259-268.

Xiao, Q., Yan, P., Ma, X., Liu, H., Perez, R., Zhu, A., Gonzales, E., Burchett, J.M., Schuler, D.R., and Cirrito, J.R. (2014). Enhancing astrocytic lysosome biogenesis facilitates Aβ clearance and attenuates amyloid plaque pathogenesis. Journal of Neuroscience *34*, 9607-9620.

Xu, H., and Ren, D. (2015). Lysosomal physiology. Annu Rev Physiol *77*, 57-80.

Yang, J., Zhao, Z., Gu, M., Feng, X., and Xu, H. (2019). Release and uptake mechanisms of vesicular Ca 2+ stores. Protein & cell *10*, 8-19.

Yasuda, S., Townsend, D., Michele, D.E., Favre, E.G., Day, S.M., and Metzger, J.M. (2005). Dystrophic heart failure blocked by membrane sealant poloxamer. Nature *436*, 1025.

Yogalingam, G., Bonten, E.J., van de Vlekkert, D., Hu, H., Moshiach, S., Connell, S.A., and d'Azzo, A. (2008). Neuraminidase 1 is a negative regulator of lysosomal exocytosis. Dev Cell *15*, 74-86.

Youle, R.J., and Narendra, D.P. (2011). Mechanisms of mitophagy. Nature reviews Molecular cell biology *12*, 9.

Young, M.F., and Fallon, J.R. (2012). Biglycan: a promising new therapeutic for neuromuscular and musculoskeletal diseases. Current opinion in genetics & development *22*, 398-400.

Yu, L., McPhee, C.K., Zheng, L., Mardones, G.A., Rong, Y., Peng, J., Mi, N., Zhao, Y., Liu, Z., Wan, F.*, et al.* (2010). Termination of autophagy and reformation of lysosomes regulated by mTOR. Nature *465*, 942-946.

Yue, Y., Skimming, J.W., Liu, M., Strawn, T., and Duan, D. (2004). Full-length dystrophin expression in half of the heart cells ameliorates β-isoproterenol-induced cardiomyopathy in mdx mice. Human Molecular Genetics *13*, 1669-1675.

Zanoteli, E., van de Vlekkert, D., Bonten, E.J., Hu, H., Mann, L., Gomero, E.M., Harris, A.J., Ghersi, G., and d'Azzo, A. (2010). Muscle degeneration in neuraminidase 1-deficient mice results from infiltration of the muscle fibers by expanded connective tissue. Biochim Biophys Acta *1802*, 659-672.

Zatz, M., Rapaport, D., Vainzof, M., Passos-Bueno, M.R., Bortolini, E.R., Rita de Cassia, M.P., and Peres, C.A. (1991). Serum creatine-kinase (CK) and pyruvate-kinase (PK) activities in Duchenne (DMD) as compared with Becker (BMD) muscular dystrophy. Journal of the neurological sciences *102*, 190-196.

Zhang, J., Kim, J., Alexander, A., Cai, S., Tripathi, D.N., Dere, R., Tee, A.R., Tait-Mulder, J., Di Nardo, A., and Han, J.M. (2013). A tuberous sclerosis complex signalling node at the peroxisome regulates mTORC1 and autophagy in response to ROS. Nature cell biology *15*, 1186.

Zhang, X., Cheng, X., Yu, L., Yang, J., Calvo, R., Patnaik, S., Hu, X., Gao, Q., Yang, M., Lawas, M.*, et al.* (2016). MCOLN1 is a ROS sensor in lysosomes that regulates autophagy. Nat Commun *7*, 12109.

Zhang, X., Li, X., and Xu, H. (2012). Phosphoinositide isoforms determine compartment-specific ion channel activity. Proc Natl Acad Sci U S A *109*, 11384-11389.

Zoncu, R., Bar-Peled, L., Efeyan, A., Wang, S., Sancak, Y., and Sabatini, D.M. (2011). mTORC1 senses lysosomal amino acids through an inside-out mechanism that requires the vacuolar H(+)-ATPase. Science *334*, 678-683.